Published for SISSA by Springer

Received: *February 5, 2024*
Accepted: *April 8, 2024*
Published: *May 9, 2024*

ATLAS Run 2 searches for electroweak production of supersymmetric particles interpreted within the pMSSM

The ATLAS collaboration

E-mail: atlas.publications@cern.ch

Abstract: A summary of the constraints from searches performed by the ATLAS collaboration for the electroweak production of charginos and neutralinos is presented. Results from eight separate ATLAS searches are considered, each using $140\,\text{fb}^{-1}$ of proton-proton data at a centre-of-mass energy of $\sqrt{s} = 13\,\text{TeV}$ collected at the Large Hadron Collider during its second data-taking run. The results are interpreted in the context of the 19-parameter phenomenological minimal supersymmetric standard model, where R-parity conservation is assumed and the lightest supersymmetric particle is assumed to be the lightest neutralino. Constraints from previous electroweak, flavour and dark matter related measurements are also considered. The results are presented in terms of constraints on supersymmetric particle masses and are compared with limits from simplified models. Also shown is the impact of ATLAS searches on parameters such as the dark matter relic density and the spin-dependent and spin-independent scattering cross-sections targeted by direct dark matter detection experiments. The Higgs boson and Z boson 'funnel regions', where a low-mass neutralino would not oversaturate the dark matter relic abundance, are almost completely excluded by the considered constraints. Example spectra for non-excluded supersymmetric models with light charginos and neutralinos are also presented.

Keywords: Beyond Standard Model, Hadron-Hadron Scattering, Supersymmetry

ArXiv ePrint: 2402.01392

https://doi.org/10.1007/JHEP05(2024)106

Contents

1 Introduction

The second data-taking run (Run 2) of the Large Hadron Collider (LHC) provided sensitivity to a variety of new-physics models well beyond that of LHC Run 1. This is due to the increase in both integrated luminosity and centre of mass energy — Run 1 corresponded to 4.6 and 20.3 fb^{-1} of proton-proton collisions at centre of mass energies of 7 and 8 TeV, respectively, whilst Run 2 searches benefitted from 140 fb^{-1} at 13 TeV. This in turn has enabled the ATLAS collaboration [1] to develop a suite of new analysis techniques sensitive to the production of electroweakly interacting particles that extends sensitivity into a new realm. Weak scale supersymmetry (SUSY) [2–7] is a theoretical extension to the Standard Model (SM) that adds a new fermion/boson SUSY partner to each boson/fermion in the SM. If fulfilled in nature, this could help to solve the fine-tuning problem [8–11]. In SUSY models that conserve R-parity [12], SUSY particles (sparticles) must be produced in pairs and the lightest SUSY particle (LSP) is stable. If the LSP is weakly interacting it constitutes a viable candidate for dark matter (DM) [13, 14]. Due to its weakly interacting nature, any LSP produced at the LHC would escape detection and lead to missing transverse momentum ($E_{\mathrm{T}}^{\mathrm{miss}}$).

LHC sparticle production cross-sections are highly dependent on the sparticle masses. The coloured sparticles (squarks and gluinos) are strongly produced and have significantly larger production cross-sections than non-coloured sparticles of equal masses, such as the sleptons (superpartners of the SM leptons) and the electroweakinos. The superpartners of the SM Higgs boson and the electroweak gauge bosons, known as higgsinos, winos and binos are collectively known as electroweakinos. They mix to form chargino ($\tilde{\chi}_i^{\pm}$, $i = 1, 2$) and

pMSSM Parameter	Meaning
$\tan\beta$	Ratio of the Higgs vacuum expectation values for the two doublets
M_A	Pseudoscalar (CP-odd) Higgs boson mass parameter
μ	Higgsino mass parameter
M_1, M_2, M_3	Bino, wino and gluino mass parameters
A_t, A_b, A_τ	Third generation trilinear couplings
$M_{\tilde{q}}$, $M_{\tilde{u}_R}$, $M_{\tilde{d}_R}$, $M_{\tilde{l}}$, $M_{\tilde{e}_R}$	First/second generation sfermion mass parameters
$M_{\tilde{Q}}$, $M_{\tilde{t}_R}$, $M_{\tilde{b}_R}$, $M_{\tilde{L}}$, $M_{\tilde{\tau}_R}$	Third generation sfermion mass parameters

Table 1. Summary of the 19 pMSSM parameters relevant to this study.

neutralino ($\tilde{\chi}^0_j$, $j = 1, 2, 3, 4$) mass eigenstates (states are ordered by increasing values of their mass). If gluino and squark masses were much heavier than low-mass electroweakinos, then SUSY production at the LHC would be dominated by direct electroweak production. The latest limits from the ATLAS collaboration on squark and gluino production [15–18] extend well beyond the TeV scale, thus making electroweak production of sparticles a promising and important probe to search for SUSY at the LHC.

Throughout the first two data-taking runs of the LHC the ATLAS and CMS collaborations have performed extensive searches for the production of electroweakinos, and in the absence of any significant excesses over the SM prediction, exclusion limits were set on SUSY model parameters [18–27]. To simplify the design and interpretation of analyses, 'simplified models' [28] are often used such that the masses of relevant sparticles (often the $\tilde{\chi}^\pm_1$, $\tilde{\chi}^0_2$ and $\tilde{\chi}^0_1$) are the only free parameters. Whilst exclusion limits using simplified models provide an easily interpretable picture of the sensitivity of analyses to specific areas of parameter space in the minimal SUSY extension to the SM (MSSM), they are far from an exhaustive exploration of the MSSM. Without any assumed mechanism for SUSY-breaking the MSSM has over a hundred parameters describing the sparticle masses and their decays. This large number of parameters can be reduced by considering the phenomenological MSSM (pMSSM) [29, 30]. This is based on the most general CP-conserving MSSM, meaning no additional CP-violating contributions, and assumes R-parity conservation, and minimal flavour violation. The first two generations of sfermions are also required to be mass degenerate and to have negligible Yukawa couplings. This leaves 19 independent weak scale parameters to consider: ten sfermion masses (five for the degenerate first two generations and five for the third generation), three trilinear couplings $A_{\tau,t,b}$ that give the couplings between the Higgs field and the third generation sfermions, the bino, wino and gluino mass parameters $M_{1,2,3}$, the bilinear Higgs mass parameter μ, the ratio of the vacuum expectation values of the Higgs fields $\tan\beta$, and the mass parameter of the pseudoscalar Higgs boson M_A. These parameters are summarised in table 1.

At the end of Run 1 a reinterpretation of the ATLAS SUSY searches was performed using 300 000 pMSSM models in this 19-dimensional parameter space [31]. The strongest direct constraints on sparticle production were found to come from searches for squarks and gluinos. A subsequent interpretation was performed restricting attention to a five-dimensional sub-space of the pMSSM to specifically assess the impact of the ATLAS Run 1 searches for the electroweak production of SUSY particles, and their corresponding constraints on DM [32]. The CMS collaboration also performed a reinterpetation of their Run 1 searches in the 19-dimensional pMSSM [33] using a global Bayesian analysis, and additional reinterpretations of LHC SUSY searches have been performed outside the LHC collaborations. These include results obtained using GAMBIT [34, 35] and MasterCode [36] that incorporate LHC searches into global likelihood fits in the 19-dimensional pMSSM or subsets of it. This paper presents the sensitivity of the searches performed with the ATLAS detector in Run 2 of the LHC to the electroweak production of SUSY particles in the pMSSM. All ATLAS results used in this paper benefit from an extensive software suite [37] that is used in data simulation, in the reconstruction and analysis of real and simulated data, in detector operations, and in the trigger and data acquisition systems of the experiment. Relative to the Run 1 reinterpretation, this analysis benefits from a broader range of search channels that were targeted throughout Run 2 due to the increased statistical precision and centre of mass energy. It also takes advantage of new tools for reinterpretation developed by the ATLAS collaboration, such as particle-level analysis evaluation using the SimpleAnalysis framework [38], preserved profile likelihood fits [39] and a new full analysis reinterpretation framework, RECAST [40, 41], as well as utilising the REANA reproducible data analysis platform [42].

The work is structured as follows: section 2 describes the analysis strategy, including the pMSSM model samples and ATLAS results considered. Section 3 then presents the results, with conclusions provided in section 4.

2 Analysis strategy

This section describes the analysis strategy used. This includes a description of the framework used to scan over the pMSSM parameters, the external constraints considered, the simulated samples produced for selected models, the choice of the scan ranges for the pMSSM parameters, and the ATLAS searches and measurements considered.

2.1 Scanning framework

A portion of the pMSSM parameter space is randomly sampled to produce a set of models. Two separate samplings (scans) are used as described in section 2.2. In both scans a flat prior is chosen as the relevant parameter ranges are relatively narrow ($<$ 2 TeV) with most of the interest in the range of O(50 GeV) to O(1 TeV). These models are then evaluated using a workflow chain summarised in figure 1.

The models are first passed through several programs to calculate various observables:

- SPheno 4.0.5 [43, 44] is used to calculate the mass spectra and decays of the SUSY particles.

- FeynHiggs 2.18 [45–52] is used to calculate relevant Higgs sector variables, such as the masses and branching fractions of the SUSY and SM Higgs bosons. As the masses of the SUSY particles strongly impact the Higgs boson masses, FeynHiggs automatically takes these into account. The changes to the Higgs sector masses, in turn, influence the

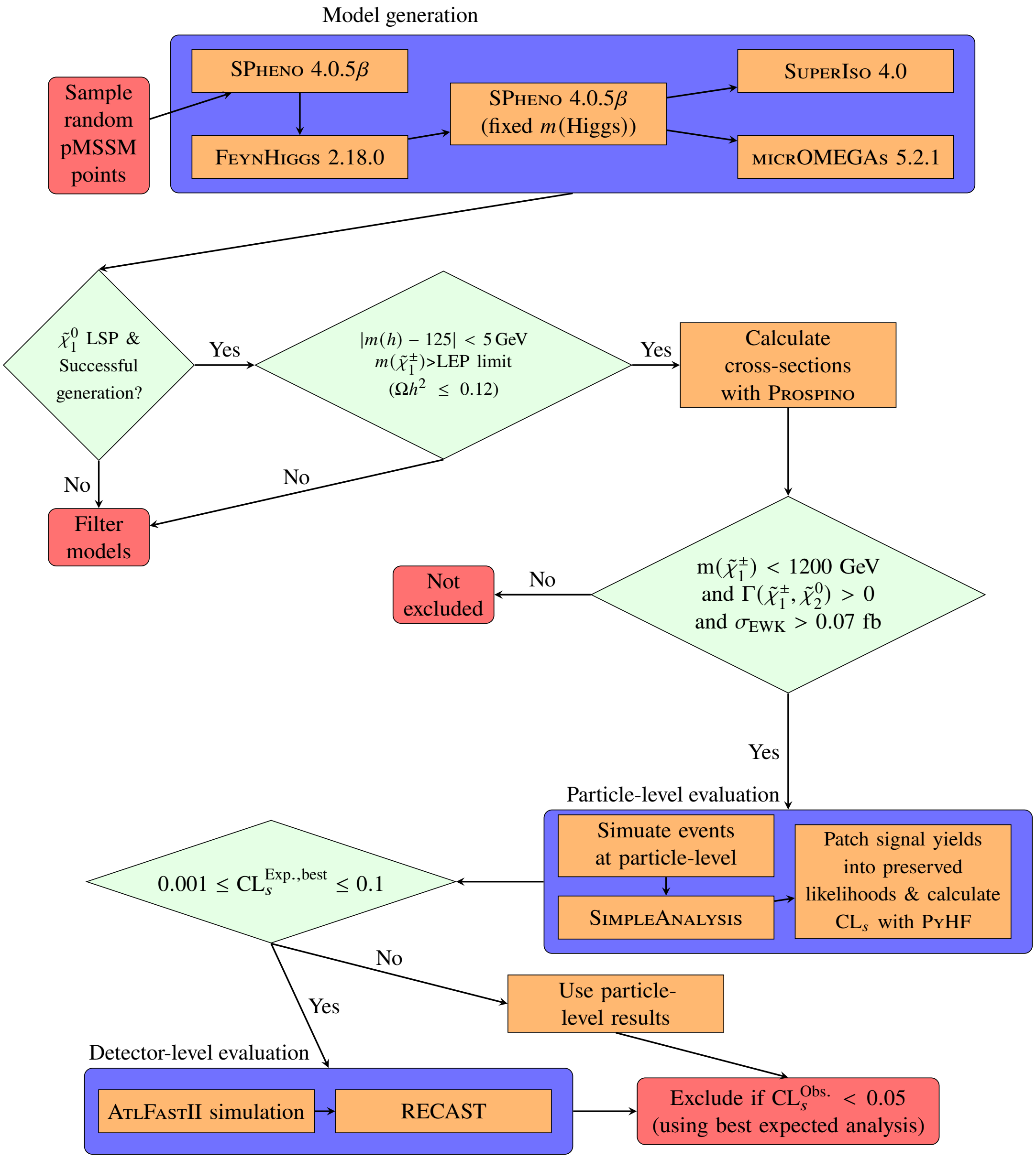

Figure 1. Workflow for the electroweak pMSSM scan, starting from sampling the pMSSM parameter space and ending at the determination of whether each model is excluded or not.

branching fractions of SUSY particles. Hence, the resulting spectrum determined with FeynHiggs is reprocessed by SPheno, which allows the calculation of SUSY branching fractions while keeping both the SUSY and Higgs sector masses constant.

- MicrOMEGAS 5.2.1 [53, 54] is used to calculate the predicted DM relic density, annihilation cross-sections, and spin (in)dependent weakly interacting massive particle (WIMP)-nucleon cross-sections. Limits on WIMP-nucleon cross-sections from direct detection experiments assume a DM candidate that saturates the observed relic density $\Omega h^2 = 0.12$ whereas the majority of pMSSM models considered here under-predict

JHEP05(2024)106

Category	Constraint	Lower bound	Upper bound	Notes
Flavour	$\mathcal{B}(b \to s\gamma)$	3.11×10^{-4}	3.87×10^{-4}	2022 PDG average (2σ window) [58].
	$\mathcal{B}(B_s \to \mu\mu)$	1.87×10^{-9}	4.31×10^{-9}	Most recent LHCb result (2σ window) [59].
	$\mathcal{B}(B^+ \to \tau\nu)$	6.10×10^{-5}	1.57×10^{-4}	2022 PDG average (2σ window) [58].
Precision electroweak	$\Delta\rho$	-0.0004	0.0018	Updated global electroweak fit by GFitter group [60] (not including CDF W mass measurement [61]).
	$\Gamma^{\mathrm{BSM}}_{\mathrm{inv}}(Z)$	—	2 MeV	Beyond-the-Standard Model contributions to precision electroweak measurements on the Z-resonance from experiments at the SLC and LEP colliders [62].
	$m(W)$	80.347 GeV	80.407 GeV	2022 PDG result (excluding CDF W mass measurement [61]) [58] but with the 2σ window expanded by 6 MeV to allow for uncertainty due to the top-quark mass in the MSSM Higgs calculation [63].
DM	Relic density	—	0.12	Latest bound from Planck [64].
	$\sigma_{\text{Spin-independent}}$			Exclusion contour on direct detection of DM from the LZ collaboration [65].
	$\sigma_{\text{Spin-dependent}}$			Exclusion contour on direct detection of DM from PICO-60 [66].

Table 2. Constraints from electroweak precision measurements, flavour physics observables and direct-detection DM searches. When used in the results in section 3, the flavour and precision electroweak constraints together correspond to the 'non-DM' external constraints, whilst 'all external constraints' includes the flavour, precision electroweak and DM constraints. In addition to these constraints, unless otherwise stated, all models considered in this paper include the LEP constraint on the chargino mass and a Higgs boson mass constraint as described in the text.

the observed relic density. Therefore all WIMP-nucleon cross-sections are scaled by $(\Omega h^2/0.12)$ for each model below the observed relic density to correct for this assuming that a second DM component makes up the remaining relic density without contributing to the DM-nucleon scattering cross-sections.

- SuperISO 4.0 [55] is used to calculate a variety of flavour observables.

Models that fail to be processed properly by one or more of these programs or contain unphysical spectra are removed. Models where the LSP is not the lightest neutralino ($\tilde{\chi}^0_1$) are removed as are models with charginos that are excluded by LEP, i.e., $m(\tilde{\chi}^\pm_1) < 103$ GeV for $\Delta\, m(\tilde{\chi}^\pm_1, \tilde{\chi}^0_1) \geq 3$ GeV [56] and $m(\tilde{\chi}^\pm_1) < 91.9$ GeV for $\Delta\, m(\tilde{\chi}^\pm_1, \tilde{\chi}^0_1) < 3$ GeV [57]. Finally, a loose bound is applied to the predicted mass of the SM Higgs boson: $120\,\text{GeV} < m(h) < 130\,\text{GeV}$. The bound on the Higgs boson mass is wider than the mass measurement precision due to the larger theoretical uncertainties in the calculation for the MSSM. A loose bound also improves the efficiency of the model generation, while the bound keeps simulated Higgs boson decays consistent with other experimental constraints. When presenting the final results, additional external constraints complementary to the ATLAS search constraints are considered based on the observables calculated by these programs. These include constraining the mass of the W boson to a window around its measured values, spin (in)dependent LSP-nucleon cross-section limits, constraints on electroweak precision observables and constraints on B-physics observables. These constraints are summarised in table 2.

The cross-sections for each electroweakino pair-production process are calculated at next-to-leading-order[1] using Prospino [68] for each model that passes the initial constraints. At this stage, a filter is applied to halt the processing of models that the ATLAS searches are very unlikely to have sensitivity to. This filter requires $m(\tilde{\chi}_1^\pm) < 1200$ GeV, as the analyses considered have no sensitivity to scenarios with a $\tilde{\chi}_1^\pm$ mass above this limit, and that the total cross-section for electroweak production of SUSY particles $\sigma_{\text{EWK}} > 7 \times 10^{-5}$ pb, as lower cross-sections would be expected to yield less than ten events in the full Run 2 data sample. In addition models with predicted stable or effectively stable $\tilde{\chi}_1^\pm$ and $\tilde{\chi}_2^0$ are also filtered, as the event generation cannot handle additional stable charginos and neutralinos. Models rejected by this filter are included in the final model sets used in section 3, but are considered to be not excluded here, even if some might be excluded by dedicated long-lived particle searches (for example the ATLAS search for heavy long-lived charged particles with large ionisation losses has sensitivity to long-lived charginos [69]).

Events are then simulated using Monte Carlo (MC) techniques for each model that passes these filters. Events are simulated at leading-order using MadGraph5_aMC@NLO 2.9.5 [70] and Pythia 8.306 [71]. Only electroweak production processes are generated, and coloured sparticles are not included in the subsequent decays. Assessing the detector effects on simulated events requires them to be processed either through a full simulation of the ATLAS detector [72] based on Geant4 [73], or a faster version of the simulation (AtlFastII), which relies on a parameterisation for the response of the calorimeters and on Geant4 for the other components of the detector, then reconstructed with the same algorithms as those used for the data. Producing such 'detector-level' reconstructed samples is computationally expensive, so instead events are initially simulated at particle-level using the SimpleAnalysis framework [38]. This includes parameterised response functions that aim to emulate detector effects such as reconstruction and identification inefficiencies and resolutions. These are typically parameterised as functions of the transverse momentum and rapidity for the different types of particles. SimpleAnalysis is used to obtain an approximate result that indicates if the model is likely to be excluded or not. Validation studies of each SimpleAnalysis implementation are performed to confirm that the yields obtained agree with the yields from fully reconstructed samples within a reasonable margin (usually around 20%). All electroweakino production processes are produced simultaneously in MadGraph and, to keep processing time manageable, up to a single additional jet from initial-state radiation is allowed in the MadGraph calculation and the 4-flavour merging scheme is used to combine them with Pythia . The number of events generated is required to correspond to at least five times the Run 2 integrated luminosity, subject to an upper limit of 250 000 events. For high cross-section models exceeding this limit, additional filtered samples are produced at particle level to improve the statistical precision of the evaluation.

ATLAS searches for SUSY typically define a set of statistically independent event selections. 'Signal regions' (SR) are event selections where a statistically significant excess of events would be observed over the SM prediction if the signal were present. These are

[1]For simplified model results published by ATLAS, Resummino [67] is used to provide additional next-to-leading-logarithm corrections to the production cross-section. To reduce resource usage, Resummino has not been applied here which could cause small differences in cross-sections for similar processes.

supplemented by auxiliary 'control regions' (CR) that are used to produce semi-data-driven estimates of SM backgrounds. A simultaneous profile likelihood fit is used to constrain the MC yields with the observed data in the CRs. The CRs are designed to be both orthogonal and similar to the SRs, whilst also having little signal contamination. When performing the statistical analysis the likelihood is constructed as a product of Poisson probability density functions, describing the observed number of events in each CR/SR, and Gaussian distributions that describe the nuisance parameters associated with each of the systematic uncertainties. Poisson distributions are used for MC statistical uncertainties, and systematic uncertainties that are correlated between different samples can be accounted for by using the same nuisance parameter. Exclusion limits are set on SUSY model parameters using the CL_s prescription [74]. The SRs and CRs in different ATLAS searches are not statistically independent and cannot be combined easily. Therefore, in this paper, only the search with the best expected exclusion limit for a given model is used to decide if a model is excluded or not.

To emulate this calculation using the particle-level signal samples and determine whether a model is excluded, a profile-likelihood fit using the procedure outlined in ref. [39] is performed using the particle-level signal yields along with a detector-level estimate of the background yields and observed data for each analysis.[2] A hypothesis test is performed using the pyhf framework [76, 77] to produce an observed and expected CL_s value for each analysis. Statistical and systematic uncertainties in the signal yields are not included in this calculation, but all background systematic and statistical uncertainties are retained. For some analyses signal contamination in the CRs is also neglected when performing the particle-level evaluation, however it is always considered when calculating the detector-level CL_s values discussed next.

Using particle-level signal yields and not applying the complete set of signal uncertainties means that the CL_s values calculated using this procedure are only approximate. To determine the final exclusion, the particle-level CL_s values are used to categorise the models as follows. Models deemed to be 'likely excluded' have an expected $CL_s < 0.001$ for at least one of the considered electroweak searches. Those deemed 'likely not excluded' have an expected $CL_s > 0.1$ for every analysis. These boundaries are chosen by checking that the particle-level classifications for a subset of models are consistent with their full detector-level evaluation. Finally, those identified as 'ambiguous' have an expected CL_s that satisfies $0.001 \leq CL_s \leq 0.1$ for at least one analysis and $CL_s \geq 0.001$ for every analysis. For the first two categories these particle-level evaluations are considered final and used for the results presented in section 3. For the models deemed 'ambiguous' detector-level MC samples are produced using the Geant4 simulation with parameterised simulation of the calorimeters. Whilst computationally expensive, the categorisation process outlined in this section ensures this only has to be done for 5%–10% of models. The full ATLAS analyses are then applied to the resulting MC samples using RECAST — a framework for re-using existing analyses to interpret new physics models. The RECAST of an analysis contains all of the original analysis steps in Docker containers [78], to allow a full re-execution of the event selection, calculation of systematic uncertainties and statistical analysis for a new signal sample. Finally, the CL_s

[2]Most Run 2 ATLAS SUSY analyses have published a 'likelihood' [39] on the HEPData platform [75], but in the cases where this was not available this was obtained internally.

Parameter	Min	Max	Note
$M_{\tilde{L}_1}$ $(=M_{\tilde{L}_2})$	10 TeV	10 TeV	Left-handed slepton (first two gens.) mass
$M_{\tilde{e}_1}$ $(=M_{\tilde{e}_2})$	10 TeV	10 TeV	Right-handed slepton (first two gens.) mass
$M_{\tilde{L}_3}$	10 TeV	10 TeV	Left-handed stau doublet mass
$M_{\tilde{e}_3}$	10 TeV	10 TeV	Right-handed stau mass
$M_{\tilde{Q}_1}$ $(=M_{\tilde{Q}_2})$	10 TeV	10 TeV	Left-handed squark (first two gens.) mass
$M_{\tilde{u}_1}$ $(=M_{\tilde{u}_2})$	10 TeV	10 TeV	Right-handed up-type squark (first two gens.) mass
$M_{\tilde{d}_1}$ $(=M_{\tilde{d}_2})$	10 TeV	10 TeV	Right-handed down-type squark (first two gens.) mass
$M_{\tilde{Q}_3}$	2 TeV	5 TeV	Left-handed squark (third gen.) mass
$M_{\tilde{u}_3}$	2 TeV	5 TeV	Right-handed top squark mass
$M_{\tilde{d}_3}$	2 TeV	5 TeV	Right-handed bottom squark mass
M_1	−2 TeV	2 TeV	Bino mass parameter
M_2	−2 TeV	2 TeV	Wino mass parameter
μ	−2 TeV	2 TeV	Bilinear Higgs boson mass parameter
M_3	1 TeV	5 TeV	Gluino mass parameter
A_t	−8 TeV	8 TeV	Trilinear top coupling
A_b	−2 TeV	2 TeV	Trilinear bottom coupling
A_τ	−2 TeV	2 TeV	Trilinear τ-lepton coupling
M_A	0 TeV	5 TeV	Pseudoscalar Higgs boson mass
$\tan\beta$	1	60	Ratio of the Higgs vacuum expectation values

Table 3. Parameter ranges that are randomly sampled for the 'EWKino' scan.

output by RECAST is used to categorise ambiguous models as excluded ($\mathrm{CL_s} < 0.05$) or not excluded ($\mathrm{CL_s} > 0.05$) based on the full detector-level analysis.

2.2 Scan configurations

Two pMSSM scans are processed with different parameter ranges and sampling strategies. In both scans, the sleptons and all squarks and gluinos are 'decoupled', i.e., mass parameters are set sufficiently high as to not influence the production or decays of the electroweakinos. The first scan focuses on general electroweakino production and is denoted the 'EWKino scan'. The parameter ranges for the EWKino scan are listed in table 3. The EWKino scan comprises 12 280 models that survive all of the constraints and filters when starting from an initial set of 20 000 models randomly sampled (with a flat prior) from these ranges.

The magnitudes of the M_1, M_2 and μ parameters, which control the bino, wino and higgsino masses respectively, are varied between 0 and 2 TeV. The ATLAS Run 2 sensitivity to electroweakinos does not extend beyond masses of 1 TeV, so these ranges capture a range

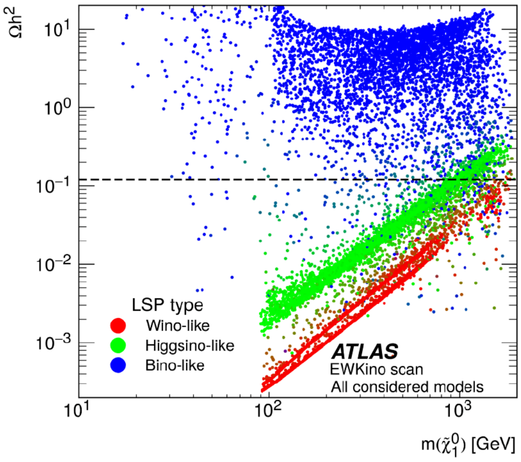

Figure 2. Scatter plot of models from the EWKino scan in the Ωh^2 versus $m(\tilde{\chi}_1^0)$ plane, coloured with RGB value set to the (wino, bino, higgsino) fraction of the LSP. The experimentally measured value of the relic density [64], $\Omega h^2 = 0.120 \pm 0.001$, is indicated by a horizontal dashed line.

of relevant senarios including those where the heavier $\tilde{\chi}_2^\pm$, $\tilde{\chi}_3^0$ and $\tilde{\chi}_4^0$ (not present in simplified models) are both below and above this limit. Whilst the third generation squark masses are scanned over and those parameters affect for example the Higgs boson mass, they have no significant impact on the phenomenology or analysis exclusion in the electroweak sector and are not included in the event generation. This is also the case for the gluino mass parameter M_3.

Figure 2 shows a scatter plot of the models from the EWKino scan in the Ωh^2 versus $m(\tilde{\chi}_1^0)$ plane, coloured by the dominant component (wino, bino or higgsino) of the LSP. The experimentally measured value of the relic density [64], $\Omega h^2 = 0.12$, is indicated by a horizontal dashed line. Here the LSP is defined as 'bino-like' if the bino fraction is greater than the wino/higgsino fraction, and similar for 'wino-like' and 'higgsino-like'. With decoupled sleptons (that limit options for co-annihilation), models with a bino-like LSP typically overestimate the DM relic density unless there are additional annihilation mechanisms available. A higgsino- or wino-like LSP, in general, provides a DM relic density prediction below the measured value, unless the LSP mass is around 1 TeV (higgsino) or 3 TeV (wino). This is because a higgsino- or wino-like LSP has enhanced co-annihilation with the chargino and/or second neutralino that by construction are close in mass to a wino- or higgsino-like LSP.

Applying the DM relic density constraint $\Omega h^2 \leq 0.12$ (where the inequality allows the neutralino LSP to be a subdominant component of DM) would thus remove almost all models in the EWKino scan with a bino-like LSP. To avoid over-saturating the relic density additional annihilation mechanisms are required for bino-like LSP models. These typically lead to models with more compressed mass splittings between the LSP and the $\tilde{\chi}_2^0$, $\tilde{\chi}_1^\pm$ as well as concentrating models in the '$Z/h/A/H$ funnel' regions. In the funnel regions the LSP mass is approximately half the mass of the Z, Higgs boson, heavy neutral scalar Higgs boson H, or pseudoscalar Higgs boson A, such that self-annihilation into a $Z/h/A/H$ is enhanced, resulting in a DM relic density below the experimental value. The ranges involved in the EWKino scan do not generate enough models in the funnel regions to demonstrate the sensitivity of the ATLAS searches. To compensate for this and to produce a sizeable

Scan name	EWKino	BinoDM
$\lvert M_1 \rvert$ range	0–2 TeV	0–500 GeV
LSP type	Neutralino	Bino-like neutralino
Number of models generated:		
Sampled	20 000	437 500
Successful generation	16 667	370 017
Correct LSP type	15 321	286 267
Satisfy DM relic density constraint $\Omega h^2 \leq 0.12$	N/A	11 122
Satisfy LEP chargino mass constraint	13 969	10 174
$120\,\text{GeV} < \text{m}(h) < 130\,\text{GeV}$	12 280	8 897
Satisfy non-DM external constraints	7 956	5 752
Satisfy all external constraints	2 460	1 769

Table 4. Set-ups for the two pMSSM scans performed and number of models passing each step and constraint. Whilst listed as part of the selections applied to produce the model set, the DM relic density is not considered in the model generation for the EWKino scan, where it is instead only used as part of the DM constraints discussed in table 2 of section 2.1.

sample of bino-LSP models with $\Omega h^2 \leq 0.12$, a second scan is performed that oversamples such models. The ranges of this scan are the same as those in table 3 except that the bino mass parameter range is tightened to $|M_1| < 500\,\text{GeV}$ in order to focus on low-mass bino models. 437,500 models are randomly sampled from these ranges with a flat prior, and only those with a bino-like LSP and $\Omega h^2 \leq 0.12$ are kept. These constraints, along with the additional filters, reduce the number of models to 8 897. This scan is referred to as the 'BinoDM' scan. In the EWKino scan the relic density constraint is not applied in the initial selection of models. Table 4 summarises the bino mass parameter ranges and the number of models passing each step of the workflow, for the two scans.

Figure 3 shows models from the EWKino and BinoDM scans plotted in the Ωh^2 versus $m(\tilde{\chi}_1^0)$ plane before the DM relic density constraint is applied, coloured by the dominant annihilation mechanism. Several regions of interest can be observed. The first are the 'Z/h funnel' regions in purple, which are particularly important for the BinoDM scan. In order to couple to the Higgs boson and Z bosons such that these annihilation mechanisms are allowed, the LSP must have a higgsino component. These 'funnel regions' are of particular interest as they can satisfy the DM relic density constraint and also have an LSP mass that overlaps with the region of sensitivity for many of the Run 2 ATLAS SUSY searches. Similarly, the A and H funnel regions are shown in green. For $m(\tilde{\chi}_1^0) > 100$ GeV, in the 'bulk region', there are a variety of other (co-)annihilation mechanisms contributing. When $m(\tilde{\chi}_1^0) > 173\,\text{GeV}$ (i.e. the LSP is similar to or greater in mass than the top quark), the $\tilde{\chi}_1^0\tilde{\chi}_1^0 \to t\bar{t}$ self-annihilation process is allowed, coloured in pink. The orange points also show models where the LSP is close in mass to a wino- or higgsino-like $\tilde{\chi}_1^\pm$ and $\tilde{\chi}_2^0$, causing enhanced co-annihilation. In general, in the BinoDM scan the DM relic density constraint

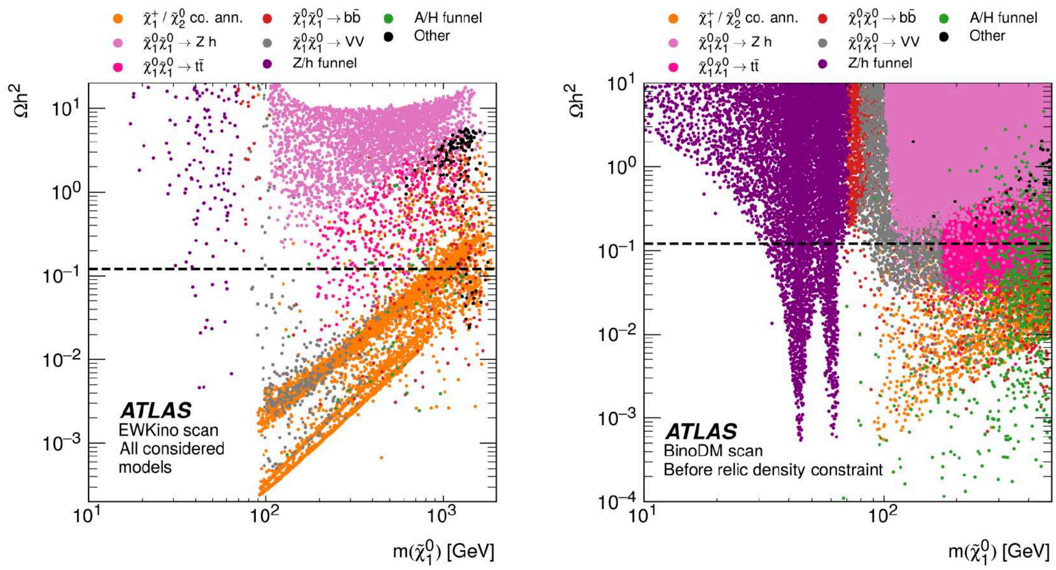

(a) EWKino scan.

(b) BinoDM scan.

Figure 3. Scatter plot of models selected from (a) the EWKino and (b) the BinoDM scan (before the relic density constraint is applied) in the Ωh^2 versus $m(\tilde{\chi}_1^0)$ plane, coloured by the dominant annihilation mechanism. No additional external constraints are applied.

favours an LSP with a bino/higgsino mix. A pure-bino LSP is disfavoured unless its mass is very close to the Z/h pole, or the $\tilde{\chi}_1^\pm/\tilde{\chi}_2^0$ are very nearby in mass.

2.3 Summary of ATLAS searches and measurements considered

This subsection describes the eight ATLAS searches and the additional constraints from ATLAS Higgs boson measurements that are included in the results in section 3. The ATLAS Run 2 searches for electroweak SUSY took a 'signature-driven' approach, meaning that multiple final states can have sensitivity to the same SUSY production mode due to differing decays of the gauge bosons in the decay chain. The simplified models used to optimise and interpret the searches typically assumed that the electroweakinos are pure bino, wino or higgsino states in terms of cross-section evaluation, with the dominant SUSY production mode being determined by the next-lightest SUSY particle (NLSP), which then decays into a particular SM final state and the LSP with a fixed branching fraction. In Run 1 the main simplified model presented was the 'bino-wino' scenario where the LSP is a pure bino with the next lightest SUSY particles being mass degenerate wino-like $\tilde{\chi}_2^0$ and $\tilde{\chi}_1^\pm$. The dominant production modes are then associated $\tilde{\chi}_1^\pm\tilde{\chi}_2^0$ production or $\tilde{\chi}_1^+\tilde{\chi}_1^-$ pair production. The larger data samples in Run 2 have enabled multiple searches targeting this scenario with complementary sensitivity in different areas of the LSP versus NLSP mass plane. Assuming boson-mediated decays, the $\tilde{\chi}_1^\pm$ decays via a W boson either leptonically or hadronically, whilst the $\tilde{\chi}_2^0$ can decay via either a Z boson, which decays leptonically or hadronically, or via a Higgs boson, which can then decay according to its SM branching fractions. The Run 1 electroweak SUSY searches focused on leptonic final states for these models as they provide a

JHEP05(2024)106

clean final state for triggering and lower SM backgrounds. The larger data samples in Run 2 have allowed more challenging final states to be probed.

Table 5 summarises the Run 2 electroweak SUSY searches considered in this analysis. The '2L0J' search [19] targeted $\tilde{\chi}_1^+\tilde{\chi}_1^-$ with W boson mediated decays into final states with exactly two opposite sign electrons or muons, low hadronic activity and missing transverse momentum. The '3L' search [23] targeted associated $\tilde{\chi}_1^{\pm}\tilde{\chi}_2^0$ production with WZ mediated decays where both the Z and W boson decay leptonically. Scenarios where the decays proceed via on-shell and off-shell Z/W bosons were targeted with separate selections. In addition to these fully leptonic searches, channels probing hadronic decays of the W or Z were considered. This incudes the 'FullHad' search [24] which considered both $\tilde{\chi}_1^+\tilde{\chi}_1^-$ and $\tilde{\chi}_1^{\pm}\tilde{\chi}_2^0$ production with boson-mediated decays (including $\tilde{\chi}_2^0$ decays into both Z and h) into final states involving hadronic jets, and the '2L2J' search [25] which targeted $\tilde{\chi}_1^{\pm}\tilde{\chi}_2^0$ where the $\tilde{\chi}_2^0$ decays leptonically via a Z and the $\tilde{\chi}_1^{\pm}$ decays hadronically. An additional dedicated search, denoted '1Lbb' [15], specifically targeted the scenario where the $\tilde{\chi}_2^0$ decays via an on-shell Higgs boson into two b-tagged jets, and the $\tilde{\chi}_1^{\pm}$ decays leptonically.

Unlike the other searches cosidered, the '4L' search [22] targeted general gauge-mediated (GGM) [79] scenarios with a gravitino LSP. However it does provide sensitivity to the pMSSM models considered in this paper that produce four leptons through long decay chains following production of the heavier electroweakinos.

For the bino-wino scenario without additional radiation, the amount of missing transverse momentum in the final state is largely determined by the mass splitting between the LSP and the $\tilde{\chi}_1^{\pm}$, $\tilde{\chi}_2^0$. Many of the analyses referred to above included multiple search regions targeting different mass splittings, however a dedicated 'compressed' [20] search was also performed that targeted models with smaller mass splittings in final states with 'soft' low-transverse momentum leptons, and high missing transverse momentum generated by the SUSY production system recoiling against initial-state radiation. This search was also the first analysis to target SUSY scenarios with a pure higgsino LSP. Finally, the only search in this paper that was optimised for pure wino LSP scenarios (while also targeting models with a higgsino LSP) is the 'disappearing-track' search [27]. This targeted anomaly-mediated SUSY breaking (AMSB) [80, 81] models that naturally give a pure wino LSP as well as providing interpretations for compressed higgsino scenarios. This search targeted long-lived charginos using a distinct signature of a short track that 'disappears' in the ATLAS tracking detector associated with missing transverse momentum.

When performing the workflow described in the previous subsection, several modifications are made for specific searches:

- In the cases where the time to run the full analysis likelihood with particle-level signal yields is too computationally expensive, the 'simplified likehood' procedure described in ref. [82] is used instead. This makes several simplifications including combining all background components into a single sample and reducing all nuisance parameters in the full likelihood to a single constrained parameter. This significantly increases the speed of the statistical fit, at the price of some accuracy. This approach is used for the compressed and 3L off-shell analyses.

Analysis	Relevant simplified models targeted
FullHad [24]	Wino $\tilde{\chi}_1^{\pm}\tilde{\chi}_2^0$ via WZ, Wino $\tilde{\chi}_1^{\pm}\tilde{\chi}_2^0$ via Wh, Wino $\tilde{\chi}_1^{+}\tilde{\chi}_1^{-}$ via WW
1Lbb [15]	Wino $\tilde{\chi}_1^{\pm}\tilde{\chi}_2^0$ via Wh
2L0J [19]	Wino $\tilde{\chi}_1^{+}\tilde{\chi}_1^{-}$ via WW, slepton pairs
2L2J [25]	Wino $\tilde{\chi}_1^{\pm}\tilde{\chi}_2^0$ via WZ
3L [23]	Wino $\tilde{\chi}_1^{\pm}\tilde{\chi}_2^0$ via WZ, Wino $\tilde{\chi}_1^{\pm}\tilde{\chi}_2^0$ via Wh, higgsino $\tilde{\chi}_1^{\pm}\tilde{\chi}_2^0\tilde{\chi}_1^0$
4L [22]	Higgsino GGM
Compressed [20]	Wino $\tilde{\chi}_1^{\pm}\tilde{\chi}_2^0$ via WZ, higgsino $\tilde{\chi}_1^{\pm}\tilde{\chi}_2^0\tilde{\chi}_1^0$
Disappearing-track [27]	Wino $\tilde{\chi}_1^{+}\tilde{\chi}_1^{-}$ and $\tilde{\chi}_1^{\pm}\tilde{\chi}_1^0$

Table 5. List of ATLAS electroweak SUSY analyses considered in this analysis, and the relevant original simplified models targeted by them.

- For the disappearing-track analysis the upper limits on production cross-sections are used to determine exclusion. This is justified in this case since the disappearing-track analysis acceptance is largely determined by the $\tilde{\chi}_1^{\pm}$ mass and lifetime, and not by other model parameters such as $\tan\beta$ or μ. Only direct $\tilde{\chi}_1^{\pm}$ and $\tilde{\chi}_1^0$ production is considered, i.e., production through decay of heavier states is ignored, leading to slightly conservative limits. A linear interpolation between the available upper limits is used to determine the appropriate limit for each pMSSM model. To ensure a reliable result, only models with chargino mass and lifetime within the ranges for which limits are available are considered. If the total production cross-section for a model, $\sigma(\tilde{\chi}_1^{\pm}\tilde{\chi}_1^0)+\sigma(\tilde{\chi}_1^{+}\tilde{\chi}_1^{-})$, is greater than the corresponding limit then the model is considered excluded.

In addition to the ATLAS SUSY searches shown in table 5, two additional constraints related to measurements of the Higgs boson are applied when assessing the ATLAS Run 2 constraints on the pMSSM models. The first is the most recent combined upper limit on the branching ratio of the Higgs boson into invisible particles of $\mathcal{B}(h \to \text{inv}) < 0.107$ [83]. Models where Higgs boson decays into SUSY particles would increase this value above this limit are considered excluded. The second constraint applied is the ATLAS combined constraint on the CP-odd Higgs boson mass in the MSSM from Higgs boson cross-sections and branching fractions [84], which is $m(A) > 480\,\text{GeV}$. This $m(A)$ bound is approximate, particularly at high $\tan\beta$ where additional SUSY corrections will contribute in the pMSSM. However, these corrections are suppressed by μ/M_{SUSY} where M_{SUSY} is the SUSY scale. In the scans presented here, μ is much smaller than M_{SUSY} such that these corrections are expected to be small.

3 Results

This section summarises the constraints from the ATLAS searches for electroweak SUSY on the pMSSM models selected by the scans described in section 2.2. To determine whether a model is excluded, the analysis with the best (i.e. smallest) expected $\mathrm{CL_s}$ of the analyses in table 5 is used. If the observed $\mathrm{CL_s}$ for that analysis is less than 0.05, the model is considered to be excluded. Statistical combinations of analyses are not performed in this study so these results provide a conservative estimate of the ATLAS constraints. As outlined in section 2.3, models with $\mathcal{B}(h \to \mathrm{inv}) \geq 0.107$ or $m(A) \leq 480\,\mathrm{GeV}$ are also considered to be excluded by ATLAS.

Throughout this section, results are presented as projections of the pMSSM models in one or two dimensions. For the one-dimensional plots the number of models satisfying different model selection criteria is presented as a function of a single pMSSM parameter or observable, along with the fraction of 'all considered models' satisfying that selection. Throughout this section 'all considered models' is the total number of models generated in each scan that satisfy the LEP chargino and LHC Higgs boson mass constraints discussed in section 2.2 (constituting 12 280 and 8 897 models for the EWKino and BinoDM scans respectively as shown in table 4). The BinoDM scan also includes the relic density requirement. The two-dimensional plots are presented in terms of the fraction of models excluded by the ATLAS Run 2 constraints described in section 2.3 in a given bin. When calculating fractional exclusion plots three sets of model selections are considered: plots labelled 'all considered models' correspond to the selection described above, plots labelled 'all non-DM constraints' include only the subset of these models that satisfy the flavour and electroweak precision measurements in table 2 and those labelled 'all external constraints' include the further subset that also satisfy the DM constraints in table 2. For the BinoDM scan the relic density requirement is applied in the initial model selection stage, meaning that the only difference between the models selected with 'all non-DM constraints' and 'all external constraints' is the application of the direct detection constraints on the spin-dependent and spin-independent cross-sections.

3.1 Constraints on the LSP mass

Figure 4 shows one-dimensional distributions of the LSP mass for models selected by the EWKino and BinoDM scans, with the fraction of models excluded in each bin being indicated by the lower panels. Figure 4(a) shows all of the EWKino scan models before and after applying the ATLAS Run 2 constraints, separated by LSP type. Figure 4(b) shows the distribution of all EWKino scan models, the distribution after non-DM external constraints are applied and finally the distribution after non-DM external constraints and the ATLAS Run 2 constraints are applied. The impact of the ATLAS constraints on the EWKino scan is most significant at lower LSP mass. Figure 4(a) shows that almost all of the models with an LSP mass below 100 GeV are bino-like LSP models, due to the LEP chargino constraint, and around 50% of these models are excluded by ATLAS. Though not shown here, these low mass bino-LSP models are also disfavoured by the DM relic density constraint — the complementarity between the ATLAS results and the DM external constraints is discussed separately in section 3.3. For an LSP mass less than 400 GeV, the ATLAS Run 2 searches exclude more than 50% of the wino LSP models in each bin, which is driven by the disappearing-track analysis. The ATLAS Run 2 exclusion fractions for both bino- and higgsino-like LSPs in the EWKino scan is less than about 20% for LSP masses above 200 GeV.

Figures 4(c) and 4(d) show the one-dimensional distribution of the LSP mass for the models in the BinoDM scan. The distribution is shown considering only the ATLAS Run 2

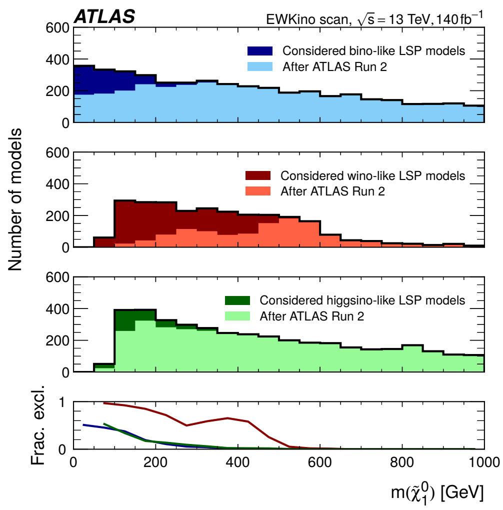

(a) EWKino scan.

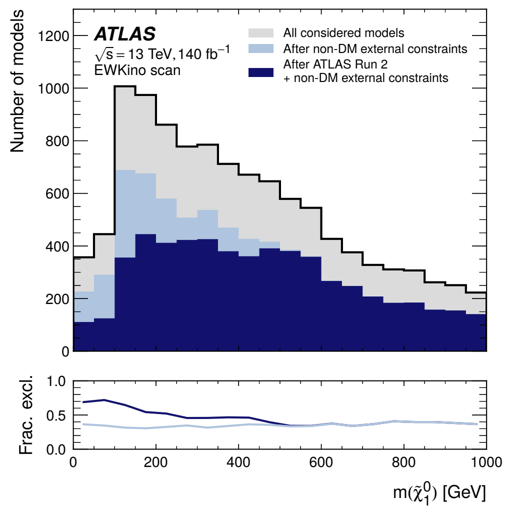

(b) EWKino scan.

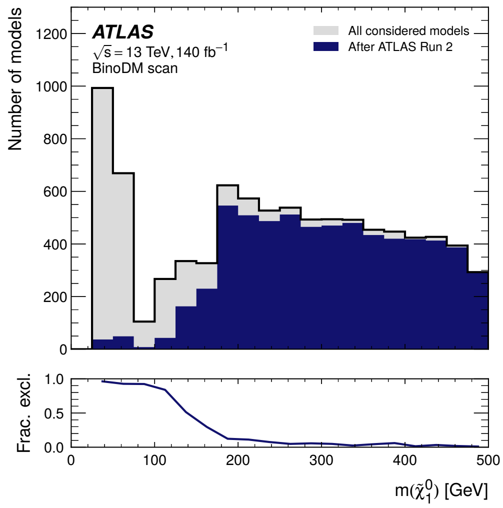

(c) BinoDM scan.

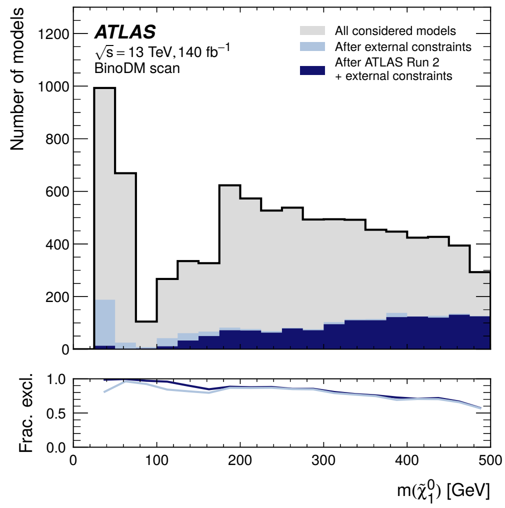

(d) BinoDM scan.

Figure 4. Distributions of the LSP mass. (a) The distribution of all considered EWKino scan models before and after the ATLAS Run 2 constraints are applied, split by the dominant component (bino, wino or higgsino) of the LSP. (b) The distribution of all considered EWKino scan models, the remaining models after non-DM external constraints are applied and the remaining models after non-DM external constraints and the ATLAS Run 2 constraints are applied. (c) The distribution of all considered BinoDM scan models before and after the ATLAS Run 2 constraints are applied. (d) The distribution of all considered BinoDM scan models, the remaining models after all the external constraints are applied and the remaining models after all external constraints and the ATLAS Run 2 constraints are applied. The lower panels show the fraction of models excluded in each case.

constraints and when also applying the external constraints. A bino-like LSP with a mass below 100 GeV is almost entirely excluded in the BinoDM scan by the ATLAS constraints, particularly when also considering external constraints. This is discussed further in the next section.

JHEP05(2024)106

3.2 Constraints on electroweakino masses and branching ratios

For the EWKino scan, figure 5 shows the fraction of models excluded by the ATLAS Run 2 electroweak searches in the $m(\tilde{\chi}_1^\pm)$–$m(\tilde{\chi}_1^0)$ and $m(\tilde{\chi}_2^0)$–$m(\tilde{\chi}_1^0)$ planes. The plots are overlaid with a contour indicating the exclusion for relevant simplified models. Assuming wino-like $\tilde{\chi}_2^0\tilde{\chi}_1^\pm$ and $\tilde{\chi}_1^\pm\tilde{\chi}_1^\pm$ production with a bino-like LSP, $\mathcal{B}(\tilde{\chi}_2^0 \to Z\tilde{\chi}_1^0) = 100\%$ and $\mathcal{B}(\tilde{\chi}_1^\pm \to W^\pm\tilde{\chi}_1^0) = 100\%$, this contour is calculated as the envelope of the exclusion contours of the 3L [23], 2L2J [25] and FullHad [24] analyses, which have complementary sensitivity for different sparticle masses. Before considering the external constraints, most of the excluded models are inside the simplified model contours, but only at very low sparticle masses does the exclusion approach 100%. For the $m(\tilde{\chi}_1^\pm)$–$m(\tilde{\chi}_1^0)$ plane, most of the models inside the contour are removed by the external constraints, primarily due to the relic density requirement suppressing most models with a bino LSP, with most of the remaining models lying along the diagonal line with small mass splittings between the lightest chargino and the LSP. The ATLAS Run 2 searches exclude at least 50% of the models, even outside the simplified model contour, up to a chargino mass around 400 GeV. For the $m(\tilde{\chi}_2^0)$–$m(\tilde{\chi}_1^0)$ plane, the region away from the compressed region still contains many models after the external constraints are applied, and there is a large region outside the simplified model contour with $m(\tilde{\chi}_2^0) > 1\,100$ GeV where the ATLAS Run 2 results exclude all of the models. These are driven by models with a wino-like $\tilde{\chi}_1^0$ and $\tilde{\chi}_1^\pm$ and a bino- or higgsino-like $\tilde{\chi}_2^0$ with a large mass splitting, where the disappearing-track analysis provides sensitivity to the compressed $\tilde{\chi}_1^0$ and $\tilde{\chi}_1^\pm$.

The same plots are shown for the BinoDM scan in figure 6. As the relic density requirement is applied to all models in this scan, there are fewer models inside the simplified model contour. The Z/h funnel regions are visible in all plots and strongly constrained by the ATLAS results. A region of 100% exclusion is observed between the funnel and compressed regions in figures 5(a) and 5(b). These are mostly models in the A-funnel region that are excluded by the ATLAS constraint $m(A) > 480$ GeV. This region is absent in figures 5(c)–5(f) due to the $\mathcal{B}(b \to s\gamma)$ external constraint that is impacted by loop contributions involving A. Similar to the EWKino scan, there are models with compressed spectra, i.e., $m(\tilde{\chi}_2^0)$ or $m(\tilde{\chi}_1^\pm) \approx m(\tilde{\chi}_1^0)$ where the ATLAS results exclude a significant fraction of the models. This illustrates the complementarity of the ATLAS searches and external constraints. To demonstrate the progress of the ATLAS Run 2 search programme relative to Run 1, figures 5(e) and 6(e) can be compared with figure 2(a) of the Run 1 electroweak reinterpretation paper [32] that reported fractional exclusion in the $m(\tilde{\chi}_1^\pm)$–$m(\tilde{\chi}_1^0)$ plane by the ATLAS searches for models selected using a profile-likelihood scan using external constraints. The distribution of models seen here is similar to those in the Run 1 analysis, however the ATLAS exclusion in the funnel region extends to higher chargino masses (the region with $\approx 100\%$ exclusion is O(100) GeV higher using the Run 2 constraints) and there is now sensitivity to the compressed region at lower masses due to the compressed and disappearing-track analyses.

Figures 5 and 6 illustrate that once external constraints are applied, many of the surviving models have compressed mass spectra. Figure 7 shows the fractions of models excluded in the $\Delta m(\tilde{\chi}_1^\pm, \tilde{\chi}_1^0) = m(\tilde{\chi}_1^\pm) - m(\tilde{\chi}_1^0)$ versus $m(\tilde{\chi}_1^\pm)$ plane once non-DM external constraints are applied. For both scans the ATLAS results have sensitivity to low chargino masses. For the EWKino scan (left plot), the highest exclusion for low chargino masses occurs for

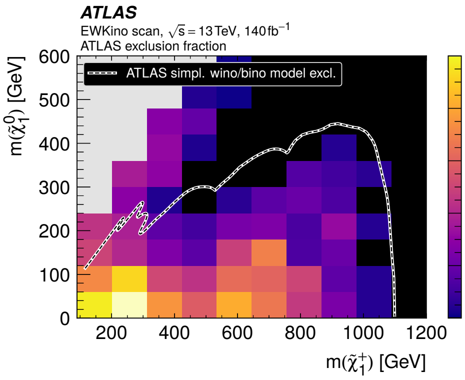

(a) All considered models.

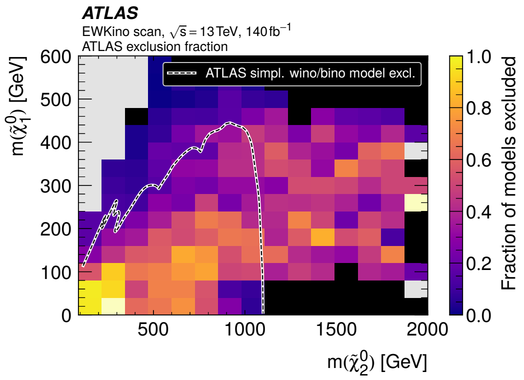

(b) All considered models.

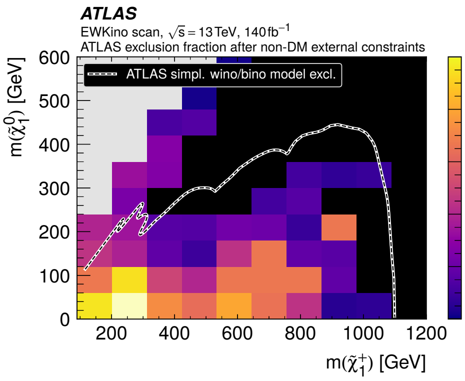

(c) Models satisfying non-DM external constraints.

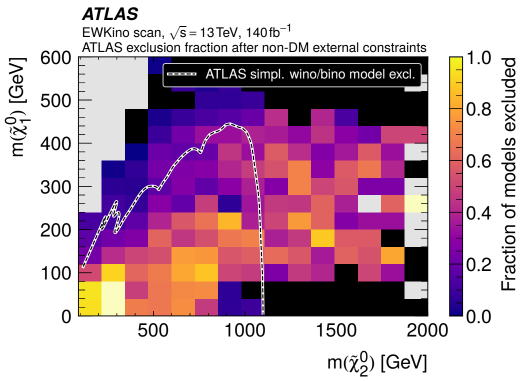

(d) Models satisfying non-DM external constraints.

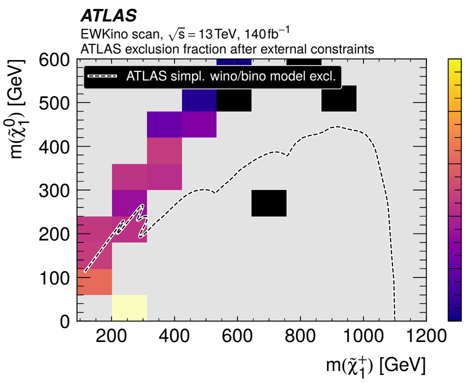

(e) Models satisfying all external constraints.

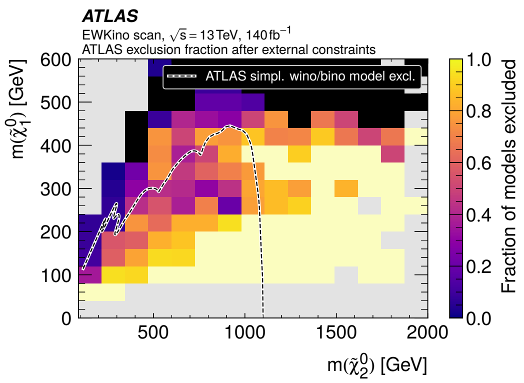

(f) Models satisfying all external constraints.

Figure 5. The fraction of EWKino scan models excluded by ATLAS Run 2 results. The first column shows the $m(\tilde{\chi}_1^\pm)$–$m(\tilde{\chi}_1^0)$ plane and the second column the $m(\tilde{\chi}_2^0)$–$m(\tilde{\chi}_1^0)$ plane. The first row includes all considered models, the second includes models that satisfy the non-DM external constraints and the third row models that satisfy all external constraints. The overlaid dashed line shows the envelope of the 3L [23], 2L2J [25] and FullHad [24] exclusion of a wino $\tilde{\chi}_1^\pm/\tilde{\chi}_2^0$ simplified model with $\mathcal{B}(\tilde{\chi}_2^0 \to Z\tilde{\chi}_1^0) = 100\%$ and $\mathcal{B}(\tilde{\chi}_1^\pm \to W^\pm\tilde{\chi}_1^0) = 100\%$. Bins in grey have no models to consider, while for bins in cream (black) all models are (not) excluded.

JHEP05(2024)106

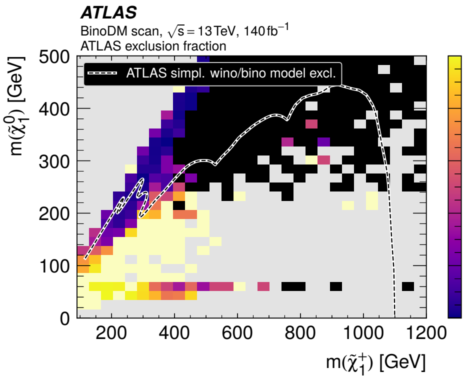

(a) All considered models.

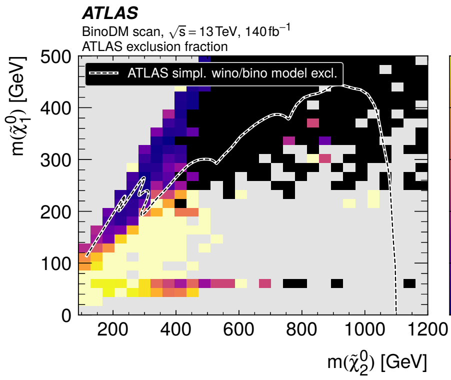

(b) All considered models.

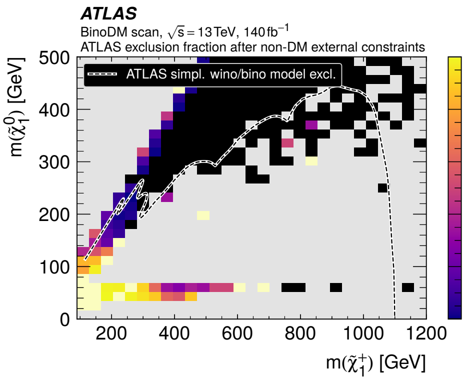

(c) Models satisfying non-DM external constraints.

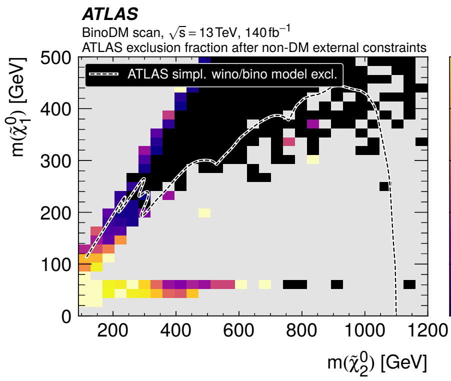

(d) Models satisfying non-DM external constraints.

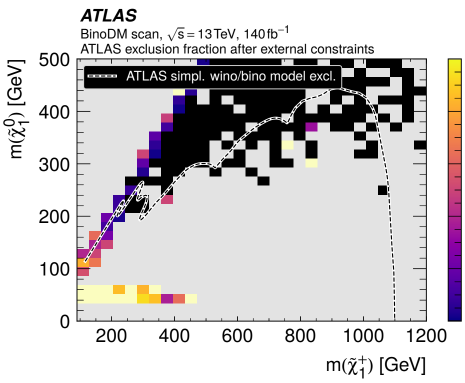

(e) Models satisfying all external constraints.

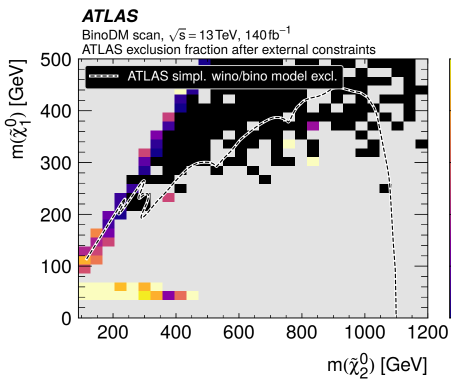

(f) Models satisfying all external constraints.

Figure 6. Fraction of BinoDM scan models excluded by the ATLAS Run 2 results. The first column shows the $m(\tilde{\chi}_1^\pm)$–$m(\tilde{\chi}_1^0)$ plane and the second column the $m(\tilde{\chi}_2^0)$–$m(\tilde{\chi}_1^0)$ plane. The first row includes all considered models, the second includes models that satisfy the non-DM external constraints and the third row models that satisfy all external constraints. The overlaid dashed line shows the envelope of the 3L [23], 2L2J [25] and FullHad [24] exclusion of a wino $\tilde{\chi}_1^\pm/\tilde{\chi}_2^0$ simplified model with $\mathcal{B}(\tilde{\chi}_2^0 \to Z\tilde{\chi}_1^0) = 100\%$ and $\mathcal{B}(\tilde{\chi}_1^\pm \to W^\pm\tilde{\chi}_1^0) = 100\%$. Bins in grey have no models to consider, while for bins in cream (black) all models are (not) excluded.

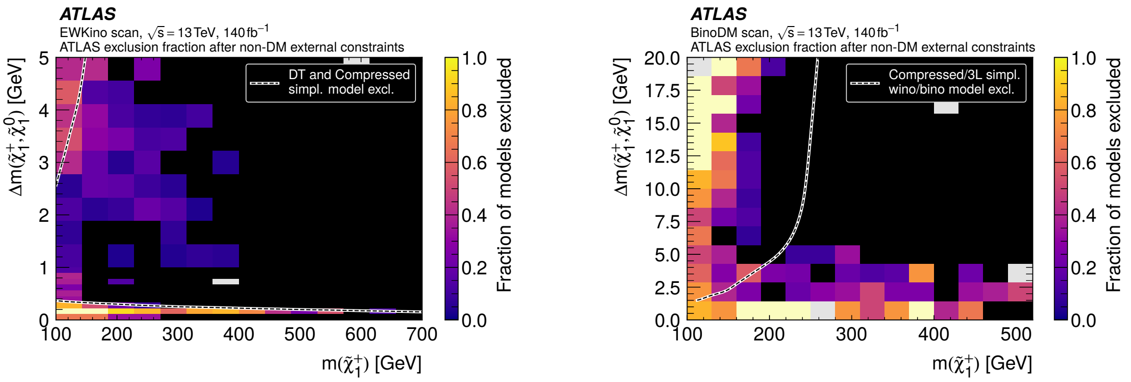

(a) EWKino scan ($\Delta m(\tilde{\chi}_1^\pm, \tilde{\chi}_1^0) < 5\,\text{GeV}$). (b) BinoDM scan ($\Delta m(\tilde{\chi}_1^\pm, \tilde{\chi}_1^0) < 20\,\text{GeV}$).

Figure 7. Fraction of EWKino (left) and BinoDM (right) scan models excluded in the $m(\tilde{\chi}_1^\pm)$–$\Delta m(\tilde{\chi}_1^\pm, \tilde{\chi}_1^0)$ plane. Only models satisfying the non-DM external constraints are included. (a) is overlaid with the disappearing-track [27] and compressed [20] exclusion of a higgsino simplified model. (b) is overlaid with the envelope of the compressed [20] and 3L [23] exclusion of a wino/bino $\tilde{\chi}_1^\pm \tilde{\chi}_2^0 \to WZ\tilde{\chi}_1^0\tilde{\chi}_1^0$ simplified model. Bins in grey have no models to consider, while for bins in cream (black) all models are (not) excluded.

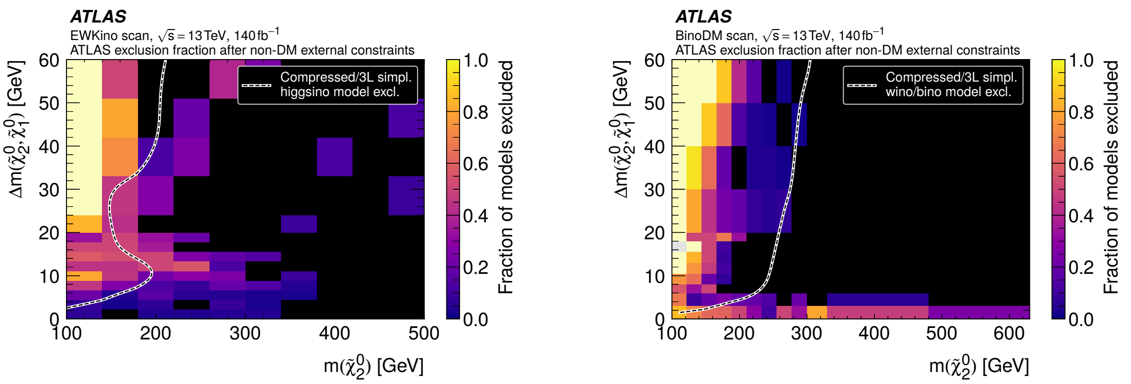

(a) EWKino scan. (b) BinoDM scan.

Figure 8. Fraction of EWKino (left) and BinoDM (right) scan models excluded in the $m(\tilde{\chi}_2^0)$–$\Delta m(\tilde{\chi}_2^0, \tilde{\chi}_1^0)$ plane. Only models satisfying the non-DM external constraints are included. The overlaid dashed lines show the envelope of the compressed [20] and 3L [23] exclusion of relevant higgsino or wino/bino $\tilde{\chi}_1^\pm \tilde{\chi}_2^0 \to WZ\tilde{\chi}_1^0\tilde{\chi}_1^0$ simplified models. Bins in grey have no models to consider, while for bins in cream (black) all models are (not) excluded.

$\Delta m(\tilde{\chi}_1^\pm, \tilde{\chi}_1^0) \approx 0.1$–$0.2\,\text{GeV}$, which is consistent with the O(160 MeV) mass splittings expected for pure wino scenarios that the disappearing-track analysis is optimised for [27]. For the BinoDM scan (right plot), at chargino masses less than 400 GeV the lowest $\Delta m(\tilde{\chi}_1^\pm, \tilde{\chi}_1^0)$ bins show exclusion fractions greater than 0.8. This can be attributed both to the disappearing-track analysis and to production mechanisms involving higher mass electroweakinos such as $\tilde{\chi}_2^\pm$ and $\tilde{\chi}_4^0$. A similar effect is seen in figure 8 that shows the fractions of models excluded for each scan in the $m(\tilde{\chi}_2^0)$–$\Delta m(\tilde{\chi}_2^0, \tilde{\chi}_1^0)$ plane. In general, many bins within the simplified

JHEP05(2024)106

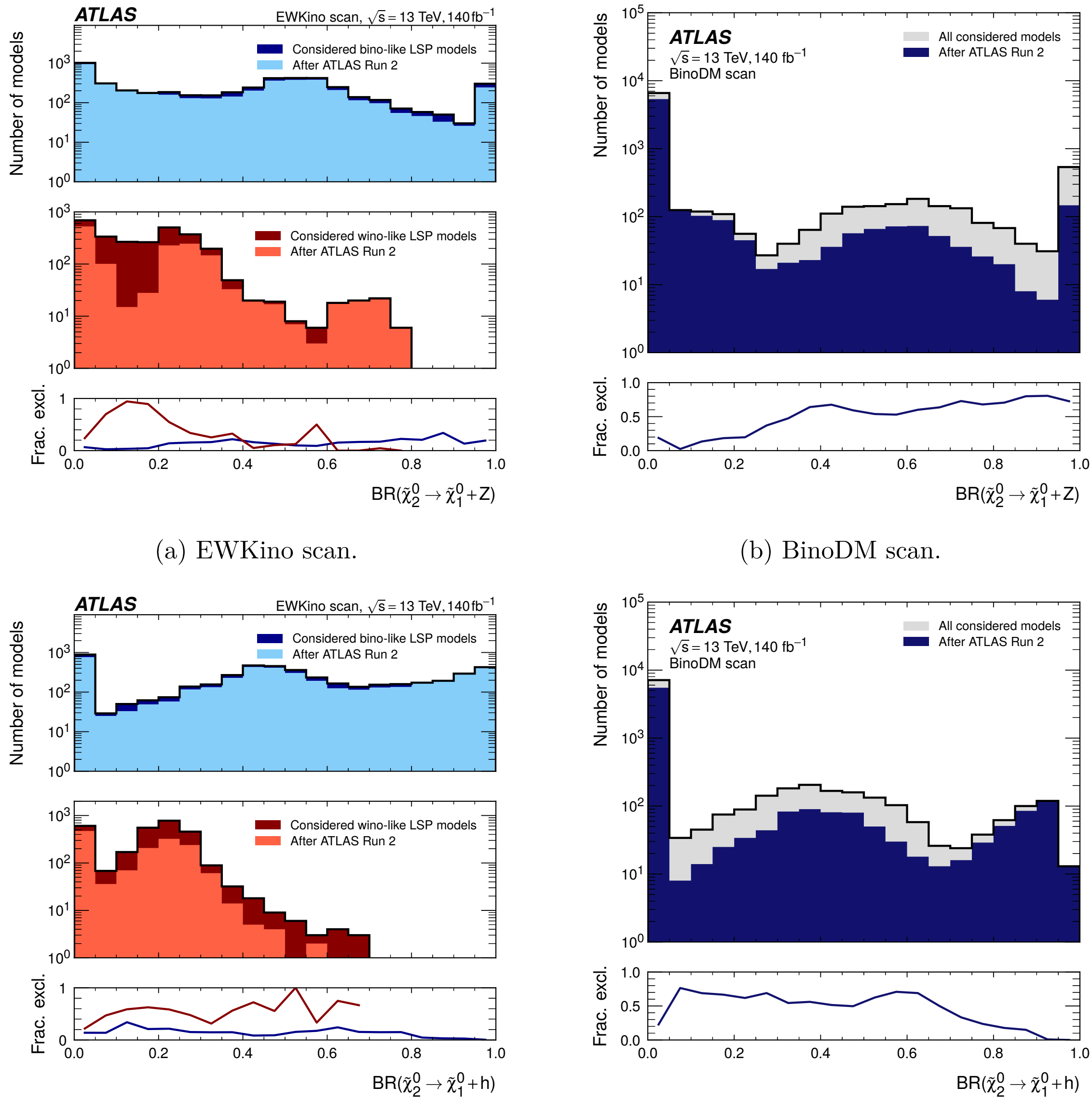

(a) EWKino scan.

(b) BinoDM scan.

(c) EWKino scan.

(d) BinoDM scan.

Figure 9. Distributions of (first row) $\mathcal{B}(\tilde{\chi}_2^0 \to \tilde{\chi}_1^0 Z)$ and (second row) $\mathcal{B}(\tilde{\chi}_2^0 \to \tilde{\chi}_1^0 h)$. The first column shows models in the EWKino scan split by LSP type and the second column models in the BinoDM scan. The distributions show all considered models before and after the ATLAS Run 2 constraints are applied. The lower panels show the fraction of models excluded in each case.

model contours in all the two-dimensional plots show less than 100% exclusion. This is mostly due to the pMSSM models having smaller branching fractions and cross-sections than the simplified models.

Simplified models used in SUSY searches typically assume fixed branching ratios into particular final states (often 100%), however in general these vary as a function of the pMSSM parameters. Figure 9 shows one-dimensional distributions of $\mathcal{B}(\tilde{\chi}_2^0 \to \tilde{\chi}_1^0 Z)$ and $\mathcal{B}(\tilde{\chi}_2^0 \to \tilde{\chi}_1^0 h)$ for both scans before and after applying the ATLAS Run 2 constraints (no external constraints are considerered here). These quantities are branching fractions for two-body decays via on-shell Z and h bosons, therefore the large peaks at zero in these distributions contain models with $\Delta m(\tilde{\chi}_2^0, \tilde{\chi}_1^0) < m(Z/h)$ such that the three-body off-shell decay modes dominate. For the EWKino scan, figures 9(a) and 9(c) are split by LSP type as the distribution and ATLAS sensitivity is distinct for each. These on-shell decay modes are not relevant to models with a higgsino-like LSP, so these are not shown. For models with a bino-like LSP in both the EWKino and BinoDM scan, the highest exclusion by the ATLAS results occurs for large values of $\mathcal{B}(\tilde{\chi}_2^0 \to \tilde{\chi}_1^0 Z)$, as expected due to the large number of searches optimised for simplified models with $\mathcal{B}(\tilde{\chi}_2^0 \to \tilde{\chi}_1^0 Z) = 100\%$ whilst only the 1Lbb search directly targets the $\tilde{\chi}_2^0 \to \tilde{\chi}_1^0 h$ decay for low mass $\tilde{\chi}_2^0$. For models with a wino-like LSP, the largest exclusion occurs when $\mathcal{B}(\tilde{\chi}_2^0 \to \tilde{\chi}_1^0 Z) \approx 15\%$ and larger $\mathcal{B}(\tilde{\chi}_2^0 \to \tilde{\chi}_1^0 h)$. These branching ratios are impacted by the mass splittings between the $\tilde{\chi}_2^0$ and $\tilde{\chi}_1^0$, which also affects the lifetime of the $\tilde{\chi}_1^\pm$. This peak in exclusion corresponds to models with a chargino lifetime of around 0.1ns that aligns with the region of sensitivity of the disappearing-track analysis.

3.3 Dark matter phenomenology

This section assesses the impact of the searches on models with particular DM annihilation phenomenology and investigates the complementarity between collider and non-collider searches for DM by considering the relic density Ωh^2 and DM-nucleon scattering cross-sections. Most direct DM detection experiments target DM scattering on nucleons. Currently, the most stringent limit on the spin-independent WIMP-nucleon scattering cross-section comes from the LUX-ZEPLIN (LZ) experiment [65] whilst the most stringent constraint on the spin-dependent WIMP-proton scattering cross-section comes from the PICO-60 experiment [66]. The impact of these limits on the models considered here is weakened by the scaling of the cross-sections by $(\Omega h^2/0.12)$ to account for lower than measured DM relic density as explained in section 2.1.

Figure 10 shows the fraction of BinoDM models excluded by the ATLAS Run 2 results in the $m(\tilde{\chi}_1^0)$–Ωh^2 plane for all considered models satisfying the non-DM external constraints and for models satisfying all external constraints. The results from the direct detection searches strongly constrain the funnel regions, and once the ATLAS Run 2 results are applied only a few models remain viable in the funnel regions. The ATLAS constraints at higher LSP masses are weaker.

To further illustrate the complementarity between the collider and non-collider results for a bino-like LSP, figure 11 shows the fraction of models in the BinoDM scan (that satisfy all non-DM external constraints) that are excluded by the ATLAS Run 2 results as function of LSP mass and WIMP-nucleon spin-independent/dependent scattering cross-sections. The ATLAS searches are observed to have a high sensitivity in regions where the direct-detection searches are insensitive and vice-versa, demonstrating the complementarity. Additionally, figure 12 shows scatter plots of Ωh^2 versus $m(\tilde{\chi}_1^0)$ with different constraints applied to the model set and each model point coloured by the dominant LSP-annihilation mechanism. The Z/h funnel regions are almost entirely excluded when considering both ATLAS Run 2 and external constraints, as are most models up to $m(\tilde{\chi}_1^0) \approx 200\,\text{GeV}$. Most models with $\tilde{\chi}_1^\pm/\tilde{\chi}_2^0$ co-annihilation as the dominant mode are still viable.

JHEP05(2024)106

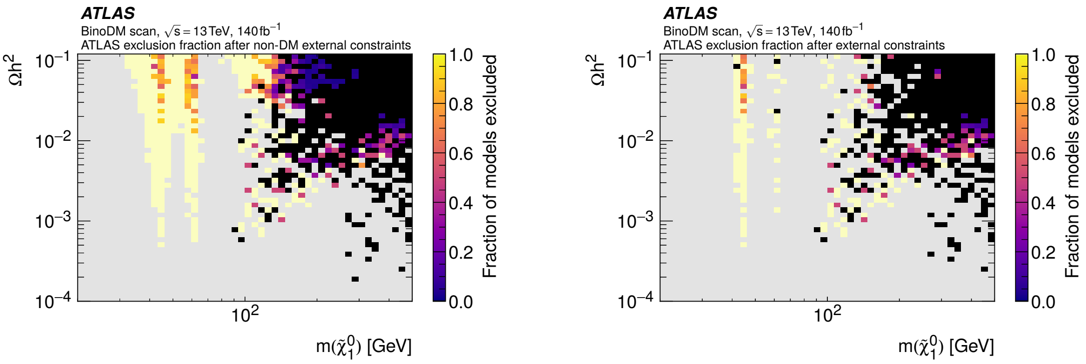

(a) Models satisfying all non-DM constraints.

(b) Models satisfying all external constraints.

Figure 10. Exclusion of models from the BinoDM scan in the $m(\tilde{\chi}_1^0)$–Ωh^2 plane with (a) all non-DM constraints applied and (b) all external constraints applied. Bins in grey have no models to consider, while for bins in cream (black) all models are (not) excluded.

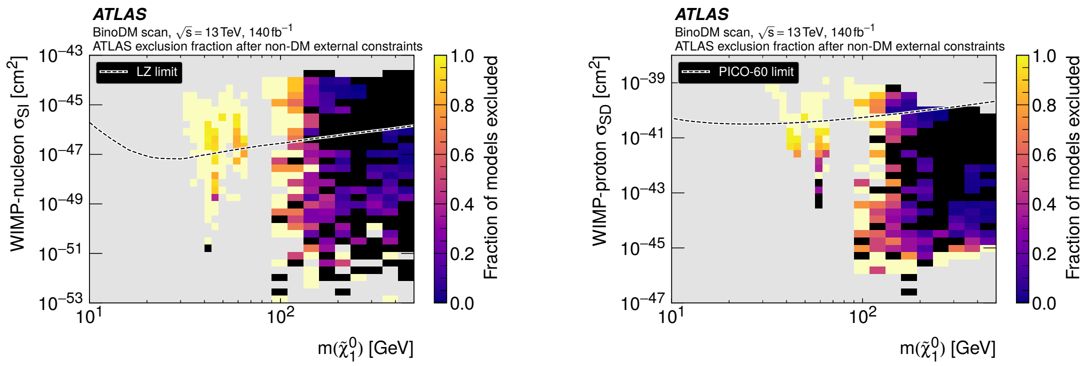

(a)

(b)

Figure 11. The fraction of models excluded by the ATLAS Run 2 searches from the BinoDM scan in (a) the WIMP-nucleon spin-independent scattering cross-section $\sigma_{\rm SI}$ versus $m(\tilde{\chi}_1^0)$ plane and (b) the WIMP-proton spin-dependent scattering cross-section $\sigma_{\rm SD}$ versus $m(\tilde{\chi}_1^0)$ plane. The pMSSM model cross-sections are scaled by $\Omega h^2/0.12$ to provide a fair comparison with the LZ [65] and PICO-60 [66] upper limit contours shown as dashed lines on the two plots, respectively. Only models that satisfy the non-DM external constraints are included. Bins in grey have no models to consider, while for bins in cream (black) all models are (not) excluded.

Finally, figure 13 illustrates the complementarity between the DM constraints and the ATLAS Run 2 constraints for the EWKino scan. One dimensional distributions of the DM relic density, the WIMP-nucleon spin-independent scattering cross-section and the WIMP-proton spin-dependent scattering cross-section are presented for models selected by the EWKino scan. For the DM relic density the distributions are presented before and after applying the ATLAS Run 2 constraints and for the scattering cross-sections one-dimensional distributions are presented after applying the relevant direct detection constraint (LZ for the spin-independent cross-section and PICO-60 for the spin-dependent cross-section), and after applying both the

JHEP05(2024)106

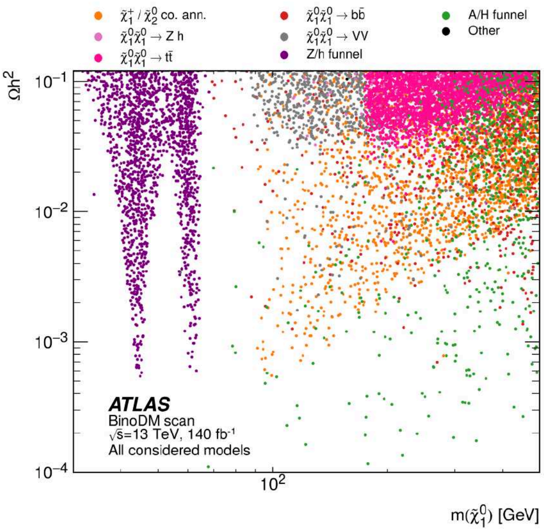

(a) All considered models.

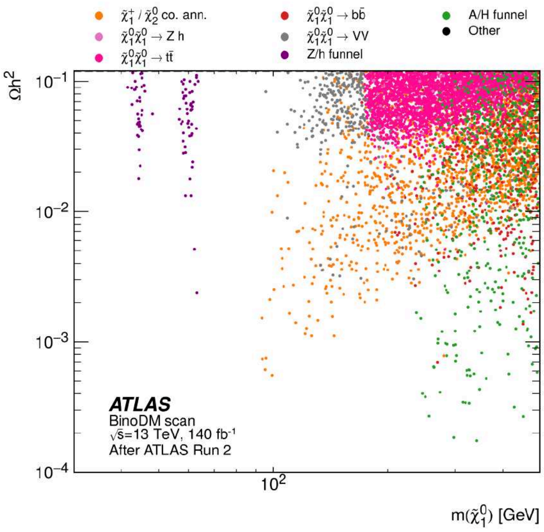

(b) Models not excluded by ATLAS.

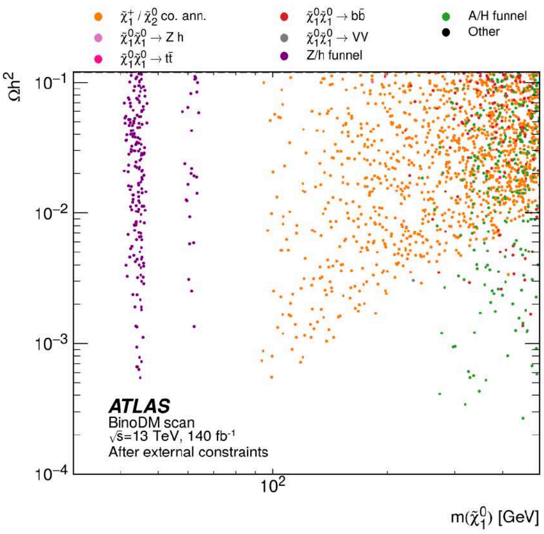

(c) Models not excluded by external constraints.

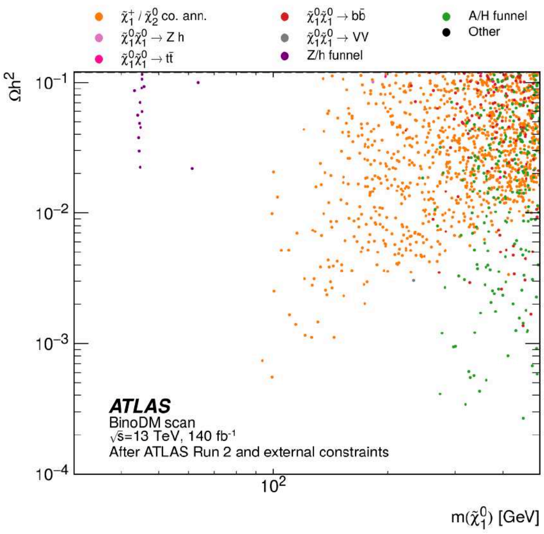

(d) Models not excluded by ATLAS or external constraints.

Figure 12. Scatter plots of models from the BinoDM scan in the $m(\tilde{\chi}_1^0)$–Ωh^2 plane, coloured by the dominant annihilation mechanism for the corresponding model. The plot is shown for all considered models, after ATLAS Run 2 constraints, after external constraints, and after both ATLAS Run 2 and external constraints.

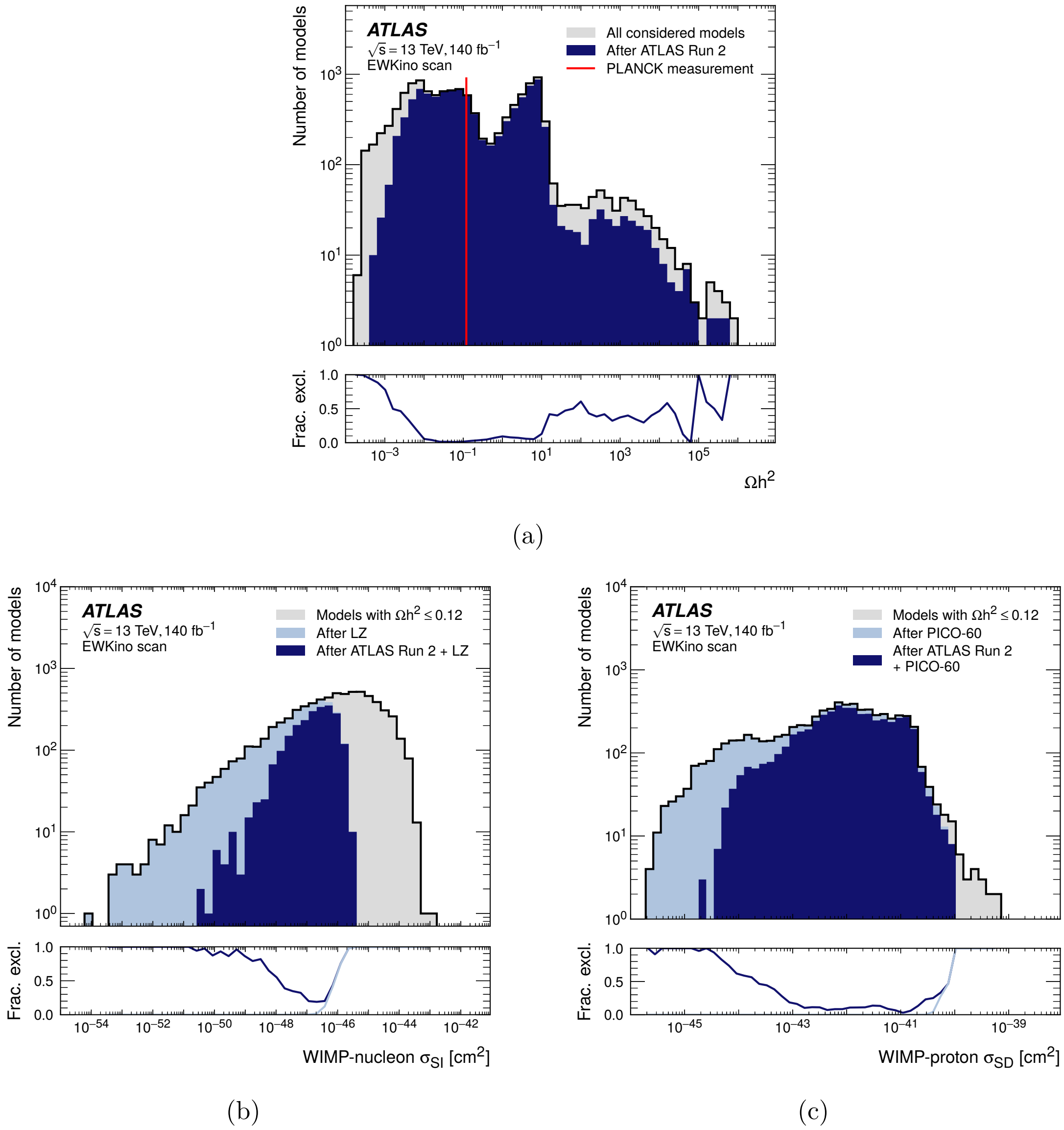

Figure 13. One-dimensional distributions of (a) the DM relic density, (b) the WIMP-nucleon spin-independent scattering cross-section and (c) the WIMP-proton spin-dependent scattering cross-section, for the EWKino scan. For (a) the distribution is shown before and after applying the ATLAS Run 2 constraints (with no additional constraints applied) with the measured relic density marked by the vertical line. The distributions in (b) and (c) are presented for all considered models that satisfy the DM relic density constraint, after applying the relevant direct detection constraint (LZ for the spin-independent cross-section and PICO-60 for the spin-dependent cross-section), and after applying both the relevant direct detection constraint and the ATLAS Run 2 constraints (with no additional external constraints applied). The pMSSM model cross-sections are scaled by $\Omega h^2/0.12$ to provide a fair comparison with the direct detection experiment limits.

direct detection constraint and the ATLAS Run 2 constraints (with no additional external constraints applied). This again demonstrates the complementarity between direct detection experiments and ATLAS searches, as ATLAS provides good exclusion of low cross-section scenarios that lie well below the LZ and PICO-60 limits.

3.4 Complementarity and overlap between ATLAS Run 2 results and external constraints

In assessing the exclusion, the $\mathrm{CL_s}$ value is taken from the ATLAS analysis with the best expected sensitivity, however for many models multiple analyses would have the required sensitivity to claim exclusion. The overlap in sensitivity between the analyses and constraints is displayed in figure 14. For the diagonal entries, the number in bold shows the percentage of all considered models excluded by that search/constraint. For the off-diagonal entries the number in each box indicates the percentage of the models excluded by the analysis/constraint in that row that were also excluded by the analysis/constraint on the column label. In general, the 2L2J and 3L searches have high overlaps with all searches except the disappearing-track search for both the EWKino and BinoDM scans, due to their abilities to probe both associated chargino-neutralino production with gauge boson-mediated decays as well as leptonic final states produced in cascade decays involving heavier electroweakinos.

The ATLAS searches exclude 100% and 99% of the models excluded by the ATLAS $\mathcal{B}(h \to \mathrm{inv})$ constraint in the EWKino and BinoDM scans respectively. This is because models with high $\mathcal{B}(h \to \mathrm{inv})$ lie in the Higgs-funnel region, which corresponds to mass ranges that the ATLAS searches considered are most sensitive to.

When examining the overlaps between the ATLAS searches and external constraints, the highest overlaps with the ATLAS searches come from the spin-independent cross-section measurement and relic density measurement for the EWKino scan, but the numbers are still relatively low (30% and 24% respectively). Alternatively, for the BinoDM scan the spin-independent cross-section measurement has a high overlap with all relevant searches and constraints.

Finally, table 6 contains a summary of the percentage of models excluded for each LSP type, for each search and constraint individually and overall. The final row shows that over 77% of models for each LSP type and scan are excluded when considering both ATLAS Run 2 and external constraints. However as these fractions are calculated from the entire model set they depend on the priors (scan ranges and strategy) used. It is therefore more useful for planning future searches to consider the models that remain unexcluded with low-mass electroweakinos that are discussed in the next section. For the EWKino scan, of the different LSP types, wino-like LSPs have the highest ATLAS Run 2 exclusion, which is almost entirely driven by the disappearing-track analysis. For the BinoDM scan, the largest individual exclusion comes from the 2L2J and 3L analyses, which, as mentioned above, have degrees of overlap. The external constraints have a large impact on both bino LSP models in the EWKino scan and the BinoDM scan, which is mainly driven by the DM constraints. The non-DM external constraints (flavour and precision electroweak) have a similar impact across the LSP types and scans, though flavour constraints have a weaker impact on models with a higgsino-like LSP.

JHEP05(2024)106

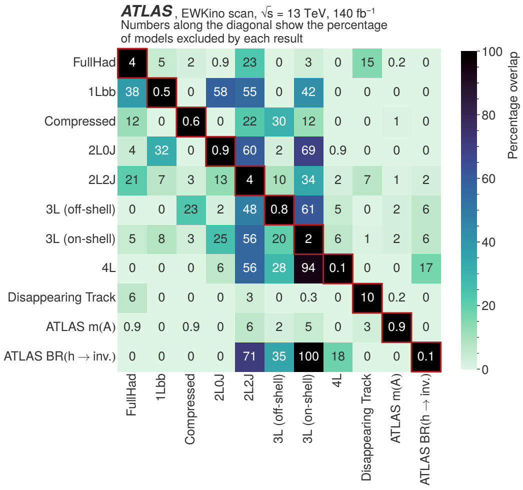

(a) EWKino scan: overlaps between searches.

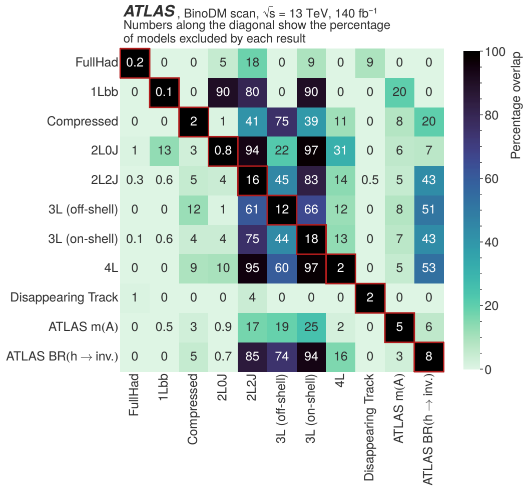

(b) BinoDM scan: overlaps between searches.

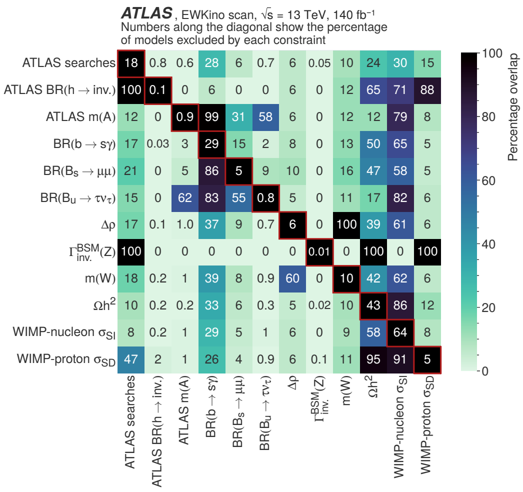

(c) EWKino scan: overlaps between external constraints.

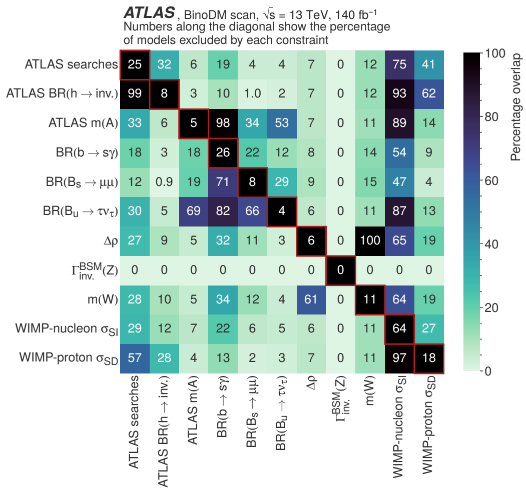

(d) BinoDM scan: overlaps between external constraints.

Figure 14. Percentage overlaps in the models excluded by each search and constraint. For the diagonal entries, the number shows the percentage of all considered models excluded by that search/constraint. For each off-diagonal square, the number and bin colour indicates the percentage of the models excluded by the result on the y axis that were also excluded by the result on the x axis, i.e. $100 \times N_{xy}/N_y$ where N_{xy} is the number of models excluded by the results on the x and y axes and N_y is the number of models excluded by the result on the y axis. The figures in (a) and (b) show the overlap of each search, while (c) and (d) show the overlap of each constraint. Figure (a) and (c) show the EWKino scan, while (b) and (d) are for the BinoDM scan. Where no models are excluded, the overlap is shown as zero.

JHEP05(2024)106

Search	EWKino scan LSP type			BinoDM
	Bino-like	Higgsino-like	Wino-like	scan
FullHad	5.3%	2.6%	3.0%	0.2%
1Lbb	1.2%	0.0%	0.0%	0.1%
Compressed	0.2%	1.4%	0.0%	1.9%
2L0J	2.2%	0.0%	0.0%	0.8%
2L2J	5.6%	2.9%	3.1%	15.9%
3L (off-shell)	1.4%	0.6%	0.0%	11.7%
3L (on-shell)	4.7%	0.8%	1.2%	17.7%
4L	0.3%	0.1%	0.0%	2.4%
Disappearing-track	0.1%	0.1%	45.7%	1.9%
Overall ATLAS Run 2 SUSY searches	**11.2%**	**5.7%**	**48.5%**	**25.0%**
$m(A) > 480\,\text{GeV}$	0.4%	1.6%	0.4%	4.8%
$\mathcal{B}(h \to \text{inv.}) \leq 0.107$	0.4%	0.0%	0.0%	8.1%
Overall ATLAS Run 2	**11.6%**	**7.2%**	**48.7%**	**28.3%**
Flavour constraints	33.8%	22.8%	32.5%	28.8%
Electroweak precision constraints	9.7%	9.8%	9.7%	10.5%
Relic density constraint	96.0%	12.8%	0.3%	N/A
Direct detection constraints	83.8%	67.7%	24.4%	64.7%
All non-DM external constraints	39.3%	29.3%	37.8%	35.4%
All external constraints	98.8%	75.8%	54.0%	80.1%
Overall ATLAS Run 2 + non-DM external	**46.7%**	**33.9%**	**67.5%**	**53.4%**
Overall ATLAS Run 2 + external	**98.9%**	**77.3%**	**83.0%**	**84.1%**

Table 6. Percentage of models excluded by each search and constraint, for each LSP type.

Figure 15 provides a visual summary of the constraints by showing the fraction of models excluded by ATLAS as a function of the masses of each electroweakino for models satisfying all of the external constraints. For both the EWKino and BinoDM scans, the bar for the LSP shows predictable behaviour where the fraction of models excluded decreases with increasing LSP mass. A similar trend is observed for all electroweakinos in the BinoDM scan. For the EWKino scan, there is an interesting effect for the $\tilde{\chi}_2^0$ where models at higher mass show high exclusion fractions. This is partly driven by wino-like LSP models, where $\Delta m(\tilde{\chi}_1^\pm, \tilde{\chi}_1^0)$ and the $\tilde{\chi}_1^\pm$ lifetime, and therefore the sensitivity of the disappearing-track analysis, are correlated with $m(\tilde{\chi}_2^0)$.

3.5 Viable pMSSM models surviving the ATLAS Run 2 constraints

One of the benefits of this study is understanding that pMSSM models have been missed by previous searches. This section presents six benchmark models with a bino-like or higgsino-like LSP that satisfy all the external constraints but are not excluded by the ATLAS Run 2 analyses considered. These have SUSY spectra that deviate from those typically encountered

JHEP05(2024)106

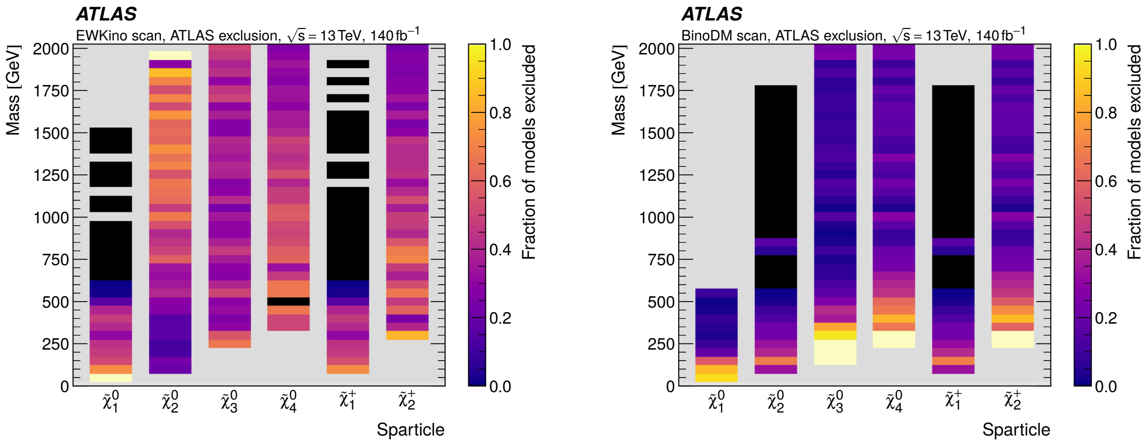

(a) EWKino scan.

(b) BinoDM scan.

Figure 15. Summary plots showing the fraction of models excluded by ATLAS across the masses of each electroweakino for models that satisfy external constraints. (a) shows the EWKino scan and (b) the BinoDM scan. Bins in grey have no models to consider, while for bins in cream (black) all models are (not) excluded.

in ATLAS simplified models, either through having different hierarchies between the bino, wino and higgsino mass parameters, mixed decay modes, or relatively light $\tilde{\chi}_3^0$, $\tilde{\chi}_2^\pm$ and $\tilde{\chi}_4^0$ that are not within the sensitivity of the FullHad or 2L2J searches. These can be used to optimise dedicated new searches for Run 3 of the LHC and beyond. Spectra are not presented here for wino-like LSPs as the main analysis targeting this scenario, the disappearing-track search, was applied as cross-section upper limits, meaning that the reason many wino-like models were not excluded is simply that they did not have a sufficiently large production cross-section.

Figure 16 shows the mass spectrum for four benchmark models with a bino-like LSP that satisfy all constraints and are not excluded by ATLAS Run 2 analyses. The $\tilde{\chi}_1^0$, $\tilde{\chi}_1^\pm$ and $\tilde{\chi}_2^0$ masses of all of these models lie within the published ATLAS simplified model contours for at least one of the SUSY searches considered in this analysis.

Figure 16(a) shows a model in the Z/h funnel region. This model differs from typical simplified models as the $\tilde{\chi}_1^\pm$ and $\tilde{\chi}_2^0$ higgsino fraction is greater than 98%. Additionally, this scenario has $\mathcal{B}(\tilde{\chi}_2^0 \to \tilde{\chi}_1^0 h) \approx \mathcal{B}(\tilde{\chi}_2^0 \to \tilde{\chi}_1^0 Z) \approx 50\%$. Scenarios such as this will therefore have smaller signal yields than typical simplified models due to the higgsino-like $\tilde{\chi}_1^\pm/\tilde{\chi}_2^0$ production cross-sections being smaller than for wino-like particles and the branching ratios to the typical $\tilde{\chi}_2^0$ decay modes being half the usual simplified model assumption of 100%.

Figure 16(b) shows a model with a wino-like $\tilde{\chi}_1^\pm$ and $\tilde{\chi}_2^0$ of similar mass with a 156 GeV mass splitting to the bino-like LSP. This scenario has relatively light A and H bosons at twice the LSP mass such that the DM relic density is reduced via the A/H funnel self-annihilation mechanisms, $\tilde{\chi}_1^0\tilde{\chi}_1^0 \to A/H$. Similar to the Z/h funnel model, this model has mixed $\tilde{\chi}_2^0$ decay modes, with $\mathcal{B}(\tilde{\chi}_2^0 \to \tilde{\chi}_1^0 h) = 77\%$ and $\mathcal{B}(\tilde{\chi}_2^0 \to \tilde{\chi}_1^0 Z) = 23\%$. The model lies just beyond the 1Lbb region of sensitivity, so despite the $\tilde{\chi}_2^0$ decay into h being dominant, the 3L search (specifically the signal regions that targeted the $\tilde{\chi}_2^0$ decay via Z) has the best sensitivity.

JHEP05(2024)106

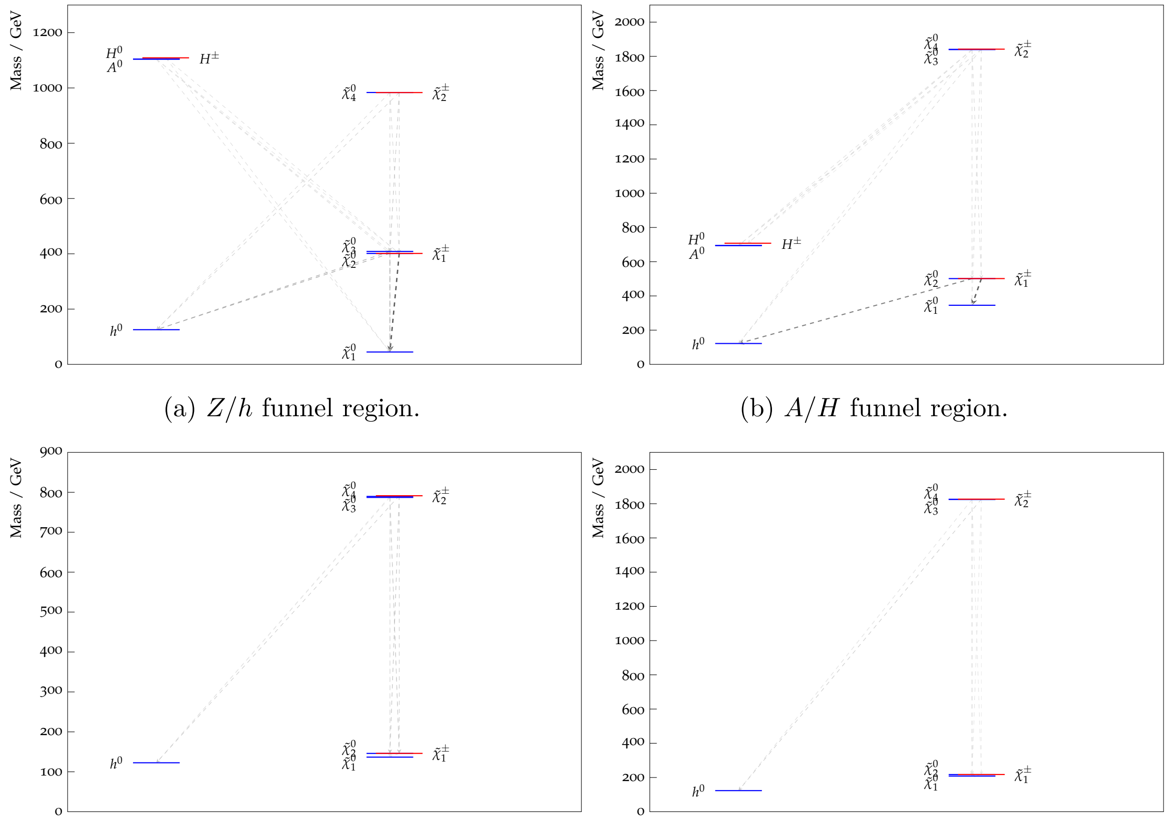

(a) Z/h funnel region.

(b) A/H funnel region.

(c) Compressed region.

(d) Compressed region.

Figure 16. Mass spectrum for four benchmark models with a bino-like LSP that satisfy all constraints and are not excluded despite having a mass-spectrum within published ATLAS simplified model contours. Produced using PySLHA [85].

Finally, two scenarios with small mass splittings between the $\tilde{\chi}_1^{\pm}$, $\tilde{\chi}_2^0$ and $\tilde{\chi}_1^0$ are shown in figures 16(c) and 16(d). These scenarios have a smaller branching fraction for the $\tilde{\chi}_2^0 \rightarrow \tilde{\chi}_1^0 \ell^+ \ell^-$ three-body decay than the simplified models used in the original compressed analysis. They are instead dominated by the radiative decay $\tilde{\chi}_2^0 \rightarrow \tilde{\chi}_1^0 \gamma$. Therefore these scenarios are not excluded despite having masses within the compressed analysis exclusion contour. In the case of figure 16(c), the $\tilde{\chi}_3^0$, $\tilde{\chi}_2^{\pm}$ and $\tilde{\chi}_4^0$ are light enough to be within reach of searches such as FullHad and 2L2J, but the production cross-section is lower due to those being higgsino-like and they all have decays through W, Z and h bosons at similar branching fractions.

Figure 17 shows the mass spectrum of two benchmark models, each with a higgsino-like LSP that satisfy all constraints and are not excluded by ATLAS Run 2 analyses. The $\tilde{\chi}_1^0$ mass and $\tilde{\chi}_2^0$ mass of these models is within the published simplified-model contours for the ATLAS 3L (off-shell) or compressed searches. As with the compressed bino LSP models discussed previously, the $\tilde{\chi}_2^0 \rightarrow \tilde{\chi}_1^0 \ell^+ \ell^-$ decay mode has a smaller branching fraction for these models than the compressed analysis simplified models, and the radiative decay is the dominant decay mode. Otherwise, the bino, wino and higgsino mass parameters are well separated in these models, making the resulting electroweakinos almost pure bino, wino or higgsinos states as would be expected in simplified models. The $\tilde{\chi}_3^0$ and $\tilde{\chi}_2^{\pm}$ each have masses under

JHEP05(2024)106

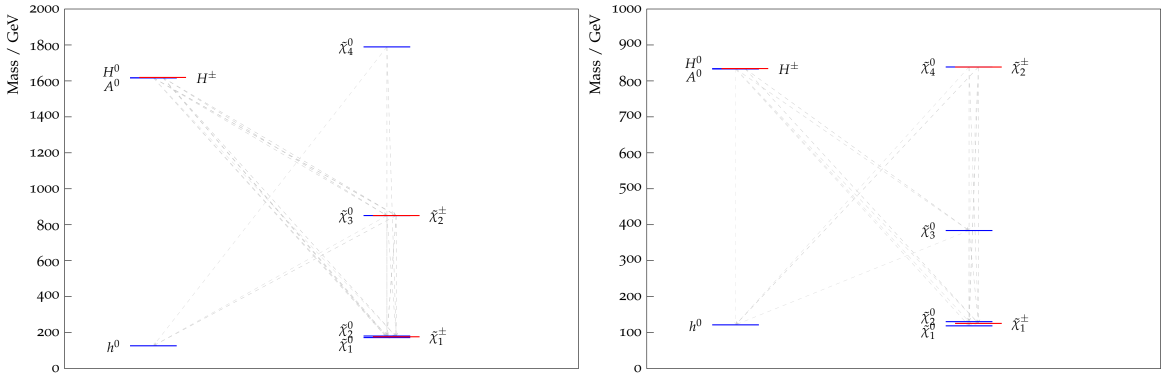

(a) (b)

Figure 17. Mass spectrum for two benchmark models with a higgsino-like LSP that satisfy all constraints and are not excluded despite having a mass-spectrum within published ATLAS simplified model contours.

a TeV and large mass-splittings with the other electroweakinos for both models. Therefore future searches could achieve sensitivity to the production of these heavier electroweakinos and their high p_{T} decay products.

4 Conclusion

This paper presents constraints from eight ATLAS Run 2 searches for electroweak SUSY, the invisible Higgs boson width and searches for additional Higgs bosons, on the phenomenological minimal SUSY standard model, or pMSSM. The selected searches are considered most relevant for the model space being considered. Two scans are performed to evaluate the sensitivity of the ATLAS Run 2 searches. The scans use flat priors across the ranges of pMSSM parameters relevant to the electroweakino sector of the pMSSM, and external constraints from electroweak, flavour and dark-matter related measurements are applied. The EWKino scan considers models where the lightest neutralino (assumed to be the dark matter candidate) can be either predominantly bino-, wino- or higgsino-like. As models with a bino-like LSP typically over-estimate the dark matter relic density unless some additional annihilation mechanisms are present, a second BinoDM scan is presented that aims to oversample the region with a bino-like LSP less than 500 GeV.

The impact of the ATLAS constraints is evaluated by considering the fraction of models that satisfy external constraints that are excluded by the selected ATLAS results. The results are presented as a function of electroweakino masses, and additional observables related to dark matter phenomenology are also presented that highlight the complementarity between collider and non-collider dark matter searches and measurements. In general, the bounds on electroweakino masses from the ATLAS searches are weaker in the pMSSM when assumptions entering the simplified models are relaxed. For some models where heavier electroweakinos are also experimentally accessible and can be constrained by the ATLAS searches, constraints beyond the simplified model contours are obtained. Highlights of the ATLAS Run 2 constraints include almost complete exclusion in the Z/h 'funnel regions' where a light bino-like LSP can avoid oversaturating the relic dark matter density through annihilating through a Z or Higgs boson, and increased sensitivity relative to Run 1 for models with more compressed mass splittings ($\Delta m(\tilde{\chi}_1^0, \tilde{\chi}_2^0)$ or $\Delta m(\tilde{\chi}_1^0, \tilde{\chi}_1^\pm)$). Example spectra for surviving SUSY models with light charginos and neutralinos are also presented that can be used to optimise future searches.

Acknowledgments

We thank CERN for the very successful operation of the LHC and its injectors, as well as the support staff at CERN and at our institutions worldwide without whom ATLAS could not be operated efficiently.

The crucial computing support from all WLCG partners is acknowledged gratefully, in particular from CERN, the ATLAS Tier-1 facilities at TRIUMF/SFU (Canada), NDGF (Denmark, Norway, Sweden), CC-IN2P3 (France), KIT/GridKA (Germany), INFN-CNAF (Italy), NL-T1 (The Netherlands), PIC (Spain), RAL (U.K.) and BNL (U.S.A.), the Tier-2 facilities worldwide and large non-WLCG resource providers. Major contributors of computing resources are listed in ref. [86].

We gratefully acknowledge the support of ANPCyT, Argentina; YerPhI, Armenia; ARC, Australia; BMWFW and FWF, Austria; ANAS, Azerbaijan; CNPq and FAPESP, Brazil; NSERC, NRC and CFI, Canada; CERN; ANID, Chile; CAS, MOST and NSFC, China; Minciencias, Colombia; MEYS CR, Czech Republic; DNRF and DNSRC, Denmark; IN2P3-CNRS and CEA-DRF/IRFU, France; SRNSFG, Georgia; BMBF, HGF and MPG, Germany; GSRI, Greece; RGC and Hong Kong SAR, China; ISF and Benoziyo Center, Israel; INFN, Italy; MEXT and JSPS, Japan; CNRST, Morocco; NWO, The Netherlands; RCN, Norway; MEiN, Poland; FCT, Portugal; MNE/IFA, Romania; MESTD, Serbia; MSSR, Slovakia; ARRS and MIZŠ, Slovenia; DSI/NRF, South Africa; MICINN, Spain; SRC and Wallenberg Foundation, Sweden; SERI, SNSF and Cantons of Bern and Geneva, Switzerland; MOST, Taipei; TENMAK, Türkiye; STFC, United Kingdom; DOE and NSF, United States of America.

Individual groups and members have received support from BCKDF, CANARIE, CRC and DRAC, Canada; PRIMUS 21/SCI/017 and UNCE SCI/013, Czech Republic; COST, ERC, ERDF, Horizon 2020, ICSC-NextGenerationEU and Marie Skłodowska-Curie Actions, European Union; Investissements d'Avenir Labex, Investissements d'Avenir Idex and ANR, France; DFG and AvH Foundation, Germany; Herakleitos, Thales and Aristeia programmes co-financed by EU-ESF and the Greek NSRF, Greece; BSF-NSF and MINERVA, Israel; Norwegian Financial Mechanism 2014–2021, Norway; NCN and NAWA, Poland; La Caixa Banking Foundation, CERCA Programme Generalitat de Catalunya and PROMETEO and GenT Programmes Generalitat Valenciana, Spain; Göran Gustafssons Stiftelse, Sweden; The Royal Society and Leverhulme Trust, United Kingdom.

In addition, individual members wish to acknowledge support from Chile: Agencia Nacional de Investigación y Desarrollo (FONDECYT 1190886, FONDECYT 1210400, FONDECYT 1230987); China: National Natural Science Foundation of China (NSFC - 12175119, NSFC 12275265); European Union: European Research Council (ERC - 948254), Horizon 2020 Framework Programme (MUCCA — CHIST-ERA-19-XAI-00), Italian Center for High Performance Computing, Big Data and Quantum Computing (ICSC, NextGenerationEU),

JHEP05(2024)106

Marie Sklodowska-Curie Actions (EU H2020 MSC IF GRANT NO 101033496); France: Agence Nationale de la Recherche (ANR-20-CE31-0013, ANR-21-CE31-0022), Investissements d'Avenir Idex (ANR-11-LABX-0012), Investissements d'Avenir Labex (ANR-11-LABX-0012); Germany: Baden-Württemberg Stiftung (BW Stiftung-Postdoc Eliteprogramme), Deutsche Forschungsgemeinschaft (DFG — CR 312/5-1); Italy: Istituto Nazionale di Fisica Nucleare (FELLINI G.A. n. 754496, ICSC, NextGenerationEU); Japan: Japan Society for the Promotion of Science (JSPS KAKENHI 22H01227, JSPS KAKENHI JP21H05085, JSPS KAKENHI JP22H04944); Netherlands: Netherlands Organisation for Scientific Research (NWO Veni 2020 — VI.Veni.202.179); Norway: Research Council of Norway (RCN-314472); Poland: Polish National Agency for Academic Exchange (PPN/PPO/2020/1/00002/U/00001), Polish National Science Centre (NCN 2021/42/E/ST2/00350, NCN OPUS nr 2022/47/B/ST2/03059, NCN UMO-2019/34/E/ST2/00393, UMO-2020/37/B/ST2/01043, UMO-2021/40/C/ST2/00187); Slovenia: Slovenian Research Agency (ARIS grant J1-3010); Spain: BBVA Foundation (LEO22-1-603), Generalitat Valenciana (Artemisa, FEDER, IDIFEDER/2018/048), La Caixa Banking Foundation (LCF/BQ/PI20/11760025), Ministry of Science and Innovation (RYC2019-028510-I, RYC2020-030254-I), PROMETEO and GenT Programmes Generalitat Valenciana (CIDEGENT/2019/023, CIDEGENT/2019/027); Sweden: Swedish Research Council (VR 2022-03845), Knut and Alice Wallenberg Foundation (KAW 2017.0100, KAW 2018.0157, KAW 2019.0447); Switzerland: Swiss National Science Foundation (SNSF — PCEFP2_194658); United Kingdom: Leverhulme Trust (Leverhulme Trust RPG-2020-004); United States of America: Neubauer Family Foundation.

References

[1] ATLAS collaboration, *The ATLAS Experiment at the CERN Large Hadron Collider*, 2008 *JINST* **3** S08003 [INSPIRE].

[2] Y.A. Golfand and E.P. Likhtman, *Extension of the Algebra of Poincare Group Generators and Violation of p Invariance*, *JETP Lett.* **13** (1971) 323 [INSPIRE].

[3] D.V. Volkov and V.P. Akulov, *Is the Neutrino a Goldstone Particle?*, *Phys. Lett. B* **46** (1973) 109 [INSPIRE].

[4] J. Wess and B. Zumino, *Supergauge Transformations in Four-Dimensions*, *Nucl. Phys. B* **70** (1974) 39 [INSPIRE].

[5] J. Wess and B. Zumino, *Supergauge Invariant Extension of Quantum Electrodynamics*, *Nucl. Phys. B* **78** (1974) 1 [INSPIRE].

[6] S. Ferrara and B. Zumino, *Supergauge Invariant Yang-Mills Theories*, *Nucl. Phys. B* **79** (1974) 413 [INSPIRE].

[7] A. Salam and J.A. Strathdee, *Supersymmetry and Non-Abelian Gauges*, *Phys. Lett. B* **51** (1974) 353 [INSPIRE].

[8] S. Weinberg, *Implications of Dynamical Symmetry Breaking*, *Phys. Rev. D* **13** (1976) 974 [INSPIRE].

[9] E. Gildener, *Gauge Symmetry Hierarchies*, *Phys. Rev. D* **14** (1976) 1667 [INSPIRE].

[10] S. Weinberg, *Implications of dynamical symmetry breaking: An Addendum*, *Phys. Rev. D* **19** (1979) 1277.

[11] L. Susskind, *Dynamics of Spontaneous Symmetry Breaking in the Weinberg-Salam Theory*, *Phys. Rev. D* **20** (1979) 2619 [INSPIRE].

[12] G.R. Farrar and P. Fayet, *Phenomenology of the Production, Decay, and Detection of New Hadronic States Associated with Supersymmetry*, *Phys. Lett. B* **76** (1978) 575 [INSPIRE].

[13] H. Goldberg, *Constraint on the Photino Mass from Cosmology*, *Phys. Rev. Lett.* **50** (1983) 1419 [*Erratum ibid.* **103** (2009) 099905] [INSPIRE].

[14] J.R. Ellis, J. Hagelin, D.V. Nanopoulos, K.A. Olive and M. Srednicki, *Supersymmetric Relics from the Big Bang*, *Nucl. Phys. B* **238** (1984) 453 [INSPIRE].

[15] ATLAS collaboration, *Search for direct production of electroweakinos in final states with one lepton, missing transverse momentum and a Higgs boson decaying into two b-jets in pp collisions at $\sqrt{s} = 13$ TeV with the ATLAS detector*, *Eur. Phys. J. C* **80** (2020) 691 [arXiv:1909.09226] [INSPIRE].

[16] ATLAS collaboration, *Search for new phenomena in final states with large jet multiplicities and missing transverse momentum using $\sqrt{s} = 13$ TeV proton-proton collisions recorded by ATLAS in Run 2 of the LHC*, *JHEP* **10** (2020) 062 [arXiv:2008.06032] [INSPIRE].

[17] ATLAS collaboration, *Search for squarks and gluinos in final states with jets and missing transverse momentum using 139 fb^{-1} of $\sqrt{s} = 13$ TeV pp collision data with the ATLAS detector*, *JHEP* **02** (2021) 143 [arXiv:2010.14293] [INSPIRE].

[18] ATLAS collaboration, *Search for squarks and gluinos in final states with one isolated lepton, jets, and missing transverse momentum at $\sqrt{s} = 13$ TeV with the ATLAS detector*, *Eur. Phys. J. C* **81** (2021) 600 [*Erratum ibid.* **81** (2021) 956] [arXiv:2101.01629] [INSPIRE].

[19] ATLAS collaboration, *Search for electroweak production of charginos and sleptons decaying into final states with two leptons and missing transverse momentum in $\sqrt{s} = 13$ TeV pp collisions using the ATLAS detector*, *Eur. Phys. J. C* **80** (2020) 123 [arXiv:1908.08215] [INSPIRE].

[20] ATLAS collaboration, *Searches for electroweak production of supersymmetric particles with compressed mass spectra in $\sqrt{s} = 13$ TeV pp collisions with the ATLAS detector*, *Phys. Rev. D* **101** (2020) 052005 [arXiv:1911.12606] [INSPIRE].

[21] ATLAS collaboration, *Search for chargino-neutralino production with mass splittings near the electroweak scale in three-lepton final states in $\sqrt{s} = 13$ TeV pp collisions with the ATLAS detector*, *Phys. Rev. D* **101** (2020) 072001 [arXiv:1912.08479] [INSPIRE].

[22] ATLAS collaboration, *Search for supersymmetry in events with four or more charged leptons in 139 fb^{-1} of $\sqrt{s} = 13$ TeV pp collisions with the ATLAS detector*, *JHEP* **07** (2021) 167 [arXiv:2103.11684] [INSPIRE].

[23] ATLAS collaboration, *Search for chargino-neutralino pair production in final states with three leptons and missing transverse momentum in $\sqrt{s} = 13$ TeV pp collisions with the ATLAS detector*, *Eur. Phys. J. C* **81** (2021) 1118 [arXiv:2106.01676] [INSPIRE].

[24] ATLAS collaboration, *Search for charginos and neutralinos in final states with two boosted hadronically decaying bosons and missing transverse momentum in pp collisions at $\sqrt{s} = 13$ TeV with the ATLAS detector*, *Phys. Rev. D* **104** (2021) 112010 [arXiv:2108.07586] [INSPIRE].

[25] ATLAS collaboration, *Searches for new phenomena in events with two leptons, jets, and missing transverse momentum in* 139 *fb*$^{-1}$ *of* $\sqrt{s} = 13$ *TeV pp collisions with the ATLAS detector*, *Eur. Phys. J. C* **83** (2023) 515 [arXiv:2204.13072] [INSPIRE].

[26] ATLAS collaboration, *Search for direct pair production of sleptons and charginos decaying to two leptons and neutralinos with mass splittings near the W-boson mass in* $\sqrt{s} = 13$ *TeV pp collisions with the ATLAS detector*, *JHEP* **06** (2023) 031 [arXiv:2209.13935] [INSPIRE].

[27] ATLAS collaboration, *Search for long-lived charginos based on a disappearing-track signature using* 136 *fb*$^{-1}$ *of pp collisions at* $\sqrt{s} = 13$ *TeV with the ATLAS detector*, *Eur. Phys. J. C* **82** (2022) 606 [arXiv:2201.02472] [INSPIRE].

[28] J. Alwall, P. Schuster and N. Toro, *Simplified Models for a First Characterization of New Physics at the LHC*, *Phys. Rev. D* **79** (2009) 075020 [arXiv:0810.3921] [INSPIRE].

[29] A. Djouadi et al., *The Minimal supersymmetric standard model: Group summary report*, in the proceedings of the *GDR (Groupement De Recherche) — Supersymetrie*, Montpellier, France, 15–17 April 1998, hep-ph/9901246 [INSPIRE].

[30] C.F. Berger, J.S. Gainer, J.A.L. Hewett and T.G. Rizzo, *Supersymmetry Without Prejudice*, *JHEP* **02** (2009) 023 [arXiv:0812.0980] [INSPIRE].

[31] ATLAS collaboration, *Summary of the ATLAS experiment's sensitivity to supersymmetry after LHC Run 1 — interpreted in the phenomenological MSSM*, *JHEP* **10** (2015) 134 [arXiv:1508.06608] [INSPIRE].

[32] ATLAS collaboration, *Dark matter interpretations of ATLAS searches for the electroweak production of supersymmetric particles in* $\sqrt{s} = 8$ *TeV proton-proton collisions*, *JHEP* **09** (2016) 175 [arXiv:1608.00872] [INSPIRE].

[33] CMS collaboration, *Phenomenological MSSM interpretation of CMS searches in pp collisions at* $\sqrt{s} = 7$ *and* 8 *TeV*, *JHEP* **10** (2016) 129 [arXiv:1606.03577] [INSPIRE].

[34] GAMBIT collaboration, *GAMBIT: The Global and Modular Beyond-the-Standard-Model Inference Tool*, *Eur. Phys. J. C* **77** (2017) 784 [*Addendum ibid.* **78** (2018) 98] [arXiv:1705.07908] [INSPIRE].

[35] GAMBIT collaboration, *A global fit of the MSSM with GAMBIT*, *Eur. Phys. J. C* **77** (2017) 879 [arXiv:1705.07917] [INSPIRE].

[36] E. Bagnaschi et al., *Likelihood Analysis of the pMSSM11 in Light of LHC* 13 *TeV Data*, *Eur. Phys. J. C* **78** (2018) 256 [arXiv:1710.11091] [INSPIRE].

[37] ATLAS collaboration, *The ATLAS collaboration Software and Firmware*, ATL-SOFT-PUB-2021-001 (2021).

[38] ATLAS collaboration, *SimpleAnalysis: Truth-level Analysis Framework*, ATL-PHYS-PUB-2022-017 (2022) [DOI:10.17181/CERN.R6S3.0QKV].

[39] ATLAS collaboration, *Reproducing searches for new physics with the ATLAS experiment through publication of full statistical likelihoods*, ATL-PHYS-PUB-2019-029 (2019).

[40] K. Cranmer and I. Yavin, *RECAST: Extending the Impact of Existing Analyses*, *JHEP* **04** (2011) 038 [arXiv:1010.2506] [INSPIRE].

[41] ATLAS collaboration, *RECAST framework reinterpretation of an ATLAS Dark Matter Search constraining a model of a dark Higgs boson decaying to two b-quarks*, ATL-PHYS-PUB-2019-032 (2019).

JHEP05(2024)106

[42] T. Šimko et al., *Scalable Declarative HEP Analysis Workflows for Containerised Compute Clouds*, Front. Big Data **4** (2021) 661501 [INSPIRE].

[43] W. Porod, *SPheno, a program for calculating supersymmetric spectra, SUSY particle decays and SUSY particle production at e^+e^- colliders*, Comput. Phys. Commun. **153** (2003) 275 [hep-ph/0301101] [INSPIRE].

[44] W. Porod and F. Staub, *SPheno 3.1: Extensions including flavour, CP-phases and models beyond the MSSM*, Comput. Phys. Commun. **183** (2012) 2458 [arXiv:1104.1573] [INSPIRE].

[45] H. Bahl et al., *Precision calculations in the MSSM Higgs-boson sector with FeynHiggs 2.14*, Comput. Phys. Commun. **249** (2020) 107099 [arXiv:1811.09073] [INSPIRE].

[46] H. Bahl, S. Heinemeyer, W. Hollik and G. Weiglein, *Reconciling EFT and hybrid calculations of the light MSSM Higgs-boson mass*, Eur. Phys. J. C **78** (2018) 57 [arXiv:1706.00346] [INSPIRE].

[47] H. Bahl and W. Hollik, *Precise prediction for the light MSSM Higgs boson mass combining effective field theory and fixed-order calculations*, Eur. Phys. J. C **76** (2016) 499 [arXiv:1608.01880] [INSPIRE].

[48] T. Hahn, S. Heinemeyer, W. Hollik, H. Rzehak and G. Weiglein, *High-Precision Predictions for the Light CP -Even Higgs Boson Mass of the Minimal Supersymmetric Standard Model*, Phys. Rev. Lett. **112** (2014) 141801 [arXiv:1312.4937] [INSPIRE].

[49] M. Frank, T. Hahn, S. Heinemeyer, W. Hollik, H. Rzehak and G. Weiglein, *The Higgs Boson Masses and Mixings of the Complex MSSM in the Feynman-Diagrammatic Approach*, JHEP **02** (2007) 047 [hep-ph/0611326] [INSPIRE].

[50] G. Degrassi, S. Heinemeyer, W. Hollik, P. Slavich and G. Weiglein, *Towards high precision predictions for the MSSM Higgs sector*, Eur. Phys. J. C **28** (2003) 133 [hep-ph/0212020] [INSPIRE].

[51] S. Heinemeyer, W. Hollik and G. Weiglein, *The Masses of the neutral CP-even Higgs bosons in the MSSM: Accurate analysis at the two loop level*, Eur. Phys. J. C **9** (1999) 343 [hep-ph/9812472] [INSPIRE].

[52] S. Heinemeyer, W. Hollik and G. Weiglein, *FeynHiggs: A Program for the calculation of the masses of the neutral CP even Higgs bosons in the MSSM*, Comput. Phys. Commun. **124** (2000) 76 [hep-ph/9812320] [INSPIRE].

[53] D. Barducci et al., *Collider limits on new physics within micrOMEGAs_4.3*, Comput. Phys. Commun. **222** (2018) 327 [arXiv:1606.03834] [INSPIRE].

[54] G. Bélanger, A. Mjallal and A. Pukhov, *Recasting direct detection limits within micrOMEGAs and implication for non-standard Dark Matter scenarios*, Eur. Phys. J. C **81** (2021) 239 [arXiv:2003.08621] [INSPIRE].

[55] F. Mahmoudi, *SuperIso v2.3: A Program for calculating flavor physics observables in Supersymmetry*, Comput. Phys. Commun. **180** (2009) 1579 [arXiv:0808.3144] [INSPIRE].

[56] LEP2 SUSY Working Group, *LEPSUSYWG, ALEPH, DELPHI, L3 and OPAL experiments*, LEPSUSYWG/01-03.1 (2001), https://lepsusy.web.cern.ch/lepsusy/Welcome.html.

[57] LEP2 SUSY Working Group, *LEPSUSYWG, ALEPH, DELPHI, L3 and OPAL experiments*, LEPSUSYWG/02-04.1 (2002), https://lepsusy.web.cern.ch/lepsusy/Welcome.html.

[58] Particle Data collaboration, *Review of Particle Physics*, Prog. Theor. Exp. Phys. **2022** (2022) 083C01 [INSPIRE].

JHEP05(2024)106

[59] LHCb collaboration, *Measurement of the $B_s^0 \to \mu^+\mu^-$ decay properties and search for the $B^0 \to \mu^+\mu^-$ and $B_s^0 \to \mu^+\mu^-\gamma$ decays*, Phys. Rev. D **105** (2022) 012010 [arXiv:2108.09283] [INSPIRE].

[60] GFITTER Group, *Update of the global electroweak fit and constraints on two-Higgs-doublet models*, Eur. Phys. J. C **78** (2018) 675 [arXiv:1803.01853] [INSPIRE].

[61] CDF collaboration, *High-precision measurement of the W boson mass with the CDF II detector*, Science **376** (2022) 170 [INSPIRE].

[62] ALEPH et al. collaborations, *Precision electroweak measurements on the Z resonance*, Phys. Rep. **427** (2006) 257 [hep-ex/0509008] [INSPIRE].

[63] S. Heinemeyer, W. Hollik, G. Weiglein and L. Zeune, *Implications of LHC search results on the W boson mass prediction in the MSSM*, JHEP **12** (2013) 084 [arXiv:1311.1663] [INSPIRE].

[64] PLANCK collaboration, *Planck 2018 results. Part VI. Cosmological parameters*, Astron. Astrophys. **641** (2020) A6 [*Erratum ibid.* **652** (2021) C4] [arXiv:1807.06209] [INSPIRE].

[65] LZ collaboration, *First Dark Matter Search Results from the LUX-ZEPLIN (LZ) Experiment*, Phys. Rev. Lett. **131** (2023) 041002 [arXiv:2207.03764] [INSPIRE].

[66] PICO collaboration, *Dark Matter Search Results from the Complete Exposure of the PICO-60 C_3F_8 Bubble Chamber*, Phys. Rev. D **100** (2019) 022001 [arXiv:1902.04031] [INSPIRE].

[67] B. Fuks, M. Klasen, D.R. Lamprea and M. Rothering, *Precision predictions for electroweak superpartner production at hadron colliders with Resummino*, Eur. Phys. J. C **73** (2013) 2480 [arXiv:1304.0790] [INSPIRE].

[68] W. Beenakker, R. Hopker and M. Spira, *PROSPINO: A Program for the production of supersymmetric particles in next-to-leading order QCD*, hep-ph/9611232 [INSPIRE].

[69] ATLAS collaboration, *Search for heavy, long-lived, charged particles with large ionisation energy loss in pp collisions at $\sqrt{s} = 13$ TeV using the ATLAS experiment and the full Run 2 dataset*, JHEP **06** (2023) 158 [arXiv:2205.06013] [INSPIRE].

[70] J. Alwall, M. Herquet, F. Maltoni, O. Mattelaer and T. Stelzer, *MadGraph 5: Going Beyond*, JHEP **06** (2011) 128 [arXiv:1106.0522] [INSPIRE].

[71] T. Sjöstrand et al., *An introduction to PYTHIA 8.2*, Comput. Phys. Commun. **191** (2015) 159 [arXiv:1410.3012] [INSPIRE].

[72] ATLAS collaboration, *The ATLAS Simulation Infrastructure*, Eur. Phys. J. C **70** (2010) 823 [arXiv:1005.4568] [INSPIRE].

[73] GEANT4 collaboration, *GEANT4 — a simulation toolkit*, Nucl. Instrum. Meth. A **506** (2003) 250 [INSPIRE].

[74] A.L. Read, *Presentation of search results: The CL_s technique*, J. Phys. G **28** (2002) 2693 [INSPIRE].

[75] E. Maguire, L.A. Heinrich and G. Watt, *HEPData: a repository for high energy physics data*, J. Phys. Conf. Ser. **898** (2017) 102006 [arXiv:1704.05473] [INSPIRE].

[76] L.A. Heinrich, M. Feickert and G. Stark, *pyhf: v0.6.3*, Zenodo (2021) [DOI:10.5281/zenodo.5426790].

[77] L.A. Heinrich, M. Feickert, G. Stark and K. Cranmer, *pyhf: pure-Python implementation of HistFactory statistical models*, J. Open Source Softw. **6** (2021) 2823 [INSPIRE].

JHEP05(2024)106

[78] D. Merkel, *Docker: lightweight linux containers for consistent development and deployment*, *Linux J.* **2014** (2014) 2.

[79] P. Meade, N. Seiberg and D. Shih, *General Gauge Mediation*, *Prog. Theor. Phys. Suppl.* **177** (2009) 143 [arXiv:0801.3278] [INSPIRE].

[80] G.F. Giudice, M.A. Luty, H. Murayama and R. Rattazzi, *Gaugino mass without singlets*, *JHEP* **12** (1998) 027 [hep-ph/9810442] [INSPIRE].

[81] L. Randall and R. Sundrum, *Out of this world supersymmetry breaking*, *Nucl. Phys. B* **557** (1999) 79 [hep-th/9810155] [INSPIRE].

[82] ATLAS collaboration, *Implementation of simplified likelihoods in HistFactory for searches for supersymmetry*, ATL-PHYS-PUB-2021-038 (2021).

[83] ATLAS collaboration, *Combination of searches for invisible decays of the Higgs boson using* $139\,fb^{-1}$ *of proton-proton collision data at* $\sqrt{s} = 13$ *TeV collected with the ATLAS experiment*, *Phys. Lett. B* **842** (2023) 137963 [arXiv:2301.10731] [INSPIRE].

[84] ATLAS collaboration, *Combined measurements of Higgs boson production and decay using up to* $80\,fb^{-1}$ *of proton-proton collision data at* $\sqrt{s} = 13$ *TeV collected with the ATLAS experiment*, *Phys. Rev. D* **101** (2020) 012002 [arXiv:1909.02845] [INSPIRE].

[85] A. Buckley, *PySLHA: a Pythonic interface to SUSY Les Houches Accord data*, *Eur. Phys. J. C* **75** (2015) 467 [arXiv:1305.4194] [INSPIRE].

[86] ATLAS collaboration, *ATLAS Computing Acknowledgements*, ATL-SOFT-PUB-2023-001 (2023).

The ATLAS collaboration

G. Aad[102], B. Abbott[120], K. Abeling[55], N.J. Abicht[49], S.H. Abidi[29], A. Aboulhorma[35e], H. Abramowicz[151], H. Abreu[150], Y. Abulaiti[117], B.S. Acharya[69a,69b,m], C. Adam Bourdarios[4], L. Adamczyk[86a], S.V. Addepalli[26], M.J. Addison[101], J. Adelman[115], A. Adiguzel[21c], T. Adye[134], A.A. Affolder[136], Y. Afik[36], M.N. Agaras[13], J. Agarwala[73a,73b], A. Aggarwal[100], C. Agheorghiesei[27c], A. Ahmad[36], F. Ahmadov[38,y], W.S. Ahmed[104], S. Ahuja[95], X. Ai[62a], G. Aielli[76a,76b], A. Aikot[163], M. Ait Tamlihat[35e], B. Aitbenchikh[35a], I. Aizenberg[169], M. Akbiyik[100], T.P.A. Åkesson[98], A.V. Akimov[37], D. Akiyama[168], N.N. Akolkar[24], S. Aktas[21a], K. Al Khoury[41], G.L. Alberghi[23b], J. Albert[165], P. Albicocco[53], G.L. Albouy[60], S. Alderweireldt[52], Z.L. Alegria[121], M. Aleksa[36], I.N. Aleksandrov[38], C. Alexa[27b], T. Alexopoulos[10], F. Alfonsi[23b], M. Algren[56], M. Alhroob[120], B. Ali[132], H.M.J. Ali[91], S. Ali[148], S.W. Alibocus[92], M. Aliev[145], G. Alimonti[71a], W. Alkakhi[55], C. Allaire[66], B.M.M. Allbrooke[146], J.F. Allen[52], C.A. Allendes Flores[137f], P.P. Allport[20], A. Aloisio[72a,72b], F. Alonso[90], C. Alpigiani[138], M. Alvarez Estevez[99], A. Alvarez Fernandez[100], M. Alves Cardoso[56], M.G. Alviggi[72a,72b], M. Aly[101], Y. Amaral Coutinho[83b], A. Ambler[104], C. Amelung[36], M. Amerl[101], C.G. Ames[109], D. Amidei[106], S.P. Amor Dos Santos[130a], K.R. Amos[163], V. Ananiev[125], C. Anastopoulos[139], T. Andeen[11], J.K. Anders[36], S.Y. Andrean[47a,47b], A. Andreazza[71a,71b], S. Angelidakis[9], A. Angerami[41,ab], A.V. Anisenkov[37], A. Annovi[74a], C. Antel[56], M.T. Anthony[139], E. Antipov[145], M. Antonelli[53], F. Anulli[75a], M. Aoki[84], T. Aoki[153], J.A. Aparisi Pozo[163], M.A. Aparo[146], L. Aperio Bella[48], C. Appelt[18], A. Apyan[26], N. Aranzabal[36], S.J. Arbiol Val[87], C. Arcangeletti[53], A.T.H. Arce[51], E. Arena[92], J-F. Arguin[108], S. Argyropoulos[54], J.-H. Arling[48], O. Arnaez[4], H. Arnold[114], G. Artoni[75a,75b], H. Asada[111], K. Asai[118], S. Asai[153], N.A. Asbah[61], K. Assamagan[29], R. Astalos[28a], S. Atashi[160], R.J. Atkin[33a], M. Atkinson[162], H. Atmani[35f], P.A. Atmasiddha[128], K. Augsten[132], S. Auricchio[72a,72b], A.D. Auriol[20], V.A. Austrup[101], G. Avolio[36], K. Axiotis[56], G. Azuelos[108,af], D. Babal[28b], H. Bachacou[135], K. Bachas[152,p], A. Bachiu[34], F. Backman[47a,47b], A. Badea[61], T.M. Baer[106], P. Bagnaia[75a,75b], M. Bahmani[18], D. Bahner[54], A.J. Bailey[163], V.R. Bailey[162], J.T. Baines[134], L. Baines[94], O.K. Baker[172], E. Bakos[15], D. Bakshi Gupta[8], V. Balakrishnan[120], R. Balasubramanian[114], E.M. Baldin[37], P. Balek[86a], E. Ballabene[23b,23a], F. Balli[135], L.M. Baltes[63a], W.K. Balunas[32], J. Balz[100], E. Banas[87], M. Bandieramonte[129], A. Bandyopadhyay[24], S. Bansal[24], L. Barak[151], M. Barakat[48], E.L. Barberio[105], D. Barberis[57b,57a], M. Barbero[102], M.Z. Barel[114], K.N. Barends[33a], T. Barillari[110], M-S. Barisits[36], T. Barklow[143], P. Baron[122], D.A. Baron Moreno[101], A. Baroncelli[62a], G. Barone[29], A.J. Barr[126], J.D. Barr[96], L. Barranco Navarro[47a,47b], F. Barreiro[99], J. Barreiro Guimarães da Costa[14a], U. Barron[151], M.G. Barros Teixeira[130a], S. Barsov[37], F. Bartels[63a], R. Bartoldus[143], A.E. Barton[91], P. Bartos[28a], A. Basan[100], M. Baselga[49], A. Bassalat[66,b], M.J. Basso[156a], C.R. Basson[101], R.L. Bates[59], S. Batlamous[35e], J.R. Batley[32], B. Batool[141], M. Battaglia[136], D. Battulga[18], M. Bauce[75a,75b], M. Bauer[36], P. Bauer[24], L.T. Bazzano Hurrell[30], J.B. Beacham[51], T. Beau[127], J.Y. Beaucamp[90], P.H. Beauchemin[158], F. Becherer[54], P. Bechtle[24], H.P. Beck[19,o], K. Becker[167], A.J. Beddall[82], V.A. Bednyakov[38], C.P. Bee[145],

JHEP05(2024)106

L.J. Beemster[15], T.A. Beermann[36], M. Begalli[83d], M. Begel[29], A. Behera[145], J.K. Behr[48], J.F. Beirer[36], F. Beisiegel[24], M. Belfkir[159], G. Bella[151], L. Bellagamba[23b], A. Bellerive[34], P. Bellos[20], K. Beloborodov[37], D. Benchekroun[35a], F. Bendebba[35a], Y. Benhammou[151], M. Benoit[29], J.R. Bensinger[26], S. Bentvelsen[114], L. Beresford[48], M. Beretta[53], E. Bergeaas Kuutmann[161], N. Berger[4], B. Bergmann[132], J. Beringer[17a], G. Bernardi[5], C. Bernius[143], F.U. Bernlochner[24], F. Bernon[36,102], A. Berrocal Guardia[13], T. Berry[95], P. Berta[133], A. Berthold[50], I.A. Bertram[91], S. Bethke[110], A. Betti[75a,75b], A.J. Bevan[94], N.K. Bhalla[54], M. Bhamjee[33c], S. Bhatta[145], D.S. Bhattacharya[166], P. Bhattarai[143], V.S. Bhopatkar[121], R. Bi[29,ai], R.M. Bianchi[129], G. Bianco[23b,23a], O. Biebel[109], R. Bielski[123], M. Biglietti[77a], M. Bindi[55], A. Bingul[21b], C. Bini[75a,75b], A. Biondini[92], C.J. Birch-sykes[101], G.A. Bird[20,134], M. Birman[169], M. Biros[133], S. Biryukov[146], T. Bisanz[49], E. Bisceglie[43b,43a], J.P. Biswal[134], D. Biswas[141], A. Bitadze[101], K. Bjørke[125], I. Bloch[48], A. Blue[59], U. Blumenschein[94], J. Blumenthal[100], G.J. Bobbink[114], V.S. Bobrovnikov[37], M. Boehler[54], B. Boehm[166], D. Bogavac[36], A.G. Bogdanchikov[37], C. Bohm[47a], V. Boisvert[95], P. Bokan[48], T. Bold[86a], M. Bomben[5], M. Bona[94], M. Boonekamp[135], C.D. Booth[95], A.G. Borbély[59], I.S. Bordulev[37], H.M. Borecka-Bielska[108], G. Borissov[91], D. Bortoletto[126], D. Boscherini[23b], M. Bosman[13], J.D. Bossio Sola[36], K. Bouaouda[35a], N. Bouchhar[163], J. Boudreau[129], E.V. Bouhova-Thacker[91], D. Boumediene[40], R. Bouquet[165], A. Boveia[119], J. Boyd[36], D. Boye[29], I.R. Boyko[38], J. Bracinik[20], N. Brahimi[62d], G. Brandt[171], O. Brandt[32], F. Braren[48], B. Brau[103], J.E. Brau[123], R. Brener[169], L. Brenner[114], R. Brenner[161], S. Bressler[169], D. Britton[59], D. Britzger[110], I. Brock[24], G. Brooijmans[41], W.K. Brooks[137f], E. Brost[29], L.M. Brown[165], L.E. Bruce[61], T.L. Bruckler[126], P.A. Bruckman de Renstrom[87], B. Brüers[48], A. Bruni[23b], G. Bruni[23b], M. Bruschi[23b], N. Bruscino[75a,75b], T. Buanes[16], Q. Buat[138], D. Buchin[110], A.G. Buckley[59], O. Bulekov[37], B.A. Bullard[143], S. Burdin[92], C.D. Burgard[49], A.M. Burger[40], B. Burghgrave[8], O. Burlayenko[54], J.T.P. Burr[32], C.D. Burton[11], J.C. Burzynski[142], E.L. Busch[41], V. Büscher[100], P.J. Bussey[59], J.M. Butler[25], C.M. Buttar[59], J.M. Butterworth[96], W. Buttinger[134], C.J. Buxo Vazquez[107], A.R. Buzykaev[37], S. Cabrera Urbán[163], L. Cadamuro[66], D. Caforio[58], H. Cai[129], Y. Cai[14a,14e], Y. Cai[14c], V.M.M. Cairo[36], O. Cakir[3a], N. Calace[36], P. Calafiura[17a], G. Calderini[127], P. Calfayan[68], G. Callea[59], L.P. Caloba[83b], D. Calvet[40], S. Calvet[40], T.P. Calvet[102], M. Calvetti[74a,74b], R. Camacho Toro[127], S. Camarda[36], D. Camarero Munoz[26], P. Camarri[76a,76b], M.T. Camerlingo[72a,72b], D. Cameron[36], C. Camincher[165], M. Campanelli[96], A. Camplani[42], V. Canale[72a,72b], A. Canesse[104], J. Cantero[163], Y. Cao[162], F. Capocasa[26], M. Capua[43b,43a], A. Carbone[71a,71b], R. Cardarelli[76a], J.C.J. Cardenas[8], F. Cardillo[163], G. Carducci[43b,43a], T. Carli[36], G. Carlino[72a], J.I. Carlotto[13], B.T. Carlson[129,q], E.M. Carlson[165,156a], L. Carminati[71a,71b], A. Carnelli[135], M. Carnesale[75a,75b], S. Caron[113], E. Carquin[137f], S. Carrá[71a], G. Carratta[23b,23a], F. Carrio Argos[33g], J.W.S. Carter[155], T.M. Carter[52], M.P. Casado[13,i], M. Caspar[48], F.L. Castillo[4], L. Castillo Garcia[13], V. Castillo Gimenez[163], N.F. Castro[130a,130e], A. Catinaccio[36], J.R. Catmore[125], V. Cavaliere[29], N. Cavalli[23b,23a], V. Cavasinni[74a,74b], Y.C. Cekmecelioglu[48], E. Celebi[21a], F. Celli[126], M.S. Centonze[70a,70b], V. Cepaitis[56], K. Cerny[122], A.S. Cerqueira[83a], A. Cerri[146], L. Cerrito[76a,76b], F. Cerutti[17a], B. Cervato[141], A. Cervelli[23b], G. Cesarini[53], S.A. Cetin[82], D. Chakraborty[115], J. Chan[170], W.Y. Chan[153], J.D. Chapman[32], E. Chapon[135], B. Chargeishvili[149b], D.G. Charlton[20], M. Chatterjee[19], C. Chauhan[133], S. Chekanov[6], S.V. Chekulaev[156a], G.A. Chelkov[38,a], A. Chen[106], B. Chen[151], B. Chen[165], H. Chen[14c], H. Chen[29], J. Chen[62c], J. Chen[142], M. Chen[126], S. Chen[153], S.J. Chen[14c], X. Chen[62c,135], X. Chen[14b,ae], Y. Chen[62a], C.L. Cheng[170], H.C. Cheng[64a], S. Cheong[143], A. Cheplakov[38], E. Cheremushkina[48], E. Cherepanova[114], R. Cherkaoui El Moursli[35e], E. Cheu[7], K. Cheung[65], L. Chevalier[135], V. Chiarella[53], G. Chiarelli[74a], N. Chiedde[102], G. Chiodini[70a], A.S. Chisholm[20], A. Chitan[27b], M. Chitishvili[163], M.V. Chizhov[38], K. Choi[11], A.R. Chomont[75a,75b], Y. Chou[103], E.Y.S. Chow[113], T. Chowdhury[33g], K.L. Chu[169], M.C. Chu[64a], X. Chu[14a,14e], J. Chudoba[131], J.J. Chwastowski[87], D. Cieri[110], K.M. Ciesla[86a], V. Cindro[93], A. Ciocio[17a], F. Cirotto[72a,72b], Z.H. Citron[169,k], M. Citterio[71a], D.A. Ciubotaru[27b], A. Clark[56], P.J. Clark[52], C. Clarry[155], J.M. Clavijo Columbie[48], S.E. Clawson[48], C. Clement[47a,47b], J. Clercx[48], Y. Coadou[102], M. Cobal[69a,69c], A. Coccaro[57b], R.F. Coelho Barrue[130a], R. Coelho Lopes De Sa[103], S. Coelli[71a], A.E.C. Coimbra[71a,71b], B. Cole[41], J. Collot[60], P. Conde Muiño[130a,130g], M.P. Connell[33c], S.H. Connell[33c], I.A. Connelly[59], E.I. Conroy[126], F. Conventi[72a,ag], H.G. Cooke[20], A.M. Cooper-Sarkar[126], A. Cordeiro Oudot Choi[127], L.D. Corpe[40], M. Corradi[75a,75b], F. Corriveau[104,w], A. Cortes-Gonzalez[18], M.J. Costa[163], F. Costanza[4], D. Costanzo[139], B.M. Cote[119], G. Cowan[95], K. Cranmer[170], D. Cremonini[23b,23a], S. Crépé-Renaudin[60], F. Crescioli[127], M. Cristinziani[141], M. Cristoforetti[78a,78b], V. Croft[114], J.E. Crosby[121], G. Crosetti[43b,43a], A. Cueto[99], T. Cuhadar Donszelmann[160], H. Cui[14a,14e], Z. Cui[7], W.R. Cunningham[59], F. Curcio[43b,43a], P. Czodrowski[36], M.M. Czurylo[63b], M.J. Da Cunha Sargedas De Sousa[57b,57a], J.V. Da Fonseca Pinto[83b], C. Da Via[101], W. Dabrowski[86a], T. Dado[49], S. Dahbi[33g], T. Dai[106], D. Dal Santo[19], C. Dallapiccola[103], M. Dam[42], G. D'amen[29], V. D'Amico[109], J. Damp[100], J.R. Dandoy[34], M.F. Daneri[30], M. Danninger[142], V. Dao[36], G. Darbo[57b], S. Darmora[6], S.J. Das[29,ai], S. D'Auria[71a,71b], C. David[156b], T. Davidek[133], B. Davis-Purcell[34], I. Dawson[94], H.A. Day-hall[132], K. De[8], R. De Asmundis[72a], N. De Biase[48], S. De Castro[23b,23a], N. De Groot[113], P. de Jong[114], H. De la Torre[115], A. De Maria[14c], A. De Salvo[75a], U. De Sanctis[76a,76b], F. De Santis[70a,70b], A. De Santo[146], J.B. De Vivie De Regie[60], D.V. Dedovich[38], J. Degens[114], A.M. Deiana[44], F. Del Corso[23b,23a], J. Del Peso[99], F. Del Rio[63a], L. Delagrange[127], F. Deliot[135], C.M. Delitzsch[49], M. Della Pietra[72a,72b], D. Della Volpe[56], A. Dell'Acqua[36], L. Dell'Asta[71a,71b], M. Delmastro[4], P.A. Delsart[60], S. Demers[172], M. Demichev[38], S.P. Denisov[37], L. D'Eramo[40], D. Derendarz[87], F. Derue[127], P. Dervan[92], K. Desch[24], C. Deutsch[24], F.A. Di Bello[57b,57a], A. Di Ciaccio[76a,76b], L. Di Ciaccio[4], A. Di Domenico[75a,75b], C. Di Donato[72a,72b], A. Di Girolamo[36], G. Di Gregorio[36], A. Di Luca[78a,78b], B. Di Micco[77a,77b], R. Di Nardo[77a,77b], C. Diaconu[102], M. Diamantopoulou[34], F.A. Dias[114], T. Dias Do Vale[142], M.A. Diaz[137a,137b], F.G. Diaz Capriles[24], M. Didenko[163], E.B. Diehl[106], L. Diehl[54], S. Díez Cornell[48], C. Diez Pardos[141], C. Dimitriadi[161,24], A. Dimitrievska[17a], J. Dingfelder[24], I-M. Dinu[27b], S.J. Dittmeier[63b], F. Dittus[36], F. Djama[102], T. Djobava[149b], J.I. Djuvsland[16], C. Doglioni[101,98], A. Dohnalova[28a], J. Dolejsi[133], Z. Dolezal[133], K.M. Dona[39], M. Donadelli[83c], B. Dong[107], J. Donini[40], A. D'Onofrio[72a,72b], M. D'Onofrio[92],

J. Dopke[134], A. Doria[72a], N. Dos Santos Fernandes[130a], P. Dougan[101], M.T. Dova[90], A.T. Doyle[59], M.A. Draguet[126], E. Dreyer[169], I. Drivas-koulouris[10], M. Drnevich[117], A.S. Drobac[158], M. Drozdova[56], D. Du[62a], T.A. du Pree[114], F. Dubinin[37], M. Dubovsky[28a], E. Duchovni[169], G. Duckeck[109], O.A. Ducu[27b], D. Duda[52], A. Dudarev[36], E.R. Duden[26], M. D'uffizi[101], L. Duflot[66], M. Dührssen[36], C. Dülsen[171], A.E. Dumitriu[27b], M. Dunford[63a], S. Dungs[49], K. Dunne[47a,47b], A. Duperrin[102], H. Duran Yildiz[3a], M. Düren[58], A. Durglishvili[149b], B.L. Dwyer[115], G.I. Dyckes[17a], M. Dyndal[86a], B.S. Dziedzic[87], Z.O. Earnshaw[146], G.H. Eberwein[126], B. Eckerova[28a], S. Eggebrecht[55], E. Egidio Purcino De Souza[127], L.F. Ehrke[56], G. Eigen[16], K. Einsweiler[17a], T. Ekelof[161], P.A. Ekman[98], S. El Farkh[35b], Y. El Ghazali[35b], H. El Jarrari[36], A. El Moussaouy[108], V. Ellajosyula[161], M. Ellert[161], F. Ellinghaus[171], N. Ellis[36], J. Elmsheuser[29], M. Elsing[36], D. Emeliyanov[134], Y. Enari[153], I. Ene[17a], S. Epari[13], J. Erdmann[49], P.A. Erland[87], M. Errenst[171], M. Escalier[66], C. Escobar[163], E. Etzion[151], G. Evans[130a], H. Evans[68], L.S. Evans[95], M.O. Evans[146], A. Ezhilov[37], S. Ezzarqtouni[35a], F. Fabbri[59], L. Fabbri[23b,23a], G. Facini[96], V. Fadeyev[136], R.M. Fakhrutdinov[37], D. Fakoudis[100], S. Falciano[75a], L.F. Falda Ulhoa Coelho[36], P.J. Falke[24], J. Faltova[133], C. Fan[162], Y. Fan[14a], Y. Fang[14a,14e], M. Fanti[71a,71b], M. Faraj[69a,69b], Z. Farazpay[97], A. Farbin[8], A. Farilla[77a], T. Farooque[107], S.M. Farrington[52], F. Fassi[35e], D. Fassouliotis[9], M. Faucci Giannelli[76a,76b], W.J. Fawcett[32], L. Fayard[66], P. Federic[133], P. Federicova[131], O.L. Fedin[37,a], G. Fedotov[37], M. Feickert[170], L. Feligioni[102], D.E. Fellers[123], C. Feng[62b], M. Feng[14b], Z. Feng[114], M.J. Fenton[160], A.B. Fenyuk[37], L. Ferencz[48], R.A.M. Ferguson[91], S.I. Fernandez Luengo[137f], P. Fernandez Martinez[13], M.J.V. Fernoux[102], J. Ferrando[48], A. Ferrari[161], P. Ferrari[114,113], R. Ferrari[73a], D. Ferrere[56], C. Ferretti[106], F. Fiedler[100], P. Fiedler[132], A. Filipčič[93], E.K. Filmer[1], F. Filthaut[113], M.C.N. Fiolhais[130a,130c,c], L. Fiorini[163], W.C. Fisher[107], T. Fitschen[101], P.M. Fitzhugh[135], I. Fleck[141], P. Fleischmann[106], T. Flick[171], M. Flores[33d,ac], L.R. Flores Castillo[64a], L. Flores Sanz De Acedo[36], F.M. Follega[78a,78b], N. Fomin[16], J.H. Foo[155], B.C. Forland[68], A. Formica[135], A.C. Forti[101], E. Fortin[36], A.W. Fortman[61], M.G. Foti[17a], L. Fountas[9,j], D. Fournier[66], H. Fox[91], P. Francavilla[74a,74b], S. Francescato[61], S. Franchellucci[56], M. Franchini[23b,23a], S. Franchino[63a], D. Francis[36], L. Franco[113], V. Franco Lima[36], L. Franconi[48], M. Franklin[61], G. Frattari[26], A.C. Freegard[94], W.S. Freund[83b], Y.Y. Frid[151], J. Friend[59], N. Fritzsche[50], A. Froch[54], D. Froidevaux[36], J.A. Frost[126], Y. Fu[62a], S. Fuenzalida Garrido[137f], M. Fujimoto[102], K.Y. Fung[64a], E. Furtado De Simas Filho[83b], M. Furukawa[153], J. Fuster[163], A. Gabrielli[23b,23a], A. Gabrielli[155], P. Gadow[36], G. Gagliardi[57b,57a], L.G. Gagnon[17a], E.J. Gallas[126], B.J. Gallop[134], K.K. Gan[119], S. Ganguly[153], Y. Gao[52], F.M. Garay Walls[137a,137b], B. Garcia[29], C. García[163], A. Garcia Alonso[114], A.G. Garcia Caffaro[172], J.E. García Navarro[163], M. Garcia-Sciveres[17a], G.L. Gardner[128], R.W. Gardner[39], N. Garelli[158], D. Garg[80], R.B. Garg[143,n], J.M. Gargan[52], C.A. Garner[155], C.M. Garvey[33a], P. Gaspar[83b], V.K. Gassmann[158], G. Gaudio[73a], V. Gautam[13], P. Gauzzi[75a,75b], I.L. Gavrilenko[37], A. Gavrilyuk[37], C. Gay[164], G. Gaycken[48], E.N. Gazis[10], A.A. Geanta[27b], C.M. Gee[136], A. Gekow[119], C. Gemme[57b], M.H. Genest[60], S. Gentile[75a,75b], A.D. Gentry[112], S. George[95],

JHEP05(2024)106

W.F. George[20], T. Geralis[46], P. Gessinger-Befurt[36], M.E. Geyik[171], M. Ghani[167], M. Ghneimat[141], K. Ghorbanian[94], A. Ghosal[141], A. Ghosh[160], A. Ghosh[7], B. Giacobbe[23b], S. Giagu[75a,75b], T. Giani[114], P. Giannetti[74a], A. Giannini[62a], S.M. Gibson[95], M. Gignac[136], D.T. Gil[86b], A.K. Gilbert[86a], B.J. Gilbert[41], D. Gillberg[34], G. Gilles[114], N.E.K. Gillwald[48], L. Ginabat[127], D.M. Gingrich[2,af], M.P. Giordani[69a,69c], P.F. Giraud[135], G. Giugliarelli[69a,69c], D. Giugni[71a], F. Giuli[36], I. Gkialas[9,j], L.K. Gladilin[37], C. Glasman[99], G.R. Gledhill[123], G. Glemža[48], M. Glisic[123], I. Gnesi[43b,f], Y. Go[29,ai], M. Goblirsch-Kolb[36], B. Gocke[49], D. Godin[108], B. Gokturk[21a], S. Goldfarb[105], T. Golling[56], M.G.D. Gololo[33g], D. Golubkov[37], J.P. Gombas[107], A. Gomes[130a,130b], G. Gomes Da Silva[141], A.J. Gomez Delegido[163], R. Gonçalo[130a,130c], G. Gonella[123], L. Gonella[20], A. Gongadze[149c], F. Gonnella[20], J.L. Gonski[41], R.Y. González Andana[52], S. González de la Hoz[163], S. Gonzalez Fernandez[13], R. Gonzalez Lopez[92], C. Gonzalez Renteria[17a], M.V. Gonzalez Rodrigues[48], R. Gonzalez Suarez[161], S. Gonzalez-Sevilla[56], G.R. Gonzalvo Rodriguez[163], L. Goossens[36], B. Gorini[36], E. Gorini[70a,70b], A. Gorišek[93], T.C. Gosart[128], A.T. Goshaw[51], M.I. Gostkin[38], S. Goswami[121], C.A. Gottardo[36], S.A. Gotz[109], M. Gouighri[35b], V. Goumarre[48], A.G. Goussiou[138], N. Govender[33c], I. Grabowska-Bold[86a], K. Graham[34], E. Gramstad[125], S. Grancagnolo[70a,70b], M. Grandi[146], C.M. Grant[1,135], P.M. Gravila[27f], F.G. Gravili[70a,70b], H.M. Gray[17a], M. Greco[70a,70b], C. Grefe[24], I.M. Gregor[48], P. Grenier[143], S.G. Grewe[110], C. Grieco[13], A.A. Grillo[136], K. Grimm[31], S. Grinstein[13,s], J.-F. Grivaz[66], E. Gross[169], J. Grosse-Knetter[55], C. Grud[106], J.C. Grundy[126], L. Guan[106], W. Guan[29], C. Gubbels[164], J.G.R. Guerrero Rojas[163], G. Guerrieri[69a,69c], F. Guescini[110], R. Gugel[100], J.A.M. Guhit[106], A. Guida[18], E. Guilloton[167,134], S. Guindon[36], F. Guo[14a,14e], J. Guo[62c], L. Guo[48], Y. Guo[106], R. Gupta[48], R. Gupta[129], S. Gurbuz[24], S.S. Gurdasani[54], G. Gustavino[36], M. Guth[56], P. Gutierrez[120], L.F. Gutierrez Zagazeta[128], M. Gutsche[50], C. Gutschow[96], C. Gwenlan[126], C.B. Gwilliam[92], E.S. Haaland[125], A. Haas[117], M. Habedank[48], C. Haber[17a], H.K. Hadavand[8], A. Hadef[50], S. Hadzic[110], A.I. Hagan[91], J.J. Hahn[141], E.H. Haines[96], M. Haleem[166], J. Haley[121], J.J. Hall[139], G.D. Hallewell[102], L. Halser[19], K. Hamano[165], M. Hamer[24], G.N. Hamity[52], E.J. Hampshire[95], J. Han[62b], K. Han[62a], L. Han[14c], L. Han[62a], S. Han[17a], Y.F. Han[155], K. Hanagaki[84], M. Hance[136], D.A. Hangal[41,ab], H. Hanif[142], M.D. Hank[128], R. Hankache[101], J.B. Hansen[42], J.D. Hansen[42], P.H. Hansen[42], K. Hara[157], D. Harada[56], T. Harenberg[171], S. Harkusha[37], M.L. Harris[103], Y.T. Harris[126], J. Harrison[13], N.M. Harrison[119], P.F. Harrison[167], N.M. Hartman[110], N.M. Hartmann[109], Y. Hasegawa[140], R. Hauser[107], C.M. Hawkes[20], R.J. Hawkings[36], Y. Hayashi[153], S. Hayashida[111], D. Hayden[107], C. Hayes[106], R.L. Hayes[114], C.P. Hays[126], J.M. Hays[94], H.S. Hayward[92], F. He[62a], M. He[14a,14e], Y. He[154], Y. He[48], N.B. Heatley[94], V. Hedberg[98], A.L. Heggelund[125], N.D. Hehir[94,*], C. Heidegger[54], K.K. Heidegger[54], W.D. Heidorn[81], J. Heilman[34], S. Heim[48], T. Heim[17a], J.G. Heinlein[128], J.J. Heinrich[123], L. Heinrich[110,ad], J. Hejbal[131], L. Helary[48], A. Held[170], S. Hellesund[16], C.M. Helling[164], S. Hellman[47a,47b], R.C.W. Henderson[91], L. Henkelmann[32], A.M. Henriques Correia[36], H. Herde[98], Y. Hernández Jiménez[145], L.M. Herrmann[24], T. Herrmann[50], G. Herten[54], R. Hertenberger[109], L. Hervas[36], M.E. Hesping[100], N.P. Hessey[156a], H. Hibi[85], E. Hill[155], S.J. Hillier [20], J.R. Hinds [107], F. Hinterkeuser [24], M. Hirose [124], S. Hirose [157], D. Hirschbuehl [171], T.G. Hitchings [101], B. Hiti [93], J. Hobbs [145], R. Hobincu [27e], N. Hod [169], M.C. Hodgkinson [139], B.H. Hodkinson [32], A. Hoecker [36], D.D. Hofer [106], J. Hofer [48], T. Holm [24], M. Holzbock [110], L.B.A.H. Hommels [32], B.P. Honan [101], J. Hong [62c], T.M. Hong [129], B.H. Hooberman [162], W.H. Hopkins [6], Y. Horii [111], S. Hou [148], A.S. Howard [93], J. Howarth [59], J. Hoya [6], M. Hrabovsky [122], A. Hrynevich [48], T. Hryn'ova [4], P.J. Hsu [65], S.-C. Hsu [138], Q. Hu [62a], Y.F. Hu [14a,14e], S. Huang [64b], X. Huang [14c], X. Huang [14a,14e], Y. Huang [139], Y. Huang [14a], Z. Huang [101], Z. Hubacek [132], M. Huebner [24], F. Huegging [24], T.B. Huffman [126], C.A. Hugli [48], M. Huhtinen [36], S.K. Huiberts [16], R. Hulsken [104], N. Huseynov [12], J. Huston [107], J. Huth [61], R. Hyneman [143], G. Iacobucci [56], G. Iakovidis [29], I. Ibragimov [141], L. Iconomidou-Fayard [66], P. Iengo [72a,72b], R. Iguchi [153], T. Iizawa [126], Y. Ikegami [84], N. Ilic [155], H. Imam [35a], M. Ince Lezki [56], T. Ingebretsen Carlson [47a,47b], G. Introzzi [73a,73b], M. Iodice [77a], V. Ippolito [75a,75b], R.K. Irwin [92], M. Ishino [153], W. Islam [170], C. Issever [18,48], S. Istin [21a,ak], H. Ito [168], J.M. Iturbe Ponce [64a], R. Iuppa [78a,78b], A. Ivina [169], J.M. Izen [45], V. Izzo [72a], P. Jacka [131,132], P. Jackson [1], R.M. Jacobs [48], B.P. Jaeger [142], C.S. Jagfeld [109], G. Jain [156a], P. Jain [54], K. Jakobs [54], T. Jakoubek [169], J. Jamieson [59], K.W. Janas [86a], M. Javurkova [103], F. Jeanneau [135], L. Jeanty [123], J. Jejelava [149a,z], P. Jenni [54,g], C.E. Jessiman [34], S. Jézéquel [4], C. Jia [62b], J. Jia [145], X. Jia [61], X. Jia [14a,14e], Z. Jia [14c], S. Jiggins [48], J. Jimenez Pena [13], S. Jin [14c], A. Jinaru [27b], O. Jinnouchi [154], P. Johansson [139], K.A. Johns [7], J.W. Johnson [136], D.M. Jones [32], E. Jones [48], P. Jones [32], R.W.L. Jones [91], T.J. Jones [92], H.L. Joos [55,36], R. Joshi [119], J. Jovicevic [15], X. Ju [17a], J.J. Junggeburth [103], T. Junkermann [63a], A. Juste Rozas [13,s], M.K. Juzek [87], S. Kabana [137e], A. Kaczmarska [87], M. Kado [110], H. Kagan [119], M. Kagan [143], A. Kahn [41], A. Kahn [128], C. Kahra [100], T. Kaji [153], E. Kajomovitz [150], N. Kakati [169], I. Kalaitzidou [54], C.W. Kalderon [29], A. Kamenshchikov [155], N.J. Kang [136], D. Kar [33g], K. Karava [126], M.J. Kareem [156b], E. Karentzos [54], I. Karkanias [152], O. Karkout [114], S.N. Karpov [38], Z.M. Karpova [38], V. Kartvelishvili [91], A.N. Karyukhin [37], E. Kasimi [152], J. Katzy [48], S. Kaur [34], K. Kawade [140], M.P. Kawale [120], C. Kawamoto [88], T. Kawamoto [62a], E.F. Kay [36], F.I. Kaya [158], S. Kazakos [107], V.F. Kazanin [37], Y. Ke [145], J.M. Keaveney [33a], R. Keeler [165], G.V. Kehris [61], J.S. Keller [34], A.S. Kelly [96], J.J. Kempster [146], K.E. Kennedy [41], P.D. Kennedy [100], O. Kepka [131], B.P. Kerridge [167], S. Kersten [171], B.P. Kerševan [93], S. Keshri [66], L. Keszeghova [28a], S. Ketabchi Haghighat [155], R.A. Khan [129], M. Khandoga [127], A. Khanov [121], A.G. Kharlamov [37], T. Kharlamova [37], E.E. Khoda [138], M. Kholodenko [37], T.J. Khoo [18], G. Khoriauli [166], J. Khubua [149b], Y.A.R. Khwaira [66], A. Kilgallon [123], D.W. Kim [47a,47b], Y.K. Kim [39], N. Kimura [96], M.K. Kingston [55], A. Kirchhoff [55], C. Kirfel [24], F. Kirfel [24], J. Kirk [134], A.E. Kiryunin [110], C. Kitsaki [10], O. Kivernyk [24], M. Klassen [63a], C. Klein [34], L. Klein [166], M.H. Klein [106], M. Klein [92], S.B. Klein [56], U. Klein [92], P. Klimek [36], A. Klimentov [29], T. Klioutchnikova [36], P. Kluit [114], S. Kluth [110], E. Kneringer [79], T.M. Knight [155], A. Knue [49], R. Kobayashi [88], D. Kobylianskii [169], S.F. Koch [126], M. Kocian [143], P. Kodyš [133], D.M. Koeck [123], P.T. Koenig [24], T. Koffas [34], O. Kolay [50], I. Koletsou [4], T. Komarek [122], K. Köneke [54], A.X.Y. Kong [1], T. Kono [118], N. Konstantinidis [96], P. Kontaxakis [56], B. Konya [98], R. Kopeliansky [68], S. Koperny [86a],

K. Korcyl[87], K. Kordas[152,e], G. Koren[151], A. Korn[96], S. Korn[55], I. Korolkov[13], N. Korotkova[37], B. Kortman[114], O. Kortner[110], S. Kortner[110], W.H. Kostecka[115], V.V. Kostyukhin[141], A. Kotsokechagia[135], A. Kotwal[51], A. Koulouris[36], A. Kourkoumeli-Charalampidi[73a,73b], C. Kourkoumelis[9], E. Kourlitis[110,ad], O. Kovanda[146], R. Kowalewski[165], W. Kozanecki[135], A.S. Kozhin[37], V.A. Kramarenko[37], G. Kramberger[93], P. Kramer[100], M.W. Krasny[127], A. Krasznahorkay[36], J.W. Kraus[171], J.A. Kremer[48], T. Kresse[50], J. Kretzschmar[92], K. Kreul[18], P. Krieger[155], S. Krishnamurthy[103], M. Krivos[133], K. Krizka[20], K. Kroeninger[49], H. Kroha[110], J. Kroll[131], J. Kroll[128], K.S. Krowpman[107], U. Kruchonak[38], H. Krüger[24], N. Krumnack[81], M.C. Kruse[51], O. Kuchinskaia[37], S. Kuday[3a], S. Kuehn[36], R. Kuesters[54], T. Kuhl[48], V. Kukhtin[38], Y. Kulchitsky[37,a], S. Kuleshov[137d,137b], M. Kumar[33g], N. Kumari[48], P. Kumari[156b], A. Kupco[131], T. Kupfer[49], A. Kupich[37], O. Kuprash[54], H. Kurashige[85], L.L. Kurchaninov[156a], O. Kurdysh[66], Y.A. Kurochkin[37], A. Kurova[37], M. Kuze[154], A.K. Kvam[103], J. Kvita[122], T. Kwan[104], N.G. Kyriacou[106], L.A.O. Laatu[102], C. Lacasta[163], F. Lacava[75a,75b], H. Lacker[18], D. Lacour[127], N.N. Lad[96], E. Ladygin[38], B. Laforge[127], T. Lagouri[137e], F.Z. Lahbabi[35a], S. Lai[55], I.K. Lakomiec[86a], N. Lalloue[60], J.E. Lambert[165], S. Lammers[68], W. Lampl[7], C. Lampoudis[152,e], A.N. Lancaster[115], E. Lançon[29], U. Landgraf[54], M.P.J. Landon[94], V.S. Lang[54], R.J. Langenberg[103], O.K.B. Langrekken[125], A.J. Lankford[160], F. Lanni[36], K. Lantzsch[24], A. Lanza[73a], A. Lapertosa[57b,57a], J.F. Laporte[135], T. Lari[71a], F. Lasagni Manghi[23b], M. Lassnig[36], V. Latonova[131], A. Laudrain[100], A. Laurier[150], S.D. Lawlor[139], Z. Lawrence[101], R. Lazaridou[167], M. Lazzaroni[71a,71b], B. Le[101], E.M. Le Boulicaut[51], B. Leban[93], A. Lebedev[81], M. LeBlanc[101], F. Ledroit-Guillon[60], A.C.A. Lee[96], S.C. Lee[148], S. Lee[47a,47b], T.F. Lee[92], L.L. Leeuw[33c], H.P. Lefebvre[95], M. Lefebvre[165], C. Leggett[17a], G. Lehmann Miotto[36], M. Leigh[56], W.A. Leight[103], W. Leinonen[113], A. Leisos[152,r], M.A.L. Leite[83c], C.E. Leitgeb[48], R. Leitner[133], K.J.C. Leney[44], T. Lenz[24], S. Leone[74a], C. Leonidopoulos[52], A. Leopold[144], C. Leroy[108], R. Les[107], C.G. Lester[32], M. Levchenko[37], J. Levêque[4], D. Levin[106], L.J. Levinson[169], M.P. Lewicki[87], D.J. Lewis[4], A. Li[5], B. Li[62b], C. Li[62a], C-Q. Li[110], H. Li[62a], H. Li[62b], H. Li[14c], H. Li[14b], H. Li[62b], J. Li[62c], K. Li[138], L. Li[62c], M. Li[14a,14e], Q.Y. Li[62a], S. Li[14a,14e], S. Li[62d,62c,d], T. Li[5], X. Li[104], Z. Li[126], Z. Li[104], Z. Li[14a,14e], S. Liang[14a,14e], Z. Liang[14a], M. Liberatore[135], B. Liberti[76a], K. Lie[64c], J. Lieber Marin[83b], H. Lien[68], K. Lin[107], R.E. Lindley[7], J.H. Lindon[2], E. Lipeles[128], A. Lipniacka[16], A. Lister[164], J.D. Little[4], B. Liu[14a], B.X. Liu[142], D. Liu[62d,62c], J.B. Liu[62a], J.K.K. Liu[32], K. Liu[62d,62c], M. Liu[62a], M.Y. Liu[62a], P. Liu[14a], Q. Liu[62d,138,62c], X. Liu[62a], X. Liu[62b], Y. Liu[14d,14e], Y.L. Liu[62b], Y.W. Liu[62a], J. Llorente Merino[142], S.L. Lloyd[94], E.M. Lobodzinska[48], P. Loch[7], T. Lohse[18], K. Lohwasser[139], E. Loiacono[48], M. Lokajicek[131,*], J.D. Lomas[20], J.D. Long[162], I. Longarini[160], L. Longo[70a,70b], R. Longo[162], I. Lopez Paz[67], A. Lopez Solis[48], N. Lorenzo Martinez[4], A.M. Lory[109], G. Löschcke Centeno[146], O. Loseva[37], X. Lou[47a,47b], X. Lou[14a,14e], A. Lounis[66], J. Love[6], P.A. Love[91], G. Lu[14a,14e], M. Lu[80], S. Lu[128], Y.J. Lu[65], H.J. Lubatti[138], C. Luci[75a,75b], F.L. Lucio Alves[14c], A. Lucotte[60], F. Luehring[68], I. Luise[145], O. Lukianchuk[66], O. Lundberg[144], B. Lund-Jensen[144], N.A. Luongo[6], M.S. Lutz[151],

JHEP05(2024)106

A.B. Lux[25], D. Lynn[29], H. Lyons[92], R. Lysak[131], E. Lytken[98], V. Lyubushkin[38], T. Lyubushkina[38], M.M. Lyukova[145], H. Ma[29], K. Ma[62a], L.L. Ma[62b], W. Ma[62a], Y. Ma[121], D.M. Mac Donell[165], G. Maccarrone[53], J.C. MacDonald[100], P.C. Machado De Abreu Farias[83b], R. Madar[40], W.F. Mader[50], T. Madula[96], J. Maeda[85], T. Maeno[29], H. Maguire[139], V. Maiboroda[135], A. Maio[130a,130b,130d], K. Maj[86a], O. Majersky[48], S. Majewski[123], N. Makovec[66], V. Maksimovic[15], B. Malaescu[127], Pa. Malecki[87], V.P. Maleev[37], F. Malek[60], M. Mali[93], D. Malito[95], U. Mallik[80], S. Maltezos[10], S. Malyukov[38], J. Mamuzic[13], G. Mancini[53], G. Manco[73a,73b], J.P. Mandalia[94], I. Mandić[93], L. Manhaes de Andrade Filho[83a], I.M. Maniatis[169], J. Manjarres Ramos[102,aa], D.C. Mankad[169], A. Mann[109], B. Mansoulie[135], S. Manzoni[36], L. Mao[62c], X. Mapekula[33c], A. Marantis[152,r], G. Marchiori[5], M. Marcisovsky[131], C. Marcon[71a], M. Marinescu[20], S. Marium[48], M. Marjanovic[120], E.J. Marshall[91], Z. Marshall[17a], S. Marti-Garcia[163], T.A. Martin[167], V.J. Martin[52], B. Martin dit Latour[16], L. Martinelli[75a,75b], M. Martinez[13,s], P. Martinez Agullo[163], V.I. Martinez Outschoorn[103], P. Martinez Suarez[13], S. Martin-Haugh[134], V.S. Martoiu[27b], A.C. Martyniuk[96], A. Marzin[36], D. Mascione[78a,78b], L. Masetti[100], T. Mashimo[153], J. Masik[101], A.L. Maslennikov[37], L. Massa[23b], P. Massarotti[72a,72b], P. Mastrandrea[74a,74b], A. Mastroberardino[43b,43a], T. Masubuchi[153], T. Mathisen[161], J. Matousek[133], N. Matsuzawa[153], J. Maurer[27b], B. Maček[93], D.A. Maximov[37], R. Mazini[148], I. Maznas[152], M. Mazza[107], S.M. Mazza[136], E. Mazzeo[71a,71b], C. Mc Ginn[29], J.P. Mc Gowan[104], S.P. Mc Kee[106], C.C. McCracken[164], E.F. McDonald[105], A.E. McDougall[114], J.A. Mcfayden[146], R.P. McGovern[128], G. Mchedlidze[149b], R.P. Mckenzie[33g], T.C. Mclachlan[48], D.J. Mclaughlin[96], S.J. McMahon[134], C.M. Mcpartland[92], R.A. McPherson[165,w], S. Mehlhase[109], A. Mehta[92], D. Melini[150], B.R. Mellado Garcia[33g], A.H. Melo[55], F. Meloni[48], A.M. Mendes Jacques Da Costa[101], H.Y. Meng[155], L. Meng[91], S. Menke[110], M. Mentink[36], E. Meoni[43b,43a], G. Mercado[115], C. Merlassino[69a,69c], L. Merola[72a,72b], C. Meroni[71a,71b], G. Merz[106], J. Metcalfe[6], A.S. Mete[6], C. Meyer[68], J-P. Meyer[135], R.P. Middleton[134], L. Mijović[52], G. Mikenberg[169], M. Mikestikova[131], M. Mikuž[93], H. Mildner[100], A. Milic[36], C.D. Milke[44], D.W. Miller[39], L.S. Miller[34], A. Milov[169], D.A. Milstead[47a,47b], T. Min[14c], A.A. Minaenko[37], I.A. Minashvili[149b], L. Mince[59], A.I. Mincer[117], B. Mindur[86a], M. Mineev[38], Y. Mino[88], L.M. Mir[13], M. Miralles Lopez[163], M. Mironova[17a], A. Mishima[153], M.C. Missio[113], A. Mitra[167], V.A. Mitsou[163], Y. Mitsumori[111], O. Miu[155], P.S. Miyagawa[94], T. Mkrtchyan[63a], M. Mlinarevic[96], T. Mlinarevic[96], M. Mlynarikova[36], S. Mobius[19], P. Moder[48], P. Mogg[109], M.H. Mohamed Farook[112], A.F. Mohammed[14a,14e], S. Mohapatra[41], G. Mokgatitswane[33g], L. Moleri[169], B. Mondal[141], S. Mondal[132], K. Mönig[48], E. Monnier[102], L. Monsonis Romero[163], J. Montejo Berlingen[13], M. Montella[119], F. Montereali[77a,77b], F. Monticelli[90], S. Monzani[69a,69c], N. Morange[66], A.L. Moreira De Carvalho[130a], M. Moreno Llácer[163], C. Moreno Martinez[56], P. Morettini[57b], S. Morgenstern[36], M. Morii[61], M. Morinaga[153], A.K. Morley[36], F. Morodei[75a,75b], L. Morvaj[36], P. Moschovakos[36], B. Moser[36], M. Mosidze[149b], T. Moskalets[54], P. Moskvitina[113], J. Moss[31,l], E.J.W. Moyse[103], O. Mtintsilana[33g], S. Muanza[102], J. Mueller[129], D. Muenstermann[91], R. Müller[19], G.A. Mullier[161], A.J. Mullin[32],

JHEP05(2024)106

J.J. Mullin[128], D.P. Mungo[155], D. Munoz Perez[163], F.J. Munoz Sanchez[101], M. Murin[101], W.J. Murray[167,134], A. Murrone[71a,71b], M. Muškinja[17a], C. Mwewa[29], A.G. Myagkov[37,a], A.J. Myers[8], G. Myers[68], M. Myska[132], B.P. Nachman[17a], O. Nackenhorst[49], A. Nag[50], K. Nagai[126], K. Nagano[84], J.L. Nagle[29,ai], E. Nagy[102], A.M. Nairz[36], Y. Nakahama[84], K. Nakamura[84], K. Nakkalil[5], H. Nanjo[124], R. Narayan[44], E.A. Narayanan[112], I. Naryshkin[37], M. Naseri[34], S. Nasri[159], C. Nass[24], G. Navarro[22a], J. Navarro-Gonzalez[163], R. Nayak[151], A. Nayaz[18], P.Y. Nechaeva[37], F. Nechansky[48], L. Nedic[126], T.J. Neep[20], A. Negri[73a,73b], M. Negrini[23b], C. Nellist[114], C. Nelson[104], K. Nelson[106], S. Nemecek[131], M. Nessi[36,h], M.S. Neubauer[162], F. Neuhaus[100], J. Neundorf[48], R. Newhouse[164], P.R. Newman[20], C.W. Ng[129], Y.W.Y. Ng[48], B. Ngair[35e], H.D.N. Nguyen[108], R.B. Nickerson[126], R. Nicolaidou[135], J. Nielsen[136], M. Niemeyer[55], J. Niermann[55,36], N. Nikiforou[36], V. Nikolaenko[37,a], I. Nikolic-Audit[127], K. Nikolopoulos[20], P. Nilsson[29], I. Ninca[48], H.R. Nindhito[56], G. Ninio[151], A. Nisati[75a], N. Nishu[2], R. Nisius[110], J-E. Nitschke[50], E.K. Nkadimeng[33g], T. Nobe[153], D.L. Noel[32], T. Nommensen[147], M.B. Norfolk[139], R.R.B. Norisam[96], B.J. Norman[34], M. Noury[35a], J. Novak[93], T. Novak[48], L. Novotny[132], R. Novotny[112], L. Nozka[122], K. Ntekas[160], N.M.J. Nunes De Moura Junior[83b], E. Nurse[96], J. Ocariz[127], A. Ochi[85], I. Ochoa[130a], S. Oerdek[48,t], J.T. Offermann[39], A. Ogrodnik[133], A. Oh[101], C.C. Ohm[144], H. Oide[84], R. Oishi[153], M.L. Ojeda[48], M.W. O'Keefe[92], Y. Okumura[153], L.F. Oleiro Seabra[130a], S.A. Olivares Pino[137d], D. Oliveira Damazio[29], D. Oliveira Goncalves[83a], J.L. Oliver[160], Ö.O. Öncel[54], A.P. O'Neill[19], A. Onofre[130a,130e], P.U.E. Onyisi[11], M.J. Oreglia[39], G.E. Orellana[90], D. Orestano[77a,77b], N. Orlando[13], R.S. Orr[155], V. O'Shea[59], L.M. Osojnak[128], R. Ospanov[62a], G. Otero y Garzon[30], H. Otono[89], P.S. Ott[63a], G.J. Ottino[17a], M. Ouchrif[35d], J. Ouellette[29], F. Ould-Saada[125], M. Owen[59], R.E. Owen[134], K.Y. Oyulmaz[21a], V.E. Ozcan[21a], F. Ozturk[87], N. Ozturk[8], S. Ozturk[82], H.A. Pacey[126], A. Pacheco Pages[13], C. Padilla Aranda[13], G. Padovano[75a,75b], S. Pagan Griso[17a], G. Palacino[68], A. Palazzo[70a,70b], S. Palestini[36], J. Pan[172], T. Pan[64a], D.K. Panchal[11], C.E. Pandini[114], J.G. Panduro Vazquez[95], H.D. Pandya[1], H. Pang[14b], P. Pani[48], G. Panizzo[69a,69c], L. Paolozzi[56], C. Papadatos[108], S. Parajuli[44], A. Paramonov[6], C. Paraskevopoulos[10], D. Paredes Hernandez[64b], K.R. Park[41], T.H. Park[155], M.A. Parker[32], F. Parodi[57b,57a], E.W. Parrish[115], V.A. Parrish[52], J.A. Parsons[41], U. Parzefall[54], B. Pascual Dias[108], L. Pascual Dominguez[151], E. Pasqualucci[75a], S. Passaggio[57b], F. Pastore[95], P. Pasuwan[47a,47b], P. Patel[87], U.M. Patel[51], J.R. Pater[101], T. Pauly[36], J. Pearkes[143], M. Pedersen[125], R. Pedro[130a], S.V. Peleganchuk[37], O. Penc[36], E.A. Pender[52], K.E. Penski[109], M. Penzin[37], B.S. Peralva[83d], A.P. Pereira Peixoto[60], L. Pereira Sanchez[47a,47b], D.V. Perepelitsa[29,ai], E. Perez Codina[156a], M. Perganti[10], L. Perini[71a,71b,*], H. Pernegger[36], O. Perrin[40], K. Peters[48], R.F.Y. Peters[101], B.A. Petersen[36], T.C. Petersen[42], E. Petit[102], V. Petousis[132], C. Petridou[152,e], A. Petrukhin[141], M. Pettee[17a], N.E. Pettersson[36], A. Petukhov[37], K. Petukhova[133], R. Pezoa[137f], L. Pezzotti[36], G. Pezzullo[172], T.M. Pham[170], T. Pham[105], P.W. Phillips[134], G. Piacquadio[145], E. Pianori[17a], F. Piazza[123], R. Piegaia[30], D. Pietreanu[27b], A.D. Pilkington[101], M. Pinamonti[69a,69c], J.L. Pinfold[2], B.C. Pinheiro Pereira[130a], A.E. Pinto Pinoargote[100,135], L. Pintucci[69a,69c],

JHEP05(2024)106

K.M. Piper[146], A. Pirttikoski[56], D.A. Pizzi[34], L. Pizzimento[64b], A. Pizzini[114], M.-A. Pleier[29], V. Plesanovs[54], V. Pleskot[133], E. Plotnikova[38], G. Poddar[4], R. Poettgen[98], L. Poggioli[127], I. Pokharel[55], S. Polacek[133], G. Polesello[73a], A. Poley[142,156a], R. Polifka[132], A. Polini[23b], C.S. Pollard[167], Z.B. Pollock[119], V. Polychronakos[29], E. Pompa Pacchi[75a,75b], D. Ponomarenko[113], L. Pontecorvo[36], S. Popa[27a], G.A. Popeneciu[27d], A. Poreba[36], D.M. Portillo Quintero[156a], S. Pospisil[132], M.A. Postill[139], P. Postolache[27c], K. Potamianos[167], P.A. Potepa[86a], I.N. Potrap[38], C.J. Potter[32], H. Potti[1], T. Poulsen[48], J. Poveda[163], M.E. Pozo Astigarraga[36], A. Prades Ibanez[163], J. Pretel[54], D. Price[101], M. Primavera[70a], M.A. Principe Martin[99], R. Privara[122], T. Procter[59], M.L. Proffitt[138], N. Proklova[128], K. Prokofiev[64c], G. Proto[110], S. Protopopescu[29], J. Proudfoot[6], M. Przybycien[86a], W.W. Przygoda[86b], J.E. Puddefoot[139], D. Pudzha[37], D. Pyatiizbyantseva[37], J. Qian[106], D. Qichen[101], Y. Qin[101], T. Qiu[52], A. Quadt[55], M. Queitsch-Maitland[101], G. Quetant[56], R.P. Quinn[164], G. Rabanal Bolanos[61], D. Rafanoharana[54], F. Ragusa[71a,71b], J.L. Rainbolt[39], J.A. Raine[56], S. Rajagopalan[29], E. Ramakoti[37], I.A. Ramirez-Berend[34], K. Ran[48,14e], N.P. Rapheeha[33g], H. Rasheed[27b], V. Raskina[127], D.F. Rassloff[63a], A. Rastogi[17a], S. Rave[100], B. Ravina[55], I. Ravinovich[169], M. Raymond[36], A.L. Read[125], N.P. Readioff[139], D.M. Rebuzzi[73a,73b], G. Redlinger[29], A.S. Reed[110], K. Reeves[26], J.A. Reidelsturz[171], D. Reikher[151], A. Rej[49], C. Rembser[36], A. Renardi[48], M. Renda[27b], M.B. Rendel[110], F. Renner[48], A.G. Rennie[160], A.L. Rescia[48], S. Resconi[71a], M. Ressegotti[57b,57a], S. Rettie[36], J.G. Reyes Rivera[107], E. Reynolds[17a], O.L. Rezanova[37], P. Reznicek[133], N. Ribaric[91], E. Ricci[78a,78b], R. Richter[110], S. Richter[47a,47b], E. Richter-Was[86b], M. Ridel[127], S. Ridouani[35d], P. Rieck[117], P. Riedler[36], E.M. Riefel[47a,47b], J.O. Rieger[114], M. Rijssenbeek[145], A. Rimoldi[73a,73b], M. Rimoldi[36], L. Rinaldi[23b,23a], T.T. Rinn[29], M.P. Rinnagel[109], G. Ripellino[161], I. Riu[13], P. Rivadeneira[48], J.C. Rivera Vergara[165], F. Rizatdinova[121], E. Rizvi[94], B.A. Roberts[167], B.R. Roberts[17a], S.H. Robertson[104,w], D. Robinson[32], C.M. Robles Gajardo[137f], M. Robles Manzano[100], A. Robson[59], A. Rocchi[76a,76b], C. Roda[74a,74b], S. Rodriguez Bosca[63a], Y. Rodriguez Garcia[22a], A. Rodriguez Rodriguez[54], A.M. Rodríguez Vera[156b], S. Roe[36], J.T. Roemer[160], A.R. Roepe-Gier[136], J. Roggel[171], O. Røhne[125], R.A. Rojas[103], C.P.A. Roland[127], J. Roloff[29], A. Romaniouk[37], E. Romano[73a,73b], M. Romano[23b], A.C. Romero Hernandez[162], N. Rompotis[92], L. Roos[127], S. Rosati[75a], B.J. Rosser[39], E. Rossi[126], E. Rossi[72a,72b], L.P. Rossi[57b], L. Rossini[54], R. Rosten[119], M. Rotaru[27b], B. Rottler[54], C. Rougier[102,aa], D. Rousseau[66], D. Rousso[32], A. Roy[162], S. Roy-Garand[155], A. Rozanov[102], Z.M.A. Rozario[59], Y. Rozen[150], X. Ruan[33g], A. Rubio Jimenez[163], A.J. Ruby[92], V.H. Ruelas Rivera[18], T.A. Ruggeri[1], A. Ruggiero[126], A. Ruiz-Martinez[163], A. Rummler[36], Z. Rurikova[54], N.A. Rusakovich[38], H.L. Russell[165], G. Russo[75a,75b], J.P. Rutherfoord[7], S. Rutherford Colmenares[32], K. Rybacki[91], M. Rybar[133], E.B. Rye[125], A. Ryzhov[44], J.A. Sabater Iglesias[56], P. Sabatini[163], H.F-W. Sadrozinski[136], F. Safai Tehrani[75a], B. Safarzadeh Samani[134], M. Safdari[143], S. Saha[165], M. Sahinsoy[110], A. Saibel[163], M. Saimpert[135], M. Saito[153], T. Saito[153], D. Salamani[36], A. Salnikov[143], J. Salt[163], A. Salvador Salas[151], D. Salvatore[43b,43a], F. Salvatore[146], A. Salzburger[36], D. Sammel[54], D. Sampsonidis[152,e], D. Sampsonidou[123], J. Sánchez[163], A. Sanchez Pineda[4], V. Sanchez Sebastian[163],

H. Sandaker[125], C.O. Sander[48], J.A. Sandesara[103], M. Sandhoff[171], C. Sandoval[22b], D.P.C. Sankey[134], T. Sano[88], A. Sansoni[53], L. Santi[75a,75b], C. Santoni[40], H. Santos[130a,130b], S.N. Santpur[17a], A. Santra[169], K.A. Saoucha[116b], J.G. Saraiva[130a,130d], J. Sardain[7], O. Sasaki[84], K. Sato[157], C. Sauer[63b], F. Sauerburger[54], E. Sauvan[4], P. Savard[155,af], R. Sawada[153], C. Sawyer[134], L. Sawyer[97], I. Sayago Galvan[163], C. Sbarra[23b], A. Sbrizzi[23b,23a], T. Scanlon[96], J. Schaarschmidt[138], P. Schacht[110], U. Schäfer[100], A.C. Schaffer[66,44], D. Schaile[109], R.D. Schamberger[145], C. Scharf[18], M.M. Schefer[19], V.A. Schegelsky[37], D. Scheirich[133], F. Schenck[18], M. Schernau[160], C. Scheulen[55], C. Schiavi[57b,57a], E.J. Schioppa[70a,70b], M. Schioppa[43b,43a], B. Schlag[143,n], K.E. Schleicher[54], S. Schlenker[36], J. Schmeing[171], M.A. Schmidt[171], K. Schmieden[100], C. Schmitt[100], N. Schmitt[100], S. Schmitt[48], L. Schoeffel[135], A. Schoening[63b], P.G. Scholer[54], E. Schopf[126], M. Schott[100], J. Schovancova[36], S. Schramm[56], F. Schroeder[171], T. Schroer[56], H-C. Schultz-Coulon[63a], M. Schumacher[54], B.A. Schumm[136], Ph. Schune[135], A.J. Schuy[138], H.R. Schwartz[136], A. Schwartzman[143], T.A. Schwarz[106], Ph. Schwemling[135], R. Schwienhorst[107], A. Sciandra[136], G. Sciolla[26], F. Scuri[74a], C.D. Sebastiani[92], K. Sedlaczek[115], P. Seema[18], S.C. Seidel[112], A. Seiden[136], B.D. Seidlitz[41], C. Seitz[48], J.M. Seixas[83b], G. Sekhniaidze[72a], S.J. Sekula[44], L. Selem[60], N. Semprini-Cesari[23b,23a], D. Sengupta[56], V. Senthilkumar[163], L. Serin[66], L. Serkin[69a,69b], M. Sessa[76a,76b], H. Severini[120], F. Sforza[57b,57a], A. Sfyrla[56], E. Shabalina[55], R. Shaheen[144], J.D. Shahinian[128], D. Shaked Renous[169], L.Y. Shan[14a], M. Shapiro[17a], A. Sharma[36], A.S. Sharma[164], P. Sharma[80], S. Sharma[48], P.B. Shatalov[37], K. Shaw[146], S.M. Shaw[101], A. Shcherbakova[37], Q. Shen[62c,5], D.J. Sheppard[142], P. Sherwood[96], L. Shi[96], X. Shi[14a], C.O. Shimmin[172], J.D. Shinner[95], I.P.J. Shipsey[126], S. Shirabe[56,h], M. Shiyakova[38,u], J. Shlomi[169], M.J. Shochet[39], J. Shojaii[105], D.R. Shope[125], B. Shrestha[120], S. Shrestha[119,aj], E.M. Shrif[33g], M.J. Shroff[165], P. Sicho[131], A.M. Sickles[162], E. Sideras Haddad[33g], A. Sidoti[23b], F. Siegert[50], Dj. Sijacki[15], F. Sili[90], J.M. Silva[20], M.V. Silva Oliveira[29], S.B. Silverstein[47a], S. Simion[66], R. Simoniello[36], E.L. Simpson[59], H. Simpson[146], L.R. Simpson[106], N.D. Simpson[98], S. Simsek[82], S. Sindhu[55], P. Sinervo[155], S. Singh[155], S. Sinha[48], S. Sinha[101], M. Sioli[23b,23a], I. Siral[36], E. Sitnikova[48], S.Yu. Sivoklokov[37,*], J. Sjölin[47a,47b], A. Skaf[55], E. Skorda[20], P. Skubic[120], M. Slawinska[87], V. Smakhtin[169], B.H. Smart[134], J. Smiesko[36], S.Yu. Smirnov[37], Y. Smirnov[37], L.N. Smirnova[37,a], O. Smirnova[98], A.C. Smith[41], E.A. Smith[39], H.A. Smith[126], J.L. Smith[92], R. Smith[143], M. Smizanska[91], K. Smolek[132], A.A. Snesarev[37], S.R. Snider[155], H.L. Snoek[114], S. Snyder[29], R. Sobie[165,w], A. Soffer[151], C.A. Solans Sanchez[36], E.Yu. Soldatov[37], U. Soldevila[163], A.A. Solodkov[37], S. Solomon[26], A. Soloshenko[38], K. Solovieva[54], O.V. Solovyanov[40], V. Solovyev[37], P. Sommer[36], A. Sonay[13], W.Y. Song[156b], J.M. Sonneveld[114], A. Sopczak[132], A.L. Sopio[96], F. Sopkova[28b], I.R. Sotarriva Alvarez[154], V. Sothilingam[63a], O.J. Soto Sandoval[137c,137b], S. Sottocornola[68], R. Soualah[116b], Z. Soumaimi[35e], D. South[48], N. Soybelman[169], S. Spagnolo[70a,70b], M. Spalla[110], D. Sperlich[54], G. Spigo[36], S. Spinali[91], D.P. Spiteri[59], M. Spousta[133], E.J. Staats[34], A. Stabile[71a,71b], R. Stamen[63a], A. Stampekis[20], M. Standke[24], E. Stanecka[87], M.V. Stange[50], B. Stanislaus[17a], M.M. Stanitzki[48], B. Stapf[48], E.A. Starchenko[37], G.H. Stark[136], J. Stark[102,aa], D.M. Starko[156b],

P. Staroba[131], P. Starovoitov[63a], S. Stärz[104], R. Staszewski[87], G. Stavropoulos[46], J. Steentoft[161], P. Steinberg[29], B. Stelzer[142,156a], H.J. Stelzer[129], O. Stelzer-Chilton[156a], H. Stenzel[58], T.J. Stevenson[146], G.A. Stewart[36], J.R. Stewart[121], M.C. Stockton[36], G. Stoicea[27b], M. Stolarski[130a], S. Stonjek[110], A. Straessner[50], J. Strandberg[144], S. Strandberg[47a,47b], M. Stratmann[171], M. Strauss[120], T. Strebler[102], P. Strizenec[28b], R. Ströhmer[166], D.M. Strom[123], R. Stroynowski[44], A. Strubig[47a,47b], S.A. Stucci[29], B. Stugu[16], J. Stupak[120], N.A. Styles[48], D. Su[143], S. Su[62a], W. Su[62d], X. Su[62a,66], K. Sugizaki[153], V.V. Sulin[37], M.J. Sullivan[92], D.M.S. Sultan[78a,78b], L. Sultanaliyeva[37], S. Sultansoy[3b], T. Sumida[88], S. Sun[106], S. Sun[170], O. Sunneborn Gudnadottir[161], N. Sur[102], M.R. Sutton[146], H. Suzuki[157], M. Svatos[131], M. Swiatlowski[156a], T. Swirski[166], I. Sykora[28a], M. Sykora[133], T. Sykora[133], D. Ta[100], K. Tackmann[48,t], A. Taffard[160], R. Tafirout[156a], J.S. Tafoya Vargas[66], E.P. Takeva[52], Y. Takubo[84], M. Talby[102], A.A. Talyshev[37], K.C. Tam[64b], N.M. Tamir[151], A. Tanaka[153], J. Tanaka[153], R. Tanaka[66], M. Tanasini[57b,57a], Z. Tao[164], S. Tapia Araya[137f], S. Tapprogge[100], A. Tarek Abouelfadl Mohamed[107], S. Tarem[150], K. Tariq[14a], G. Tarna[102,27b], G.F. Tartarelli[71a], P. Tas[133], M. Tasevsky[131], E. Tassi[43b,43a], A.C. Tate[162], G. Tateno[153], Y. Tayalati[35e,v], G.N. Taylor[105], W. Taylor[156b], A.S. Tee[170], R. Teixeira De Lima[143], P. Teixeira-Dias[95], J.J. Teoh[155], K. Terashi[153], J. Terron[99], S. Terzo[13], M. Testa[53], R.J. Teuscher[155,w], A. Thaler[79], O. Theiner[56], N. Themistokleous[52], T. Theveneaux-Pelzer[102], O. Thielmann[171], D.W. Thomas[95], J.P. Thomas[20], E.A. Thompson[17a], P.D. Thompson[20], E. Thomson[128], Y. Tian[55], V. Tikhomirov[37,a], Yu.A. Tikhonov[37], S. Timoshenko[37], D. Timoshyn[133], E.X.L. Ting[1], P. Tipton[172], S.H. Tlou[33g], A. Thourji[40], K. Todome[154], S. Todorova-Nova[133], S. Todt[50], M. Togawa[84], J. Tojo[89], S. Tokár[28a], K. Tokushuku[84], O. Toldaiev[68], R. Tombs[32], M. Tomoto[84,111], L. Tompkins[143,n], K.W. Topolnicki[86b], E. Torrence[123], H. Torres[102,aa], E. Torró Pastor[163], M. Toscani[30], C. Tosciri[39], M. Tost[11], D.R. Tovey[139], A. Traeet[16], I.S. Trandafir[27b], T. Trefzger[166], A. Tricoli[29], I.M. Trigger[156a], S. Trincaz-Duvoid[127], D.A. Trischuk[26], B. Trocmé[60], C. Troncon[71a], L. Truong[33c], M. Trzebinski[87], A. Trzupek[87], F. Tsai[145], M. Tsai[106], A. Tsiamis[152,e], P.V. Tsiareshka[37], S. Tsigaridas[156a], A. Tsirigotis[152,r], V. Tsiskaridze[155], E.G. Tskhadadze[149a], M. Tsopoulou[152,e], Y. Tsujikawa[88], I.I. Tsukerman[37], V. Tsulaia[17a], S. Tsuno[84], K. Tsuri[118], D. Tsybychev[145], Y. Tu[64b], A. Tudorache[27b], V. Tudorache[27b], A.N. Tuna[61], S. Turchikhin[57b,57a], I. Turk Cakir[3a], R. Turra[71a], T. Turtuvshin[38,x], P.M. Tuts[41], S. Tzamarias[152,e], P. Tzanis[10], E. Tzovara[100], F. Ukegawa[157], P.A. Ulloa Poblete[137c,137b], E.N. Umaka[29], G. Unal[36], M. Unal[11], A. Undrus[29], G. Unel[160], J. Urban[28b], P. Urquijo[105], P. Urrejola[137a], G. Usai[8], R. Ushioda[154], M. Usman[108], Z. Uysal[21b], V. Vacek[132], B. Vachon[104], K.O.H. Vadla[125], T. Vafeiadis[36], A. Vaitkus[96], C. Valderanis[109], E. Valdes Santurio[47a,47b], M. Valente[156a], S. Valentinetti[23b,23a], A. Valero[163], E. Valiente Moreno[163], A. Vallier[102,aa], J.A. Valls Ferrer[163], D.R. Van Arneman[114], T.R. Van Daalen[138], A. Van Der Graaf[49], P. Van Gemmeren[6], M. Van Rijnbach[125,36], S. Van Stroud[96], I. Van Vulpen[114], M. Vanadia[76a,76b], W. Vandelli[36], M. Vandenbroucke[135], E.R. Vandewall[121], D. Vannicola[151], L. Vannoli[57b,57a], R. Vari[75a], E.W. Varnes[7], C. Varni[17b], T. Varol[148], D. Varouchas[66], L. Varriale[163], K.E. Varvell[147], M.E. Vasile[27b], L. Vaslin[84], G.A. Vasquez[165], A. Vasyukov[38], F. Vazeille[40], T. Vazquez Schroeder[36], J. Veatch[31], V. Vecchio[101], M.J. Veen[103], I. Veliscek[126], L.M. Veloce[155], F. Veloso[130a,130c], S. Veneziano[75a], A. Ventura[70a,70b], S. Ventura Gonzalez[135], A. Verbytskyi[110], M. Verducci[74a,74b], C. Vergis[24], M. Verissimo De Araujo[83b], W. Verkerke[114], J.C. Vermeulen[114], C. Vernieri[143], M. Vessella[103], M.C. Vetterli[142,af], A. Vgenopoulos[152,e], N. Viaux Maira[137f], T. Vickey[139], O.E. Vickey Boeriu[139], G.H.A. Viehhauser[126], L. Vigani[63b], M. Villa[23b,23a], M. Villaplana Perez[163], E.M. Villhauer[52], E. Vilucchi[53], M.G. Vincter[34], G.S. Virdee[20], A. Vishwakarma[52], A. Visibile[114], C. Vittori[36], I. Vivarelli[146], E. Voevodina[110], F. Vogel[109], J.C. Voigt[50], P. Vokac[132], Yu. Volkotrub[86a], J. Von Ahnen[48], E. Von Toerne[24], B. Vormwald[36], V. Vorobel[133], K. Vorobev[37], M. Vos[163], K. Voss[141], J.H. Vossebeld[92], M. Vozak[114], L. Vozdecky[94], N. Vranjes[15], M. Vranjes Milosavljevic[15], M. Vreeswijk[114], R. Vuillermet[36], O. Vujinovic[100], I. Vukotic[39], S. Wada[157], C. Wagner[103], J.M. Wagner[17a], W. Wagner[171], S. Wahdan[171], H. Wahlberg[90], M. Wakida[111], J. Walder[134], R. Walker[109], W. Walkowiak[141], A. Wall[128], T. Wamorkar[6], A.Z. Wang[136], C. Wang[100], C. Wang[62c], H. Wang[17a], J. Wang[64a], R.-J. Wang[100], R. Wang[61], R. Wang[6], S.M. Wang[148], S. Wang[62b], T. Wang[62a], W.T. Wang[80], W. Wang[14a], X. Wang[14c], X. Wang[162], X. Wang[62c], Y. Wang[62d], Y. Wang[14c], Z. Wang[106], Z. Wang[62d,51,62c], Z. Wang[106], A. Warburton[104], R.J. Ward[20], N. Warrack[59], A.T. Watson[20], H. Watson[59], M.F. Watson[20], E. Watton[59,134], G. Watts[138], B.M. Waugh[96], C. Weber[29], H.A. Weber[18], M.S. Weber[19], S.M. Weber[63a], C. Wei[62a], Y. Wei[126], A.R. Weidberg[126], E.J. Weik[117], J. Weingarten[49], M. Weirich[100], C. Weiser[54], C.J. Wells[48], T. Wenaus[29], B. Wendland[49], T. Wengler[36], N.S. Wenke[110], N. Wermes[24], M. Wessels[63a], A.M. Wharton[91], A.S. White[61], A. White[8], M.J. White[1], D. Whiteson[160], L. Wickremasinghe[124], W. Wiedenmann[170], C. Wiel[50], M. Wielers[134], C. Wiglesworth[42], D.J. Wilbern[120], H.G. Wilkens[36], D.M. Williams[41], H.H. Williams[128], S. Williams[32], S. Willocq[103], B.J. Wilson[101], P.J. Windischhofer[39], F.I. Winkel[30], F. Winklmeier[123], B.T. Winter[54], J.K. Winter[101], M. Wittgen[143], M. Wobisch[97], Z. Wolffs[114], J. Wollrath[160], M.W. Wolter[87], H. Wolters[130a,130c], A.F. Wongel[48], E.L. Woodward[41], S.D. Worm[48], B.K. Wosiek[87], K.W. Woźniak[87], S. Wozniewski[55], K. Wraight[59], C. Wu[20], J. Wu[14a,14e], M. Wu[64a], M. Wu[113], S.L. Wu[170], X. Wu[56], Y. Wu[62a], Z. Wu[135], J. Wuerzinger[110,ad], T.R. Wyatt[101], B.M. Wynne[52], S. Xella[42], L. Xia[14c], M. Xia[14b], J. Xiang[64c], M. Xie[62a], X. Xie[62a], S. Xin[14a,14e], A. Xiong[123], J. Xiong[17a], D. Xu[14a], H. Xu[62a], L. Xu[62a], R. Xu[128], T. Xu[106], Y. Xu[14b], Z. Xu[52], Z. Xu[14c], B. Yabsley[147], S. Yacoob[33a], Y. Yamaguchi[154], E. Yamashita[153], H. Yamauchi[157], T. Yamazaki[17a], Y. Yamazaki[85], J. Yan[62c], S. Yan[126], Z. Yan[25], H.J. Yang[62c,62d], H.T. Yang[62a], S. Yang[62a], T. Yang[64c], X. Yang[36], X. Yang[14a], Y. Yang[44], Y. Yang[62a], Z. Yang[62a], W-M. Yao[17a], Y.C. Yap[48], H. Ye[14c], H. Ye[55], J. Ye[14a], S. Ye[29], X. Ye[62a], Y. Yeh[96], I. Yeletskikh[38], B.K. Yeo[17b], M.R. Yexley[96], P. Yin[41], K. Yorita[168], S. Younas[27b], C.J.S. Young[36], C. Young[143], C. Yu[14a,14e,ah], Y. Yu[62a], M. Yuan[106], R. Yuan[62b], L. Yue[96], M. Zaazoua[62a], B. Zabinski[87], E. Zaid[52], Z.K. Zak[87], T. Zakareishvili[149b], N. Zakharchuk[34], S. Zambito[56], J.A. Zamora Saa[137d,137b], J. Zang[153], D. Zanzi[54], O. Zaplatilek[132], C. Zeitnitz[171], H. Zeng[14a], J.C. Zeng[162], D.T. Zenger Jr[26], O. Zenin[37],

JHEP05(2024)106

T. Ženiš[28a], S. Zenz[94], S. Zerradi[35a], D. Zerwas[66], M. Zhai[14a,14e], B. Zhang[14c], D.F. Zhang[139], J. Zhang[62b], J. Zhang[6], K. Zhang[14a,14e], L. Zhang[14c], P. Zhang[14a,14e], R. Zhang[170], S. Zhang[106], S. Zhang[44], T. Zhang[153], X. Zhang[62c], X. Zhang[62b], Y. Zhang[62c,5], Y. Zhang[96], Y. Zhang[14c], Z. Zhang[17a], Z. Zhang[66], H. Zhao[138], T. Zhao[62b], Y. Zhao[136], Z. Zhao[62a], A. Zhemchugov[38], J. Zheng[14c], K. Zheng[162], X. Zheng[62a], Z. Zheng[143], D. Zhong[162], B. Zhou[106], H. Zhou[7], N. Zhou[62c], Y. Zhou[7], C.G. Zhu[62b], J. Zhu[106], Y. Zhu[62c], Y. Zhu[62a], X. Zhuang[14a], K. Zhukov[37], V. Zhulanov[37], N.I. Zimine[38], J. Zinsser[63b], M. Ziolkowski[141], L. Živković[15], A. Zoccoli[23b,23a], K. Zoch[61], T.G. Zorbas[139], O. Zormpa[46], W. Zou[41], L. Zwalinski[36]

[1] *Department of Physics, University of Adelaide, Adelaide, Australia*
[2] *Department of Physics, University of Alberta, Edmonton AB, Canada*
[3] [(a)] *Department of Physics, Ankara University, Ankara;* [(b)] *Division of Physics, TOBB University of Economics and Technology, Ankara, Türkiye*
[4] *LAPP, Université Savoie Mont Blanc, CNRS/IN2P3, Annecy, France*
[5] *APC, Université Paris Cité, CNRS/IN2P3, Paris, France*
[6] *High Energy Physics Division, Argonne National Laboratory, Argonne IL, United States of America*
[7] *Department of Physics, University of Arizona, Tucson AZ, United States of America*
[8] *Department of Physics, University of Texas at Arlington, Arlington TX, United States of America*
[9] *Physics Department, National and Kapodistrian University of Athens, Athens, Greece*
[10] *Physics Department, National Technical University of Athens, Zografou, Greece*
[11] *Department of Physics, University of Texas at Austin, Austin TX, United States of America*
[12] *Institute of Physics, Azerbaijan Academy of Sciences, Baku, Azerbaijan*
[13] *Institut de Física d'Altes Energies (IFAE), Barcelona Institute of Science and Technology, Barcelona, Spain*
[14] [(a)] *Institute of High Energy Physics, Chinese Academy of Sciences, Beijing;* [(b)] *Physics Department, Tsinghua University, Beijing;* [(c)] *Department of Physics, Nanjing University, Nanjing;* [(d)] *School of Science, Shenzhen Campus of Sun Yat-sen University;* [(e)] *University of Chinese Academy of Science (UCAS), Beijing, China*
[15] *Institute of Physics, University of Belgrade, Belgrade, Serbia*
[16] *Department for Physics and Technology, University of Bergen, Bergen, Norway*
[17] [(a)] *Physics Division, Lawrence Berkeley National Laboratory, Berkeley CA;* [(b)] *University of California, Berkeley CA, United States of America*
[18] *Institut für Physik, Humboldt Universität zu Berlin, Berlin, Germany*
[19] *Albert Einstein Center for Fundamental Physics and Laboratory for High Energy Physics, University of Bern, Bern, Switzerland*
[20] *School of Physics and Astronomy, University of Birmingham, Birmingham, United Kingdom*
[21] [(a)] *Department of Physics, Bogazici University, Istanbul;* [(b)] *Department of Physics Engineering, Gaziantep University, Gaziantep;* [(c)] *Department of Physics, Istanbul University, Istanbul, Türkiye*
[22] [(a)] *Facultad de Ciencias y Centro de Investigaciónes, Universidad Antonio Nariño, Bogotá;* [(b)] *Departamento de Física, Universidad Nacional de Colombia, Bogotá, Colombia*
[23] [(a)] *Dipartimento di Fisica e Astronomia A. Righi, Università di Bologna, Bologna;* [(b)] *INFN Sezione di Bologna, Italy*
[24] *Physikalisches Institut, Universität Bonn, Bonn, Germany*
[25] *Department of Physics, Boston University, Boston MA, United States of America*
[26] *Department of Physics, Brandeis University, Waltham MA, United States of America*
[27] [(a)] *Transilvania University of Brasov, Brasov;* [(b)] *Horia Hulubei National Institute of Physics and Nuclear Engineering, Bucharest;* [(c)] *Department of Physics, Alexandru Ioan Cuza University of Iasi, Iasi;* [(d)] *National Institute for Research and Development of Isotopic and Molecular Technologies, Physics Department, Cluj-Napoca;* [(e)] *National University of Science and Technology Politechnica, Bucharest;* [(f)] *West University in Timisoara, Timisoara;* [(g)] *Faculty of Physics, University of Bucharest, Bucharest, Romania*

JHEP05(2024)106

[28] [(a)] Faculty of Mathematics, Physics and Informatics, Comenius University, Bratislava; [(b)] Department of Subnuclear Physics, Institute of Experimental Physics of the Slovak Academy of Sciences, Kosice, Slovak Republic
[29] Physics Department, Brookhaven National Laboratory, Upton NY, United States of America
[30] Universidad de Buenos Aires, Facultad de Ciencias Exactas y Naturales, Departamento de Física, y CONICET, Instituto de Física de Buenos Aires (IFIBA), Buenos Aires, Argentina
[31] California State University, CA, United States of America
[32] Cavendish Laboratory, University of Cambridge, Cambridge, United Kingdom
[33] [(a)] Department of Physics, University of Cape Town, Cape Town; [(b)] iThemba Labs, Western Cape; [(c)] Department of Mechanical Engineering Science, University of Johannesburg, Johannesburg; [(d)] National Institute of Physics, University of the Philippines Diliman (Philippines); [(e)] University of South Africa, Department of Physics, Pretoria; [(f)] University of Zululand, KwaDlangezwa; [(g)] School of Physics, University of the Witwatersrand, Johannesburg, South Africa
[34] Department of Physics, Carleton University, Ottawa ON, Canada
[35] [(a)] Faculté des Sciences Ain Chock, Réseau Universitaire de Physique des Hautes Energies - Université Hassan II, Casablanca; [(b)] Faculté des Sciences, Université Ibn-Tofail, Kénitra; [(c)] Faculté des Sciences Semlalia, Université Cadi Ayyad, LPHEA-Marrakech; [(d)] LPMR, Faculté des Sciences, Université Mohamed Premier, Oujda; [(e)] Faculté des sciences, Université Mohammed V, Rabat; [(f)] Institute of Applied Physics, Mohammed VI Polytechnic University, Ben Guerir, Morocco
[36] CERN, Geneva, Switzerland
[37] Affiliated with an institute covered by a cooperation agreement with CERN
[38] Affiliated with an international laboratory covered by a cooperation agreement with CERN
[39] Enrico Fermi Institute, University of Chicago, Chicago IL, United States of America
[40] LPC, Université Clermont Auvergne, CNRS/IN2P3, Clermont-Ferrand, France
[41] Nevis Laboratory, Columbia University, Irvington NY, United States of America
[42] Niels Bohr Institute, University of Copenhagen, Copenhagen, Denmark
[43] [(a)] Dipartimento di Fisica, Università della Calabria, Rende; [(b)] INFN Gruppo Collegato di Cosenza, Laboratori Nazionali di Frascati, Italy
[44] Physics Department, Southern Methodist University, Dallas TX, United States of America
[45] Physics Department, University of Texas at Dallas, Richardson TX, United States of America
[46] National Centre for Scientific Research "Demokritos", Agia Paraskevi, Greece
[47] [(a)] Department of Physics, Stockholm University; [(b)] Oskar Klein Centre, Stockholm, Sweden
[48] Deutsches Elektronen-Synchrotron DESY, Hamburg and Zeuthen, Germany
[49] Fakultät Physik, Technische Universität Dortmund, Dortmund, Germany
[50] Institut für Kern- und Teilchenphysik, Technische Universität Dresden, Dresden, Germany
[51] Department of Physics, Duke University, Durham NC, United States of America
[52] SUPA - School of Physics and Astronomy, University of Edinburgh, Edinburgh, United Kingdom
[53] INFN e Laboratori Nazionali di Frascati, Frascati, Italy
[54] Physikalisches Institut, Albert-Ludwigs-Universität Freiburg, Freiburg, Germany
[55] II. Physikalisches Institut, Georg-August-Universität Göttingen, Göttingen, Germany
[56] Département de Physique Nucléaire et Corpusculaire, Université de Genève, Genève, Switzerland
[57] [(a)] Dipartimento di Fisica, Università di Genova, Genova; [(b)] INFN Sezione di Genova, Italy
[58] II. Physikalisches Institut, Justus-Liebig-Universität Giessen, Giessen, Germany
[59] SUPA - School of Physics and Astronomy, University of Glasgow, Glasgow, United Kingdom
[60] LPSC, Université Grenoble Alpes, CNRS/IN2P3, Grenoble INP, Grenoble, France
[61] Laboratory for Particle Physics and Cosmology, Harvard University, Cambridge MA, United States of America
[62] [(a)] Department of Modern Physics and State Key Laboratory of Particle Detection and Electronics, University of Science and Technology of China, Hefei; [(b)] Institute of Frontier and Interdisciplinary Science and Key Laboratory of Particle Physics and Particle Irradiation (MOE), Shandong University, Qingdao; [(c)] School of Physics and Astronomy, Shanghai Jiao Tong University, Key Laboratory for Particle Astrophysics and Cosmology (MOE), SKLPPC, Shanghai; [(d)] Tsung-Dao Lee Institute, Shanghai; [(e)] School of Physics and Microelectronics, Zhengzhou University, China

[63] [(a)] Kirchhoff-Institut für Physik, Ruprecht-Karls-Universität Heidelberg, Heidelberg; [(b)] Physikalisches Institut, Ruprecht-Karls-Universität Heidelberg, Heidelberg, Germany
[64] [(a)] Department of Physics, Chinese University of Hong Kong, Shatin, N.T., Hong Kong; [(b)] Department of Physics, University of Hong Kong, Hong Kong; [(c)] Department of Physics and Institute for Advanced Study, Hong Kong University of Science and Technology, Clear Water Bay, Kowloon, Hong Kong, China
[65] Department of Physics, National Tsing Hua University, Hsinchu, Taiwan
[66] IJCLab, Université Paris-Saclay, CNRS/IN2P3, 91405, Orsay, France
[67] Centro Nacional de Microelectrónica (IMB-CNM-CSIC), Barcelona, Spain
[68] Department of Physics, Indiana University, Bloomington IN, United States of America
[69] [(a)] INFN Gruppo Collegato di Udine, Sezione di Trieste, Udine; [(b)] ICTP, Trieste; [(c)] Dipartimento Politecnico di Ingegneria e Architettura, Università di Udine, Udine, Italy
[70] [(a)] INFN Sezione di Lecce; [(b)] Dipartimento di Matematica e Fisica, Università del Salento, Lecce, Italy
[71] [(a)] INFN Sezione di Milano; [(b)] Dipartimento di Fisica, Università di Milano, Milano, Italy
[72] [(a)] INFN Sezione di Napoli; [(b)] Dipartimento di Fisica, Università di Napoli, Napoli, Italy
[73] [(a)] INFN Sezione di Pavia; [(b)] Dipartimento di Fisica, Università di Pavia, Pavia, Italy
[74] [(a)] INFN Sezione di Pisa; [(b)] Dipartimento di Fisica E. Fermi, Università di Pisa, Pisa, Italy
[75] [(a)] INFN Sezione di Roma; [(b)] Dipartimento di Fisica, Sapienza Università di Roma, Roma, Italy
[76] [(a)] INFN Sezione di Roma Tor Vergata; [(b)] Dipartimento di Fisica, Università di Roma Tor Vergata, Roma, Italy
[77] [(a)] INFN Sezione di Roma Tre; [(b)] Dipartimento di Matematica e Fisica, Università Roma Tre, Roma, Italy
[78] [(a)] INFN-TIFPA; [(b)] Università degli Studi di Trento, Trento, Italy
[79] Universität Innsbruck, Department of Astro and Particle Physics, Innsbruck, Austria
[80] University of Iowa, Iowa City IA, United States of America
[81] Department of Physics and Astronomy, Iowa State University, Ames IA, United States of America
[82] Istinye University, Sariyer, Istanbul, Türkiye
[83] [(a)] Departamento de Engenharia Elétrica, Universidade Federal de Juiz de Fora (UFJF), Juiz de Fora; [(b)] Universidade Federal do Rio De Janeiro COPPE/EE/IF, Rio de Janeiro; [(c)] Instituto de Física, Universidade de São Paulo, São Paulo; [(d)] Rio de Janeiro State University, Rio de Janeiro, Brazil
[84] KEK, High Energy Accelerator Research Organization, Tsukuba, Japan
[85] Graduate School of Science, Kobe University, Kobe, Japan
[86] [(a)] AGH University of Krakow, Faculty of Physics and Applied Computer Science, Krakow; [(b)] Marian Smoluchowski Institute of Physics, Jagiellonian University, Krakow, Poland
[87] Institute of Nuclear Physics Polish Academy of Sciences, Krakow, Poland
[88] Faculty of Science, Kyoto University, Kyoto, Japan
[89] Research Center for Advanced Particle Physics and Department of Physics, Kyushu University, Fukuoka, Japan
[90] Instituto de Física La Plata, Universidad Nacional de La Plata and CONICET, La Plata, Argentina
[91] Physics Department, Lancaster University, Lancaster, United Kingdom
[92] Oliver Lodge Laboratory, University of Liverpool, Liverpool, United Kingdom
[93] Department of Experimental Particle Physics, Jožef Stefan Institute and Department of Physics, University of Ljubljana, Ljubljana, Slovenia
[94] School of Physics and Astronomy, Queen Mary University of London, London, United Kingdom
[95] Department of Physics, Royal Holloway University of London, Egham, United Kingdom
[96] Department of Physics and Astronomy, University College London, London, United Kingdom
[97] Louisiana Tech University, Ruston LA, United States of America
[98] Fysiska institutionen, Lunds universitet, Lund, Sweden
[99] Departamento de Física Teorica C-15 and CIAFF, Universidad Autónoma de Madrid, Madrid, Spain
[100] Institut für Physik, Universität Mainz, Mainz, Germany
[101] School of Physics and Astronomy, University of Manchester, Manchester, United Kingdom
[102] CPPM, Aix-Marseille Université, CNRS/IN2P3, Marseille, France
[103] Department of Physics, University of Massachusetts, Amherst MA, United States of America
[104] Department of Physics, McGill University, Montreal QC, Canada
[105] School of Physics, University of Melbourne, Victoria, Australia

[106] Department of Physics, University of Michigan, Ann Arbor MI, United States of America
[107] Department of Physics and Astronomy, Michigan State University, East Lansing MI, United States of America
[108] Group of Particle Physics, University of Montreal, Montreal QC, Canada
[109] Fakultät für Physik, Ludwig-Maximilians-Universität München, München, Germany
[110] Max-Planck-Institut für Physik (Werner-Heisenberg-Institut), München, Germany
[111] Graduate School of Science and Kobayashi-Maskawa Institute, Nagoya University, Nagoya, Japan
[112] Department of Physics and Astronomy, University of New Mexico, Albuquerque NM, United States of America
[113] Institute for Mathematics, Astrophysics and Particle Physics, Radboud University/Nikhef, Nijmegen, The Netherlands
[114] Nikhef National Institute for Subatomic Physics and University of Amsterdam, Amsterdam, The Netherlands
[115] Department of Physics, Northern Illinois University, DeKalb IL, United States of America
[116] [(a)] New York University Abu Dhabi, Abu Dhabi; [(b)] University of Sharjah, Sharjah, United Arab Emirates
[117] Department of Physics, New York University, New York NY, United States of America
[118] Ochanomizu University, Otsuka, Bunkyo-ku, Tokyo, Japan
[119] Ohio State University, Columbus OH, United States of America
[120] Homer L. Dodge Department of Physics and Astronomy, University of Oklahoma, Norman OK, United States of America
[121] Department of Physics, Oklahoma State University, Stillwater OK, United States of America
[122] Palacký University, Joint Laboratory of Optics, Olomouc, Czech Republic
[123] Institute for Fundamental Science, University of Oregon, Eugene, OR, United States of America
[124] Graduate School of Science, Osaka University, Osaka, Japan
[125] Department of Physics, University of Oslo, Oslo, Norway
[126] Department of Physics, Oxford University, Oxford, United Kingdom
[127] LPNHE, Sorbonne Université, Université Paris Cité, CNRS/IN2P3, Paris, France
[128] Department of Physics, University of Pennsylvania, Philadelphia PA, United States of America
[129] Department of Physics and Astronomy, University of Pittsburgh, Pittsburgh PA, United States of America
[130] [(a)] Laboratório de Instrumentação e Física Experimental de Partículas - LIP, Lisboa; [(b)] Departamento de Física, Faculdade de Ciências, Universidade de Lisboa, Lisboa; [(c)] Departamento de Física, Universidade de Coimbra, Coimbra; [(d)] Centro de Física Nuclear da Universidade de Lisboa, Lisboa; [(e)] Departamento de Física, Universidade do Minho, Braga; [(f)] Departamento de Física Teórica y del Cosmos, Universidad de Granada, Granada (Spain); [(g)] Departamento de Física, Instituto Superior Técnico, Universidade de Lisboa, Lisboa, Portugal
[131] Institute of Physics of the Czech Academy of Sciences, Prague, Czech Republic
[132] Czech Technical University in Prague, Prague, Czech Republic
[133] Charles University, Faculty of Mathematics and Physics, Prague, Czech Republic
[134] Particle Physics Department, Rutherford Appleton Laboratory, Didcot, United Kingdom
[135] IRFU, CEA, Université Paris-Saclay, Gif-sur-Yvette, France
[136] Santa Cruz Institute for Particle Physics, University of California Santa Cruz, Santa Cruz CA, United States of America
[137] [(a)] Departamento de Física, Pontificia Universidad Católica de Chile, Santiago; [(b)] Millennium Institute for Subatomic physics at high energy frontier (SAPHIR), Santiago; [(c)] Instituto de Investigación Multidisciplinario en Ciencia y Tecnología, y Departamento de Física, Universidad de La Serena; [(d)] Universidad Andres Bello, Department of Physics, Santiago; [(e)] Instituto de Alta Investigación, Universidad de Tarapacá, Arica; [(f)] Departamento de Física, Universidad Técnica Federico Santa María, Valparaíso, Chile
[138] Department of Physics, University of Washington, Seattle WA, United States of America
[139] Department of Physics and Astronomy, University of Sheffield, Sheffield, United Kingdom
[140] Department of Physics, Shinshu University, Nagano, Japan
[141] Department Physik, Universität Siegen, Siegen, Germany
[142] Department of Physics, Simon Fraser University, Burnaby BC, Canada

[143] *SLAC National Accelerator Laboratory, Stanford CA, United States of America*
[144] *Department of Physics, Royal Institute of Technology, Stockholm, Sweden*
[145] *Departments of Physics and Astronomy, Stony Brook University, Stony Brook NY, United States of America*
[146] *Department of Physics and Astronomy, University of Sussex, Brighton, United Kingdom*
[147] *School of Physics, University of Sydney, Sydney, Australia*
[148] *Institute of Physics, Academia Sinica, Taipei, Taiwan*
[149] [(a)] *E. Andronikashvili Institute of Physics, Iv. Javakhishvili Tbilisi State University, Tbilisi;* [(b)] *High Energy Physics Institute, Tbilisi State University, Tbilisi;* [(c)] *University of Georgia, Tbilisi, Georgia*
[150] *Department of Physics, Technion, Israel Institute of Technology, Haifa, Israel*
[151] *Raymond and Beverly Sackler School of Physics and Astronomy, Tel Aviv University, Tel Aviv, Israel*
[152] *Department of Physics, Aristotle University of Thessaloniki, Thessaloniki, Greece*
[153] *International Center for Elementary Particle Physics and Department of Physics, University of Tokyo, Tokyo, Japan*
[154] *Department of Physics, Tokyo Institute of Technology, Tokyo, Japan*
[155] *Department of Physics, University of Toronto, Toronto ON, Canada*
[156] [(a)] *TRIUMF, Vancouver BC;* [(b)] *Department of Physics and Astronomy, York University, Toronto ON, Canada*
[157] *Division of Physics and Tomonaga Center for the History of the Universe, Faculty of Pure and Applied Sciences, University of Tsukuba, Tsukuba, Japan*
[158] *Department of Physics and Astronomy, Tufts University, Medford MA, United States of America*
[159] *United Arab Emirates University, Al Ain, United Arab Emirates*
[160] *Department of Physics and Astronomy, University of California Irvine, Irvine CA, United States of America*
[161] *Department of Physics and Astronomy, University of Uppsala, Uppsala, Sweden*
[162] *Department of Physics, University of Illinois, Urbana IL, United States of America*
[163] *Instituto de Física Corpuscular (IFIC), Centro Mixto Universidad de Valencia - CSIC, Valencia, Spain*
[164] *Department of Physics, University of British Columbia, Vancouver BC, Canada*
[165] *Department of Physics and Astronomy, University of Victoria, Victoria BC, Canada*
[166] *Fakultät für Physik und Astronomie, Julius-Maximilians-Universität Würzburg, Würzburg, Germany*
[167] *Department of Physics, University of Warwick, Coventry, United Kingdom*
[168] *Waseda University, Tokyo, Japan*
[169] *Department of Particle Physics and Astrophysics, Weizmann Institute of Science, Rehovot, Israel*
[170] *Department of Physics, University of Wisconsin, Madison WI, United States of America*
[171] *Fakultät für Mathematik und Naturwissenschaften, Fachgruppe Physik, Bergische Universität Wuppertal, Wuppertal, Germany*
[172] *Department of Physics, Yale University, New Haven CT, United States of America*

[a] *Also Affiliated with an institute covered by a cooperation agreement with CERN*
[b] *Also at An-Najah National University, Nablus, Palestine*
[c] *Also at Borough of Manhattan Community College, City University of New York, New York NY, United States of America*
[d] *Also at Center for High Energy Physics, Peking University, China*
[e] *Also at Center for Interdisciplinary Research and Innovation (CIRI-AUTH), Thessaloniki, Greece*
[f] *Also at Centro Studi e Ricerche Enrico Fermi, Italy*
[g] *Also at CERN, Geneva, Switzerland*
[h] *Also at Département de Physique Nucléaire et Corpusculaire, Université de Genève, Genève, Switzerland*
[i] *Also at Departament de Fisica de la Universitat Autonoma de Barcelona, Barcelona, Spain*
[j] *Also at Department of Financial and Management Engineering, University of the Aegean, Chios, Greece*
[k] *Also at Department of Physics, Ben Gurion University of the Negev, Beer Sheva, Israel*
[l] *Also at Department of Physics, California State University, Sacramento, United States of America*
[m] *Also at Department of Physics, King's College London, London, United Kingdom*
[n] *Also at Department of Physics, Stanford University, Stanford CA, United States of America*
[o] *Also at Department of Physics, University of Fribourg, Fribourg, Switzerland*

JHEP05(2024)106

[p] *Also at Department of Physics, University of Thessaly, Greece*
[q] *Also at Department of Physics, Westmont College, Santa Barbara, United States of America*
[r] *Also at Hellenic Open University, Patras, Greece*
[s] *Also at Institucio Catalana de Recerca i Estudis Avancats, ICREA, Barcelona, Spain*
[t] *Also at Institut für Experimentalphysik, Universität Hamburg, Hamburg, Germany*
[u] *Also at Institute for Nuclear Research and Nuclear Energy (INRNE) of the Bulgarian Academy of Sciences, Sofia, Bulgaria*
[v] *Also at Institute of Applied Physics, Mohammed VI Polytechnic University, Ben Guerir, Morocco*
[w] *Also at Institute of Particle Physics (IPP), Canada*
[x] *Also at Institute of Physics and Technology, Mongolian Academy of Sciences, Ulaanbaatar, Mongolia*
[y] *Also at Institute of Physics, Azerbaijan Academy of Sciences, Baku, Azerbaijan*
[z] *Also at Institute of Theoretical Physics, Ilia State University, Tbilisi, Georgia*
[aa] *Also at L2IT, Université de Toulouse, CNRS/IN2P3, UPS, Toulouse, France*
[ab] *Also at Lawrence Livermore National Laboratory, Livermore, United States of America*
[ac] *Also at National Institute of Physics, University of the Philippines Diliman (Philippines), Philippines*
[ad] *Also at Technical University of Munich, Munich, Germany*
[ae] *Also at The Collaborative Innovation Center of Quantum Matter (CICQM), Beijing, China*
[af] *Also at TRIUMF, Vancouver BC, Canada*
[ag] *Also at Università di Napoli Parthenope, Napoli, Italy*
[ah] *Also at University of Chinese Academy of Sciences (UCAS), Beijing, China*
[ai] *Also at University of Colorado Boulder, Department of Physics, Colorado, United States of America*
[aj] *Also at Washington College, Chestertown, MD, United States of America*
[ak] *Also at Yeditepe University, Physics Department, Istanbul, Türkiye*
[*] *Deceased*

JHEP05(2024)106